NATIONAL COOPERATIVE HIGHWAY RESEARCH PROGRAM

NCHRP Report 410

Silica Fume Concrete for Bridge Decks

Transportation Research Board
National Research Council

NATIONAL COOPERATIVE HIGHWAY RESEARCH PROGRAM

Report 410

Silica Fume Concrete for Bridge Decks

D. WHITING and R. DETWILER
Construction Technology Laboratories, Inc.
Skokie, IL

Subject Areas

Bridges, Other Structures, and Hydraulics and Hydrology
Materials and Construction

Research Sponsored by the American Association of State Highway and Transportation Officials in Cooperation with the Federal Highway Administration

TRANSPORTATION RESEARCH BOARD
NATIONAL RESEARCH COUNCIL

NATIONAL ACADEMY PRESS
Washington, D.C. 1998

NATIONAL COOPERATIVE HIGHWAY RESEARCH PROGRAM

Systematic, well-designed research provides the most effective approach to the solution of many problems facing highway administrators and engineers. Often, highway problems are of local interest and can best be studied by highway departments individually or in cooperation with their state universities and others. However, the accelerating growth of highway transportation develops increasingly complex problems of wide interest to highway authorities. These problems are best studied through a coordinated program of cooperative research.

In recognition of these needs, the highway administrators of the American Association of State Highway and Transportation Officials initiated in 1962 an objective national highway research program employing modern scientific techniques. This program is supported on a continuing basis by funds from participating member states of the Association and it receives the full cooperation and support of the Federal Highway Administration, United States Department of Transportation.

The Transportation Research Board of the National Research Council was requested by the Association to administer the research program because of the Board's recognized objectivity and understanding of modern research practices. The Board is uniquely suited for this purpose as it maintains an extensive committee structure from which authorities on any highway transportation subject may be drawn; it possesses avenues of communications and cooperation with federal, state and local governmental agencies, universities, and industry; its relationship to the National Research Council is an insurance of objectivity; it maintains a full-time research correlation staff of specialists in highway transportation matters to bring the findings of research directly to those who are in a position to use them.

The program is developed on the basis of research needs identified by chief administrators of the highway and transportation departments and by committees of AASHTO. Each year, specific areas of research needs to be included in the program are proposed to the National Research Council and the Board by the American Association of State Highway and Transportation Officials. Research projects to fulfill these needs are defined by the Board, and qualified research agencies are selected from those that have submitted proposals. Administration and surveillance of research contracts are the responsibilities of the National Research Council and the Transportation Research Board.

The needs for highway research are many, and the National Cooperative Highway Research Program can make significant contributions to the solution of highway transportation problems of mutual concern to many responsible groups. The program, however, is intended to complement rather than to substitute for or duplicate other highway research programs.

Note: The Transportation Research Board, the National Research Council, the Federal Highway Administration, the American Association of State Highway and Transportation Officials, and the individual states participating in the National Cooperative Highway Research Program do not endorse products or manufacturers. Trade or manufacturers' names appear herein solely because they are considered essential to the object of this report.

NCHRP REPORT 410

Project 18-3 FY'95

ISSN 0077-5614

ISBN 0-309-06270-5

L. C. Catalog Card No. 98-60937

Price $30.00

NOTICE

The project that is the subject of this report was a part of the National Cooperative Highway Research Program conducted by the Transportation Research Board with the approval of the Governing Board of the National Research Council. Such approval reflects the Governing Board's judgment that the program concerned is of national importance and appropriate with respect to both the purposes and resources of the National Research Council.

The members of the technical committee selected to monitor this project and to review this report were chosen for recognized scholarly competence and with due consideration for the balance of disciplines appropriate to the project. The opinions and conclusions expressed or implied are those of the research agency that performed the research, and, while they have been accepted as appropriate by the technical committee, they are not necessarily those of the Transportation Research Board, the National Research Council, the American Association of State Highway and Transportation Officials, or the Federal Highway Administration, U.S. Department of Transportation.

Each report is reviewed and accepted for publication by the technical committee according to procedures established and monitored by the Transportation Research Board Executive Committee and the Governing Board of the National Research Council.

Published reports of the

NATIONAL COOPERATIVE HIGHWAY RESEARCH PROGRAM

are available from:

Transportation Research Board
National Research Council
2101 Constitution Avenue, N.W.
Washington, D.C. 20418

and can be ordered through the Internet at:

http://www.nas.edu/trb/index.html

Printed in the United States of America

FOREWORD

By Staff
Transportation Research Board

This report contains the findings of a study that was performed to determine the effects of the form and dosage of silica fume admixtures and other concrete mixture parameters on the concrete properties most relevant to bridge-deck applications and to develop recommendations for silica fume concrete mixtures suitable for these applications. The report provides a comprehensive description of the research, including provisions to help highway engineers select silica fume concrete mixtures and adopt construction practices that should enhance bridge-deck performance. The contents of this report will be of immediate interest to bridge and construction engineers and others involved in the design, construction, and rehabilitation of bridge decks.

The use of silica fume concrete for bridge decks and bridge-deck overlays has become a widely accepted practice by many state highway agencies, primarily because of its favorable effects on transport properties and compressive strength. However, cracking in some bridge decks constructed with silica fume concrete has led to some concern about its suitability for these applications.

Under NCHRP Project 18-3, "Silica Fume Concrete for Bridge Decks," Construction Technology Laboratories, Inc. of Skokie, Illinois, was assigned the task of determining the effects of the form and dosage of silica fume admixtures and other concrete mixture parameters on the concrete properties most relevant to bridge-deck applications, and recommending concrete mixtures and construction practices for enhancing the deck's performance. To accomplish these objectives, the researchers developed a statistically valid experiment design for a laboratory investigation, prepared test specimens, and performed laboratory tests. The report documents the work performed under NCHRP Project 18-3 and describes the relevance of silica fume concrete mixtures and construction practices to the performance of bridge decks and bridge-deck overlays.

The recommended silica fume concrete mixtures and construction practices, described in this report, will enhance the performance of bridge deck and bridge-deck overlays. Highway agencies are encouraged to incorporate the research findings and recommendations into their specifications for bridge deck and bridge-deck overlay construction.

CONTENTS

AUTHOR ACKNOWLEDGMENTS

The research reported herein was performed under NCHRP Project 18-3 by Construction Technology Laboratories, Inc. (CTL). Dr. David Whiting, Senior Principal Engineer, was the principal investigator. Dr. Rachel Detwiler, Principal Engineer, served as co-investigator and co-authored this report. Mr. Thomas Weinman, Senior Engineer, also served as co-investigator and directed the cracking tendency testing. Dr. Eric Lagergren of the National Institutes of Standards and Technology (NIST), Computing and Applied Mathematic Laboratory, performed the statistical analysis of data under a subcontract to CTL.

SILICA FUME CONCRETE FOR BRIDGE DECKS

SUMMARY

Since the first installations during the mid-1980s in the state of Ohio, the use of silica fume in highway applications has progressively increased. Because of its low diffusivity to chloride ions and good bonding characteristics, silica fume concrete can extend the life of bridge decks by postponing chloride-induced corrosion of reinforcing steel. Although the majority of projects have consisted of thin bonded overlays for restoration of deck riding surfaces, some full-depth deck placements also have been carried out. The majority of such projects have been successful; however, in some cases, instances of unanticipated and premature cracking have occurred. While cracking of thin overlays has been attributed to early plastic shrinkage prior to setting of the concrete, the causes of full-depth deck cracking are less well understood. Cracking, in some instances, has been attributed to the use of silica fume, especially when used at high percentages by weight of the portland cement.

The amount of silica fume used in concrete mixtures for placement of bridge decks and overlays needs to be optimized from both economic and performance viewpoints. Most conventional concrete mixtures used for such applications exhibit strength values that exceed minimum strength requirements by a significant amount. Thus, the very high strengths achievable through the use of large amounts of silica fume may be neither necessary nor desirable. The accompanying increase in elastic modulus may make the concrete matrix more brittle and prone to cracking. It is also believed that silica fume mixtures may, under certain circumstances, exhibit a higher degree of drying shrinkage than conventional concretes. While penetration of chloride ions into the deck may be reduced through use of silica fume, more information is needed on the nature of the relationship so that excessive amounts of silica fume may be avoided.

In this project, a number of important physical properties of concrete were selected for study with respect to use of silica fume. Primary properties were defined as those having the greatest impact on observed problems, as well as representing the primary reason why silica fume has been adopted as a protective strategy. These included drying shrinkage, cracking tendency (under restrained conditions), and chloride ion ingress. Secondary properties included compressive strength, elastic modulus, thermal expansion coefficient, and bond of overlay to deck substrate concrete. In addition, workability and handling characteristics were qualitatively assessed. Mixtures were prepared representing both full-depth bridge decks and deck overlay concretes. Silica fume content was varied from zero (conventional concrete) to 12 percent replacement

of cement by mass. The water-to-cementitious materials ratio (w/cm) was varied from 0.35 to 0.45 for the full-depth mixtures and from 0.30 to 0.40 for the overlay mixtures. Overlay mixtures were moist cured for 3 days, and full-depth mixtures were cured for 7 days. Further work on cracking tendency was carried out using only 1 day of moist curing.

Results of laboratory testing indicated that silica fume had similar effects on drying shrinkage and tendency to cracking. At early ages (1 to 4 days), an increase in the amount of silica fume will increase drying shrinkage and decrease the time to cracking. The w/cm has less effect on shrinkage or cracking when curing is minimal. At later ages, drying shrinkage is primarily a function of w/cm and, if given sufficient moist curing (7 days or more), silica fume will not promote, and may even reduce, the tendency to cracking of full-depth concrete mixtures. Overlay mixtures, because of their higher paste contents, exhibit higher drying shrinkage and are more susceptible to cracking. The use of Type K (shrinkage-compensating) cement does not decrease drying shrinkage, but does significantly reduce the tendency toward cracking under restrained conditions in full-depth concrete mixtures.

Findings with respect to chloride diffusivity indicate that, for any given w/cm, the diffusivity drops as silica fume is increased. The most sensitive region is in the lower range of silica fume contents where diffusivity changes at a faster rate as small amounts of silica fume are added. At levels of silica fume over 4 to 6 percent, it takes a much greater addition to effect a large change in diffusivity. As silica fume is expensive, a point of diminishing returns may be reached as one adds silica fume over about 6 percent. At lower w/cm values, increasing the silica fume content above the 6 percent level has little effect on diffusivity. Therefore, considerable savings can be effected with little loss in performance by restricting addition of silica fume to a maximum of 6 percent by mass of total cementitious materials in the mix.

For compressive strength, the expected association with both w/cm and silica fume content was seen. In all cases, strength increased with a decrease in w/cm. As was seen for chloride diffusivity, a "plateau" effect on strength was seen as silica fume content was increased. That is, beyond a level of about 6 percent silica fume there was much less of an increase in strength as the silica fume content was increased. While data with respect to elastic modulus were more complex, in the majority of cases moduli increased as the amount of silica fume in the mix increased. This reinforces the conclusion that silica fume contents greater than about 6 percent are unnecessary for bridge-deck applications.

This final report also includes a plan for field installation of silica fume concrete test sections and a suggested implementation strategy. The field plan is designed to include silica fume and newly developed "ternary" mixtures containing blends of silica fume and other pozzolans in fabrication of full-depth concrete bridge-deck sections. Suggested test section layouts, experimental variables, installation procedures, and insitu and long-term testing protocols are included in the field plan. The implementation plan includes an outline for a 1-day short course on bridge-deck applications of silica fume concrete and other suggested means for distribution of project findings.

CHAPTER 1

INTRODUCTION AND RESEARCH APPROACH

PROBLEM STATEMENT

The use of silica fume concrete for bridge decks and bridge-deck overlays has become a widely accepted practice by many state highway agencies, primarily because of its favorable effects on transport properties and compressive strengths. However, cracking of some bridge decks constructed with silica fume concrete has led to a certain degree of concern about the use of this material for such applications.

A great deal of research has been performed on the effects of concrete-mixture variables on the properties of silica fume concrete. This research, however, has not provided clear conclusions concerning the concrete mixtures that are well suited for bridge-deck applications. Further research is needed to address the properties of silica fume concrete that significantly influence the performance of bridge decks and to develop recommendations for suitable mixtures.

OBJECTIVES AND SCOPE

The objectives of this laboratory study were as follows:

- To determine the effect of form and amount of silica fume (also known as condensed silica fume and "microsilica"), as well as other mix design parameters, on the properties of silica fume concrete most pertinent to bridge deck and overlay placements.
- To develop information concerning the ability of silica fume concrete to restrict the ingress of chloride ions, the tendency of silica fume concrete to crack, the means of reducing any potential for cracking, and the bond of silica fume concrete overlays to deck concrete and optimization of the mix for desired overlay performance.

The scope and research approach of the study included the following:

- Statistically valid experimental design of the study so that response surface methodology (a statistical technique in which results of a multiple regression analysis are mapped onto a contour plot) could be used to determine effects of silica fume content and water-to-cementitious material ratios (w/cm) on response variables.
- Preparation of a series of concrete mixtures, including both overlay and full-depth concretes, over a practical range of w/cm and silica fume contents.
- Preparation of test specimens for determination of drying shrinkage, cracking tendency, chloride ion diffusivity, compressive strength, elastic modulus, strength of bond to concrete substrate, and coefficient of thermal expansion as a function of w/cm and silica fume content.
- Regression analysis of the data, construction of response surfaces in contour plot format, and interpretation of the plots in terms of trends with respect to silica fume content and w/cm for all variables modeled.

BACKGROUND AND CURRENT KNOWLEDGE

Silica Fume

Silica fume (also referred to as condensed silica fume or "microsilica") is generally a by-product material from the production of silicon metal or ferrosilicon alloys in electric arc furnaces. Chemically, it has a very high (generally over 85 percent) content of amorphous silica (SiO_2) and consists of very fine spherical particles. Its average fineness (surface area/unit mass) of about 20,000 m^2/kg (*1*) is two orders of magnitude finer than even the most finely ground portland cements, whose average particle diameters are of the order of 0.1 μm. This results in a very highly reactive material when exposed to the lime-rich environment of a portland cement system. The silica fume quickly forms calcium silicate hydrate, filling in the normally weak interstitial spaces between the cement paste matrix and aggregate particles, which results in a dense, strong, and relatively impermeable material. It should be noted that for silica fume contents typical of U.S. practice, silica fume concrete mixes have an unusually high water demand, and fairly high amounts of high-range water-reducing (HRWR) agents must be used in order to obtain a workable concrete at reasonable w/cm.

Use of Silica Fume in Highway Applications

Silica fume was first employed on an experimental basis in the Scandinavian countries in the 1950s (*2*). The development of HRWR in Europe and Japan in the early 1970s

allowed silica fume concrete to be produced with acceptable workability at low w/cm. However, the use of silica fume concrete in highway applications in the United States did not begin until the mid-1980s with trial placements of full-depth decks and overlays in the state of Ohio (*3*).

In a summary article published in 1993, Luther (*4*) discusses the use and performance of silica fume concrete in bridges from the early 1984–87 placements to late 1991. He notes its use by nearly 30 state highway agencies, though frequency of use was certainly not the same among the agencies; for example, states such as Ohio and New York place many silica fume concrete overlays every year, while others were exploring the use of silica fume concrete on an experimental basis. An article also published in 1993 by Ozyildirim (*5*) discusses the increasing popularity of high-performance concretes containing silica fume for the production of concretes with low chloride ion diffusivities. Various types of mixes, containing a fairly wide range of silica fume contents and w/cm, have been employed for these applications. Silica fume contents have ranged from 5 to 12 percent (up to 15 percent in some experimental applications), and w/cm ratios have ranged from 0.3 to 0.4. As yet, however, there is no consensus on what constitutes an optimum silica fume concrete mix design for these applications. Luther stresses the care that must be taken with the placement of silica fume concrete overlays, especially with regard to the timing of finishing operations and the need for immediate application of moist curing and maintenance of a saturated environment for at least 3 to 7 days after placement using soaker hoses or other means. Similar cautions with regard to curing of silica fume concrete have been also given by others (*6, 7*). Manufacturers of silica fume admixtures have included detailed sets of such recommendations on proper finishing and curing techniques in their product literature. An excellent summary of information on properties and applications of silica fume is contained in an ACI Committee 234 document, "Guide for the Use of Silica Fume in Concrete" (*8*).

Concern with Use of Silica Fume in Bridge-Deck Applications

While it has been fairly well documented that silica fume concrete will provide a durable, low permeability concrete, one area which has received considerable attention is the apparent increased susceptibility of silica fume concrete to cracking, both in the plastic and hardened states. In the plastic state, the concrete has not yet hardened, its tensile strength is low, and shrinkage cracks can develop, especially at the surface where drying is greater. The risk is especially high in silica fume concretes as the fine particle size of the fume decreases bleeding rates and capacities of the concrete. Because of the lack of bleeding in silica fume concrete, water lost from the surface due to evaporation cannot be readily replaced. Precautions that should be taken include (1) strict adherence to specifications regarding evaporation rates and cessation of concrete placement if relative humidities are low and temperatures and wind speeds are high, (2) expediting finishing of concrete and use of fog sprays during finishing, (3) use of evaporation-retarding agents during and immediately after finishing, and (4) initiation of wet curing as soon as possible after finishing. Use of these techniques has, in general, reduced the incidence of plastic shrinkage cracking in silica fume concrete and allowed the successful placement of many hundreds of silica fume concrete overlays.

Unfortunately, plastic shrinkage is not the only mechanism that will cause cracking in concrete at early ages. A more subtle effect, termed "autogenous shrinkage," is present in all concretes but may be accentuated in silica fume concrete. As cement hydrates, a cement "gel" is formed. The volume of this gel is less than the sum of the volumes of its constituents (i.e., cement and water) because the water combined with the cement during hydration (the chemically bound water) has a lower specific volume than the specific volume of free water (*9*). This results in an overall shrinkage as the cement hydrates. In conventional concretes, this shrinkage is ultimately offset by the expansion produced when external water is drawn into the gel structure, causing swelling. However, in concretes prepared with low w/cm ratios, water will not be able to enter from the external environment because of the very low permeability of the gel. Thus, the only water present in the system is chemically and physically bound water, both of which have a lower specific volume than free water, resulting in an overall volume decrease (i.e., shrinkage). The situation is aggravated when silica fume is used because of the formation of an even finer cement gel having a lower specific volume and having a greater proclivity toward autogenous shrinkage. This has been confirmed in experiments carried out by Paillere et al. (*10*) and McDonald (*11*). However, in both of these studies, the silica fume dosage ranged from 15 to 20 percent, much higher than is generally used in bridge-deck applications. Recent work carried out under NCHRP Project 12-37 (*12*) using a restrained ring test similar to that used in the present research program (see Chapter 2) indicated that silica fume concretes cracked at an earlier age than conventional concrete. However, the number of specimens tested was limited and further work (carried out under Project 18-3) was warranted.

RESEARCH APPROACH

Design of Experiments

Based on examination of AASHTO and state bridge-deck specifications, two classes of concrete mixture were included in this laboratory study. These were (1) a "full-depth" mixture containing 368 kg/m^3 (620 lb/yd^3) of cementitious materials and 19-mm (¾-in.) maximum size coarse aggregate and (2) an "overlay" mixture containing 415 kg/m^3 (700 lb/yd^3) of cementitious materials and 9.5-mm (⅜-in.) maximum size coarse aggregate. For each mix design, separate test mixtures were prepared over a range of w/cm and silica fume contents. While the majority of batches used standard Type I/II portland cement and dry-densified silica fume, additional mixtures

were prepared with slurry-formulated silica fume as well as Type K shrinkage-compensating cement. The particular combinations studied were selected based on a statistically valid "central-composite" experimental design (see Appendix C). For both full-depth and overlay mixtures, the silica fume content ranged from none (control) to 12 percent by mass of cementitious materials. For full-depth mixtures, w/cm ranged from 0.35 to 0.45. For overlay mixtures, w/cm ranged from 0.30 to 0.40. Nine mixtures were prepared for each class of concrete. For each mixture, a total of three separate test batches were prepared. Batches were prepared in rounds such that no two replicate batches were prepared on the same day. Specimens for each test procedure were prepared following appropriate AASHTO or ASTM procedures. Specimens prepared from full-depth mixtures were moist cured for 7 days prior to initiation of testing. Specimens prepared from overlay concretes were moist cured for 3 days prior to start of testing.

Laboratory Testing

A laboratory test program was designed to obtain needed information on the characteristics of silica fume concretes directly relating to concerns with early age cracking, strength, chloride diffusivity, and other important properties. Brief descriptions of tests included in this program are given below:

- Drying shrinkage was measured on beam specimens after 4, 7, 14, and 28 days, and 8, 16, 44, and 64 weeks at a temperature of 23 ± 1.7 °C (73.4 ± 3 °F) and 50 ± 4 percent relative humidity.
- Cracking tendency was measured according to a restrained-ring method developed under NCHRP Project 12-37 and described in *NCHRP Report 380* (*12*). Testing was carried out in two distinct phases. In the first phase, testing was carried out across the complete range of mixtures and materials included in the experimental design. In the second phase, a full-factorial design was carried out on full-depth mixtures on a more restricted range of variables with increased replication of testing.
- Chloride ion ingress was measured using a modification of AASHTO T 259 (*13*) allowing for more precise determination of chloride profiles in concretes where low levels of chloride penetration are found. Concretes were exposed to chloride solution for 180 days, then sampled for chlorides at close increments from the surface. The resultant chloride profile was used to calculate chloride diffusivity coefficients for each mixture.
- For each mix, compressive strength was measured on moist-cured test cylinders at each of four test ages: 7, 28, 56, and 90 days. Modulus of elasticity in compression was measured on the same specimens at 28 and 90 days of age.
- Coefficient of thermal expansion was measured on air-dry test prisms after completion of drying shrinkage testing (64 weeks of drying).
- Bond strength of overlays to concrete substrates was measured after casting each overlay mixture onto a reinforced concrete base slab. Bond strength testing was carried out at 28 and 90 days of age.

Statistical Analysis and Modeling

For the analysis of the majority of the data generated under this research program, the central composite design was chosen to study the effects of silica fume content and w/cm on the various physical properties of the concrete mixtures. The central composite design is well suited to what is termed "response surface methodology." In this approach, a multivariate relationship between the independent variables and the response variable is developed from multiple regression analysis of the data. Response surface designs are most useful when the factors examined are known to be important, and interest centers on understanding the relationship of a property of interest to these factors and on optimizing the factors. After a satisfactory equation has been developed, results are displayed graphically using contour plots. As two variables (i.e., w/cm and silica fume content) were investigated, results were then displayed as contour plots. The response variable can be easily viewed as increasing (or decreasing) contours in the region of interest.

From these analyses, statistical models were constructed using response surface methodology. These models were intended to illustrate the significance of major variables (i.e., silica fume content and w/cm) and trends in physical properties of concrete with respect to the major variables studied. The models were not meant as predictors of actual values of physical properties to be expected for in-service concretes. Statistical analyses were carried out on drying shrinkage, restrained-ring cracking data, chloride diffusivity coefficients, compressive strength, and elastic moduli data. For data that were inconsistent or subject to wide variability, such as the initial restrained-ring cracking or overlay bond data, no formal statistical analyses were performed.

APPLICABILITY OF RESULTS TO HIGHWAY PRACTICE

The results of this investigation are immediately applicable to highway construction practice. The results indicate that acceptable performance of silica fume concretes can be obtained at moderate levels of silica fume content (6 to 8 percent) and that high levels of silica fume are neither necessary nor desirable. Moist curing of silica fume concretes is essential, with 7 days of continuous moist curing recommended. Provided that moderate levels of silica fume are used and adequate moist curing is applied, the tendency toward shrinkage and cracking of silica fume concrete is no greater than that of conventional mixtures in current use for casting of concrete bridge decks and overlays.

CHAPTER 2

FINDINGS

FINDINGS OF THE LABORATORY STUDY

In this chapter, the findings of the laboratory tests of full-depth and overlay silica fume concrete mixtures are presented. Major findings, with respect to drying shrinkage, cracking tendency, chloride diffusivity, compressive strength, modulus of elasticity, overlay bond strength, and coefficient of thermal expansion, are given. Detailed data and the analyses on which the findings are based can be found in Appendices B and C of this report.

DRYING SHRINKAGE

Drying shrinkage measurements were carried out on full-depth and overlay concrete mixtures. Drying shrinkage over time of these two types of mixtures is shown in Figure 1. Depicted are shrinkage versus age relationships for two "control" concrete mixtures (not containing silica fume) and two concrete mixtures with 6 percent silica fume by mass of cementitious materials. The w/cm represents the mid-point of the range used for each mixture. It is clear from this comparison (and by comparing other equivalent mixtures for the two types of concrete) that the overlay concretes exhibit higher shrinkage than corresponding concretes having the full-depth mix design. This is especially true at later ages. The higher shrinkage of the overlay mixes can be attributed to (1) higher paste content of these mixtures and (2) shorter moist curing time of the overlay mixtures (3 versus 7 days). Although the overlay mixtures were produced at lower w/cm ratios than the full-depth mixtures, the beneficial effects of lower w/cm on shrinkage were overcome by those factors previously noted. When data from the full-depth or overlay sets are examined independently, however, it becomes evident that a decrease in w/cm does have the beneficial effect of reducing shrinkage in most cases.

Multivariate regression analyses were carried out on drying shrinkage data and contour plots constructed to illustrate relationships between w/cm, silica fume content, and drying shrinkage. Contour plots for ultimate (64-week) shrinkage are shown in Figure 2 for the full-depth mixtures. There is the expected influence of w/cm on shrinkage; as w/cm increases, there is a corresponding increase in shrinkage. The increase is sharper (i.e., it takes less of a change in w/cm to produce a given change in shrinkage) as the silica fume content is increased. However, at a fixed w/cm, the changes in shrinkage are sensitive to change in silica fume content only at the extremes of w/cm used, primarily at the lower end. At the midpoint of w/cm for the full-depth mixtures, there is virtually no change in shrinkage as silica fume content is increased.

At early ages, a different behavior with respect to shrinkage is exhibited. There is much less sensitivity to changes in w/cm at lower silica fume contents. In contrast to the 64-week results, at only 4 days of drying, increases in silica fume content up to about 6 percent result in increases in drying shrinkage at all levels of w/cm, as is clearly seen from examination of Figure 3. As one proceeds along any horizontal level of w/cm, increasingly higher drying shrinkage contours are intercepted as silica fume content increases up to 6 percent. Trends were similar for overlay mixtures, although here the increase in drying shrinkage is proportional to the increase in silica fume content. There is a higher sensitivity of drying shrinkage to changes in silica fume content at early ages. At later ages, there is a greater sensitivity of drying shrinkage to changes in w/cm.

Comparisons were made between drying shrinkage of full-depth mixtures prepared with conventional Type I/II cement, and equivalent mixtures prepared with Type K (shrinkage-compensating) cement. Type K cement concretes exhibited higher levels of drying shrinkage. While this appears to be in conflict with the use of Type K cement as a "shrinkage-compensating" product, it should be noted that the major benefit of Type K cement is that its initial expansion induces compressive forces in the concrete member due to restraint by the reinforcement (*14*), so that these compressive forces must subsequently be overcome by drying shrinkage before crack-producing tensile forces can develop. Thus, Type K cement concrete can actually show a higher unrestrained drying shrinkage, and, because of the initial expansion, still function as intended.

Comparisons were also made between dry-densified and slurry forms of silica fume with respect to drying shrinkage behavior. No statistically significant differences were found.

CRACKING TENDENCY

Cracking tendency of concrete mixtures was evaluated using the restrained-ring test procedure described in *NCHRP*

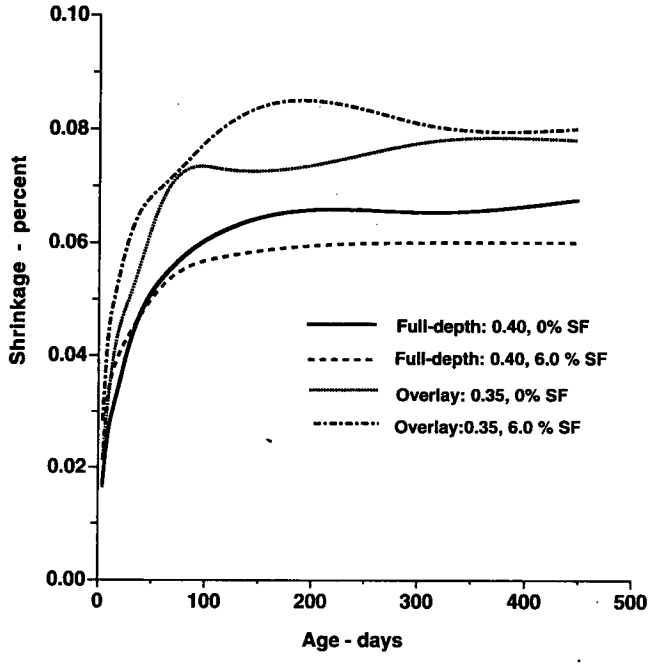

Figure 1. Comparison of shrinkage of selected full-depth and overlay concretes.

Report 380 (*12*). The test subjects a concrete specimen to drying shrinkage stresses while under restrained conditions. Details concerning test methodology are given in Appendix B. Good correlation between results of this technique and actual cracking of bridge decks under field conditions has been reported (*12*). In the first series of tests (Phase I), while all mixtures prepared under the test program were compared, the number of replicates was limited and statistical treatment of the data was restricted. However, Table 1 does compare the percentage of each type of mixture exhibiting cracking during the Phase I testing. It can be seen that overlay mixes exhibited the highest (100 percent) tendency toward cracking, followed by full-depth mixes (44 percent) and, finally, Type K cement concretes, which exhibited no cracking during the 90-day period of test. Results were not surprising, considering the higher shrinkage exhibited by the overlay mixtures, and the shrinkage-compensating characteristics of the Type K material.

Restrained-ring cracking tests consisted of a full-factorial examination of variables (w/cm, silica fume content, and curing time) for the full-depth mixtures only. Analysis of Variance (ANOVA) techniques were used to investigate significance of the variables with respect to time-to-cracking. The results are presented in Table 2a and 2b. Cure time was found to be extremely important with regards to age at cracking time. Specimens cured for 7 days, on the average, took significantly longer to crack than specimens cured for only 1 day. For specimens cured for only 1 day, the silica fume content had a significant effect. Specimens prepared with 6 and 9 percent silica fume cracked at significantly earlier ages than the control (no silica fume) specimens. For specimens cured for 7 days, the silica fume content had no effect on time-to-cracking. For both 1 and 7 days of curing, there was no statistically significant effect of w/cm on age at cracking. Again, these results substantiated the generally held belief that silica fume mixtures are more sensitive to curing practices than

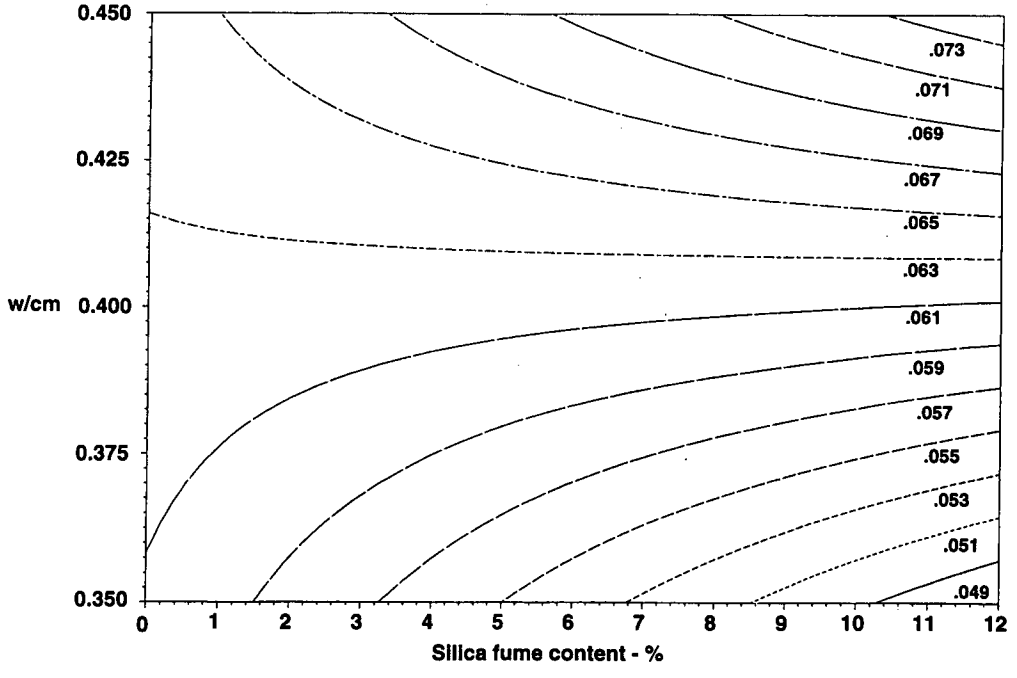

Figure 2. Contour plots for 64-week shrinkage of full-depth concrete mixtures.

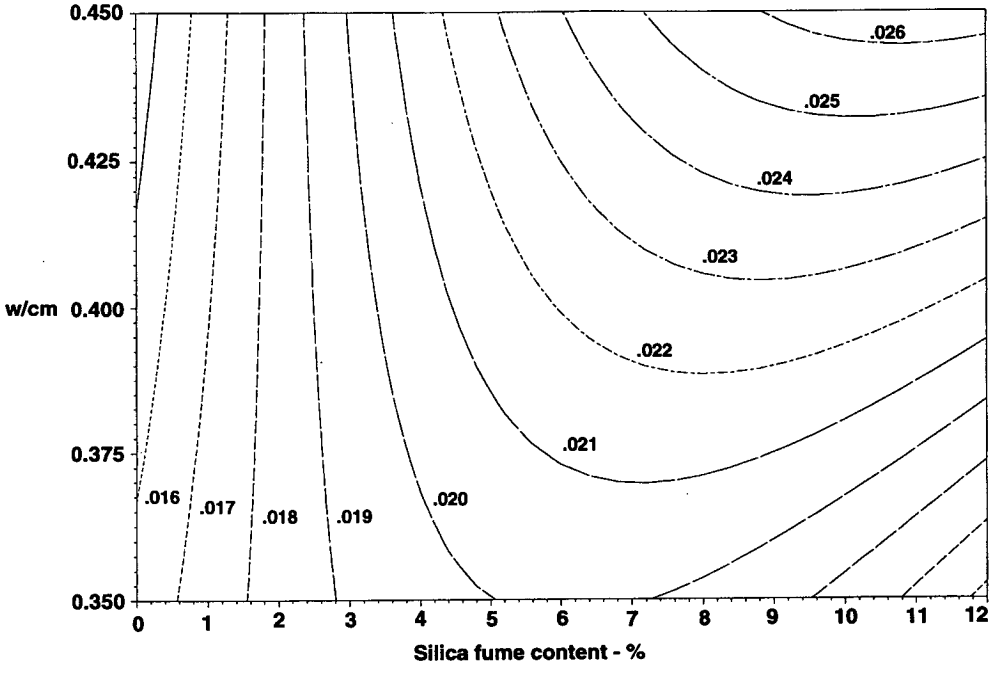

Figure 3. Contour plots for 4-day shrinkage of full-depth concrete mixtures.

conventional concretes, and extended moist curing is necessary to achieve the desired level of performance.

CHLORIDE DIFFUSIVITY

Chloride diffusivities were measured over a 180-day ponding period for all mixtures in the test program. Curing procedures are described in Appendix B. Ponding was done according to the procedure described in AASHTO T 259 Resistance of Concrete to Chloride Ion Penetration. However, the period of moist curing was shortened to 3 days for the overlay and slurry mixtures and 7 days for the full depth and Type K mixtures. At the end of the exposure period, 100-mm (4-in.) diameter cores were taken and milled in a lathe in 1-mm (0.04-in.) layers. Each layer was analyzed separately for acid soluble chloride ion in order to obtain a more detailed profile of chloride ion ingress. Further details of the experimental procedure can be found in Appendix B. Chloride profiles were constructed using a procedure in which 1-mm increments are milled off from a core taken from the test specimens and the resulting powder is chemically analyzed for total chloridation (*15*), and apparent diffusion coefficients obtained by a least-squares regression fit to Ficks's second law (*16*). It is recognized that the values obtained represent an average diffusivity taken over the period of ponding, as diffusivity will change as the concrete continues to hydrate. The numerical values obtained are shown in Tables B-14 through B-17. The apparent diffusion coefficients for the full-depth mixtures are shown in Figure 4. While there are differences between replicate rounds, the overall decrease in diffusivity as silica fume is added to the concrete is apparent. The same trends can be seen for the overlay mixtures (Figure 5). For all practical purposes, the particular type of mix (i.e., overlay or full-depth) has little effect on the apparent diffusion coefficient. The important factors are the silica fume content, and, to a lesser extent, the w/cm. This can be seen graphically in Figures 6 and 7, which show chloride profiles after 180 days of ponding. Figure 6 illustrates the effect of silica fume addition at a constant level of w/cm. The effect of silica fume is quite apparent; for instance, at 12 mm (0.5 in.) depth, the use of only 6 percent silica fume effectively stops penetration of chloride to this level, while control concrete exhibits relatively high amounts of chloride at the same depth. Figure 7 shows the effect of w/cm, which, as indicated, is not as strong. A more complete description of the methods used to analyze and interpret the data, as well as assumptions made and their limitations, is given in Appendix B.

TABLE 1 Percentage of specimens exhibiting cracking in Phase I cracking test program

Mixture Type	Percentage of Specimens Cracked
Full-Depth	44
Overlay	100
Type K (1)	0

(1) Full-depth mixes prepared using Type K cement.

TABLE 2a Time to first crack, days, for full-depth concretes cured for 1 day

	Silica Fume Content		
w/cm	0%	6%	9%
0.45	33	19	17
	36	14	18
	27	17	11
	27	13	16
	22	23	20
0.40	24	17	30
	26	12	17
	22	23	11
	24	18	22
	31	10	14
0.35	35	13	11
	43	12	23
	22	14	18
	24	28	28
	35	17	21

TABLE 2b Time to first crack, days, for full-depth concretes cured for 7 days

	Silica Fume Content		
w/cm	0%	6%	9%
0.45	33	25	30
	35	20	46
	38	19	28
	40	20	28
	33	16	31
0.40	36	49	51
	24	18	14
	34	25	34
	18	21	55
	50	56	52
0.35	53	29	67
	29	57	32
	32	17	53
	28	37	66
	32	64	30

Multivariate contour plots for full-depth mixtures are shown in Figure 8. For any given w/cm ratio, as silica fume is increased, the diffusivity drops. The most sensitive region is in the lower range of silica fume contents. Here the contour lines are "tighter" and diffusivity changes at a faster rate as small amounts of silica fume are added. At the midpoint of the range of w/cm used in this study, apparent diffusion coefficient drops from approximately 42×10^{-13} m^2/sec at zero percent silica fume content to 20×10^{-13} m^2/sec at 4 percent silica fume. At silica fume levels over 6 percent, it takes a much greater addition to effect a large change in diffusivity. Again, at a w/cm of 0.40, apparent diffusion coefficient decreases from 16×10^{-13} m^2/sec at 6 percent fume to 12×10^{-13} m^2/sec at 12 percent silica fume, a much smaller absolute decrease than seen for the initial addition of 4 percent silica fume. As silica fume is expensive, a point of diminishing returns may be reached as one adds silica fume over about 6 percent. In fact, at the lower w/cm values, diffusivity is relatively insensitive to addition of silica fume above the 6 percent level. From the contour plot, it can again be seen that the effect of w/cm is much less than that of silica fume content. The effect of w/cm is strongest at very low silica fume contents. For any fixed silica fume content, the effect of w/cm on diffusivity is more linear. That is, approximately the same change in diffusivity is found at all levels of w/cm. Again, however, at the lower silica fume contents, the contours are much tighter, a larger range of diffusivity being encompassed by the same range of w/cm. Over 5 percent silica fume content, there is only a small effect of w/cm on diffusivity. Contour plots for overlay mixtures (see Appendix C) followed similar trends with respect to w/cm and silica fume content.

Comparisons were made between dry-densified and slurry forms of silica fume, and between Type I/II and Type K concrete mixtures with respect to chloride diffusivity. No statistically significant differences were found in either case.

COMPRESSIVE STRENGTH

Compressive strengths were measured after 7, 28, 56, and 90 days of moist curing. Results for full-depth mixes are shown in Figure 9. Examination of these data indicates that highest strengths are achieved by reduction of the w/cm of the mix. The silica fume content, by itself, has less effect on

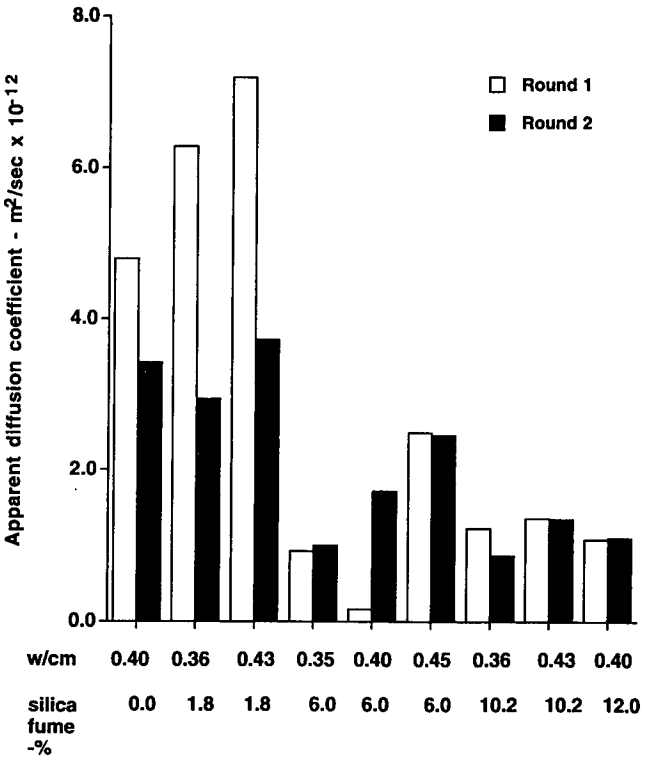

Figure 4. Apparent chloride diffusion coefficients of full-depth concrete mixtures.

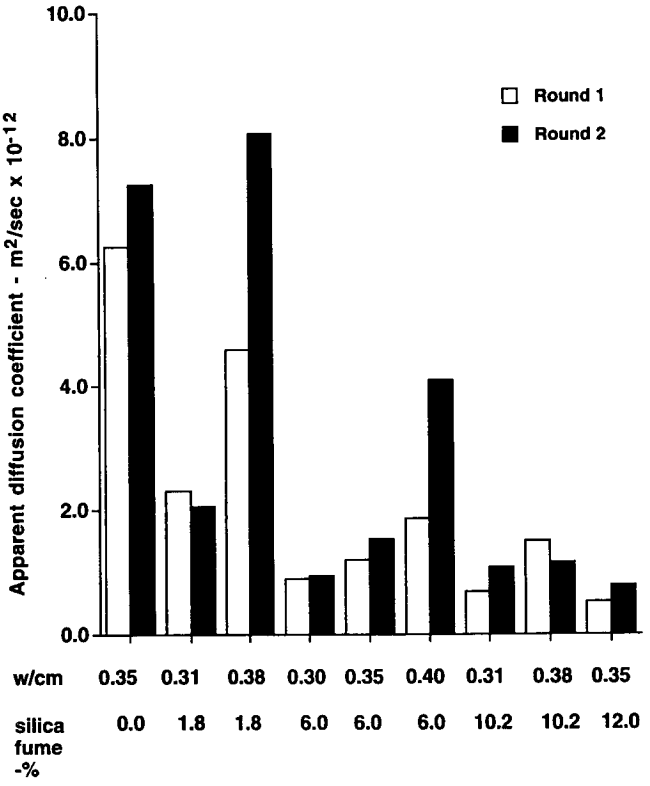

Figure 5. Apparent chloride diffusion coefficients of overlay concrete mixtures.

strength. This can be seen from examination of the data for the mixes at 0.40 w/cm and silica fume content of 0, 6, and 12 percent. While there is an increase of up to 10 MPa (1,450 psi) when increasing silica fume content from zero to 6 percent, there is much less of an increase, if any, when increasing silica fume content further from 6 to 12 percent. Highest strengths are obtained at the lowest w/cm. For all mixes, an increase in moist curing time results in an increase in strength, although in some cases increases are negligible between 56 and 90 days age. Data for overlay mixtures are presented in Figure 10. Here, there is a more linear increase in strength with silica fume content, although the highest strengths are still obtained at the lowest w/cm.

Results of multivariate regression modeling are shown in Figure 11 for the full-depth mixtures. At any given silica fume content, an increase in w/cm will result in progressively lower strengths. With respect to silica fume content, however, the relationship is less sensitive. In fact, at the midpoint w/cm (0.40), there is a plateau reached at about 42 to 43 MPa (6,100 to 6,200 psi), corresponding to approximately 6 to 8 percent silica fume; further increases in silica fume content have little effect on strength. Overlay mixtures (Figure 12) show somewhat similar trends. While there is no plateau with respect to silica fume content, the mixtures are less sensitive to changes in silica fume content than they are to changes in w/cm. Results for 90-day compressive strengths showed similar trends. It appears from all mixes

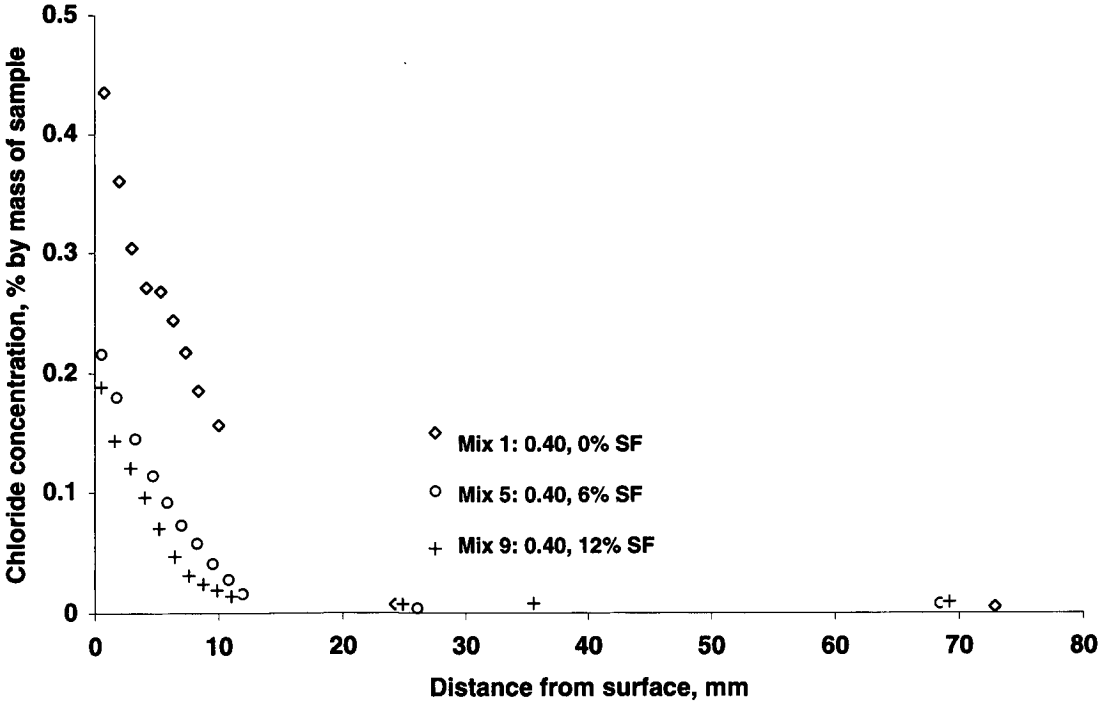

Figure 6. Acid-soluble chloride profiles for full-depth concretes: Mixes 1, 5, and 9.

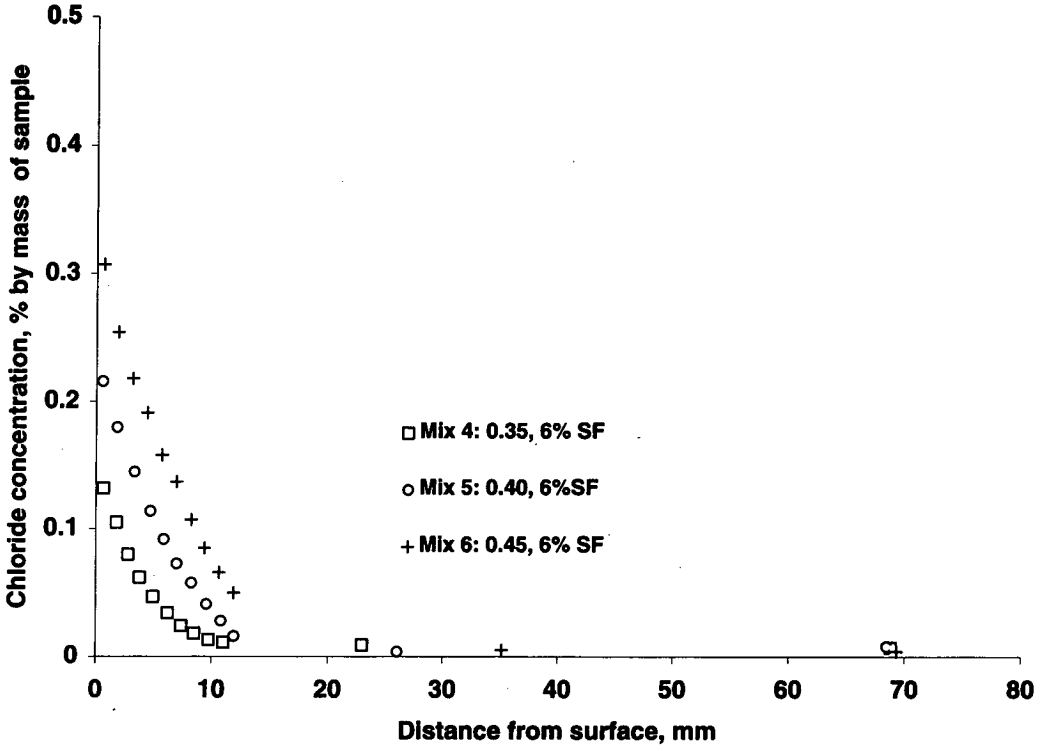

Figure 7. Acid-soluble chloride profiles for full-depth concretes: Mixes 4, 5, and 6.

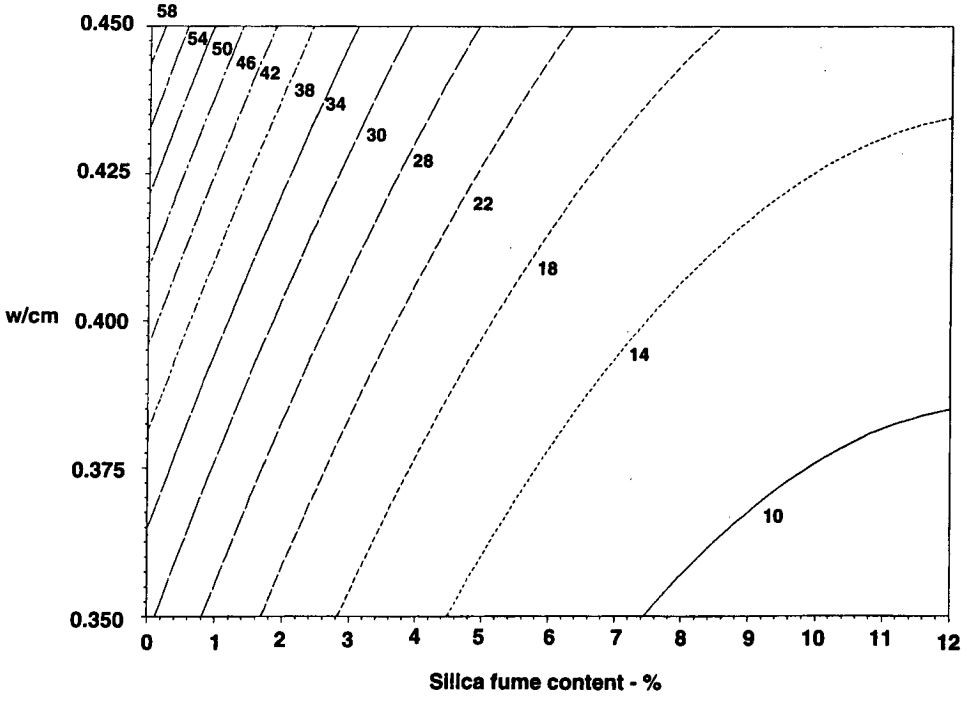

Figure 8. Contour plots for diffusivity coefficients of full-depth concrete mixtures.

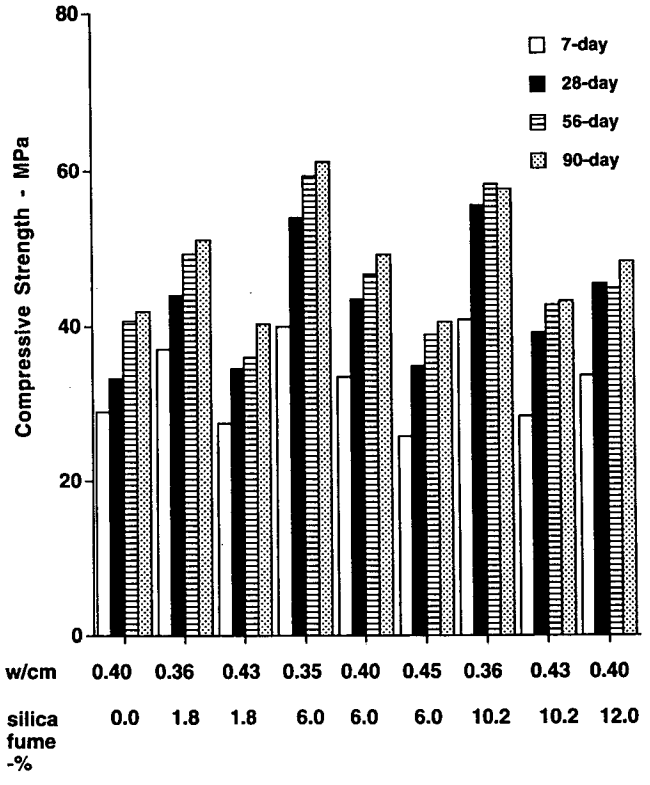

Figure 9. Compressive strength of full-depth concrete mixtures.

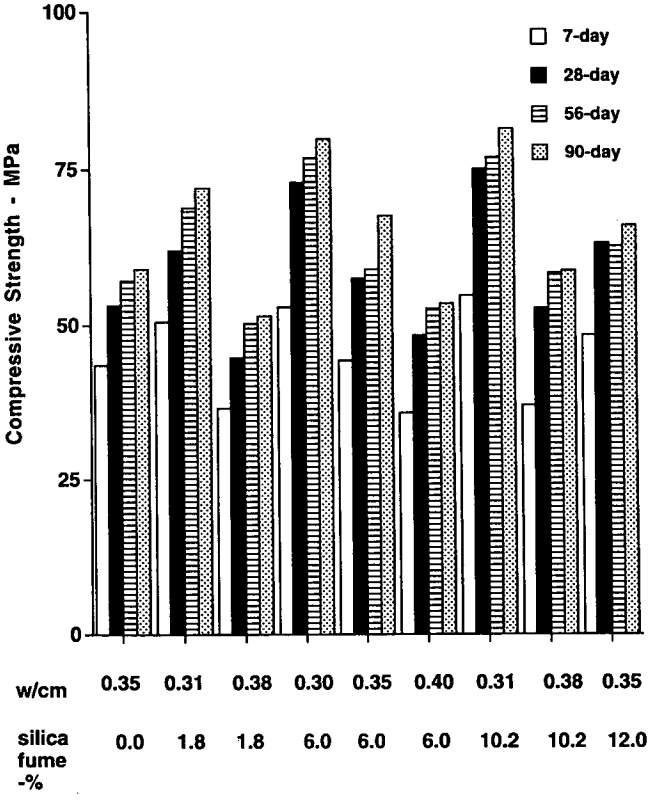

Figure 10. Compressive strength of overlay concrete mixtures.

tested that the optimum level of silica fume for reasonable increases in compressive strength is about 6 percent, similar to what was seen for chloride diffusivity.

Comparison analyses of Type I/II versus Type K cement concretes indicate that there is a statistically significant difference in strength, and that, on the average, an increase of about 5 MPa (725 psi) was obtained for the Type K mixtures over the corresponding Type I/II mixtures. There was no consistent difference in strength for dry-densified as opposed to slurry silica fume mixtures.

MODULUS OF ELASTICITY

Elastic moduli of full-depth mixtures measured at 28 and 90 days of age are shown in Figure 13. At either age, there is less spread in the data than for compressive strength. For example, at 28 days, the difference in strength between mixtures having the highest and lowest compressive strengths is 52 percent of the mean strength, while the range in modulus for the same set of mixtures is only 22 percent of the mean modulus. Similar behavior is seen for the overlay mixtures, as shown in Figure 14. Statistical modeling was carried out for elastic moduli data at 28 and 90 days of age, and there was an overall trend toward increasing elastic modulus as the amount of silica fume in the concrete was increased.

Comparison analyses were also carried out on elastic modulus for Type K versus Type I/II cement concretes and slurry versus densified forms of silica fume. No significant differences in elastic modulus were found between the two types of cement or two types of fume.

BOND STRENGTH

Bond strength of overlay concretes to concrete substrate was measured using a pull-off bond procedure (*17*). Testing details are described in Appendix B. Concretes were mixed and cast at elevated temperatures (35 °C[95 °F]) to simulate casting under severe hot-weather conditions, where problems with overlay placements are especially prevalent. Results of bond measurements, carried out at 28 and 90 days after overlayment, are shown in Figure 15. While the highest bond strengths appear to be associated, for the most part, with silica fume contents of 6 percent and above, the differences in many cases are small considering the inherent variability of the test procedure. Analysis of variance (ANOVA) carried out on these data indicated no significant differences between the mixtures at either 28 or 90 days of age. However, all test results exceeded the recommended minimum criteria (*18, 19*) for overlay bond strengths.

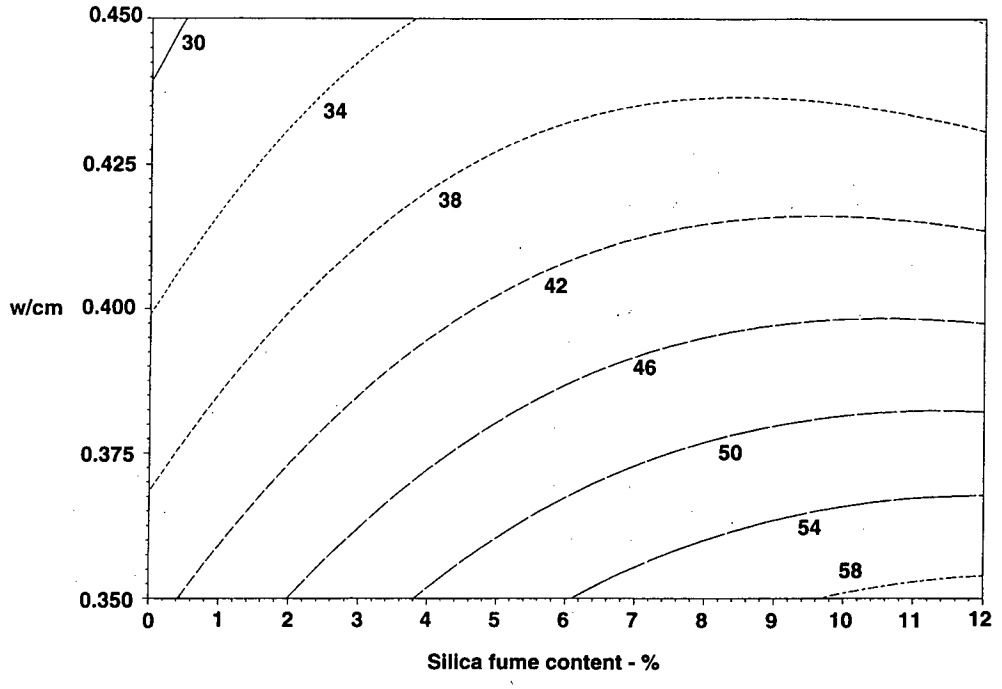

Figure 11. Contour plots for 28-day compressive strength of full-depth concrete mixtures.

COEFFICIENT OF THERMAL EXPANSION

Significant differences in coefficient of thermal expansion between repair and existing concretes, or between overlays and substrates, may induce stresses capable of causing bond failure or other distress. Results of measurements of coefficient of thermal expansion (CTE) on selected full-depth and overlay mixes are shown in Tables 3 and 4. Differences within the full-depth set (Table 3) are small. While results of tests on the overlay mixtures (Table 4) do show a decrease in

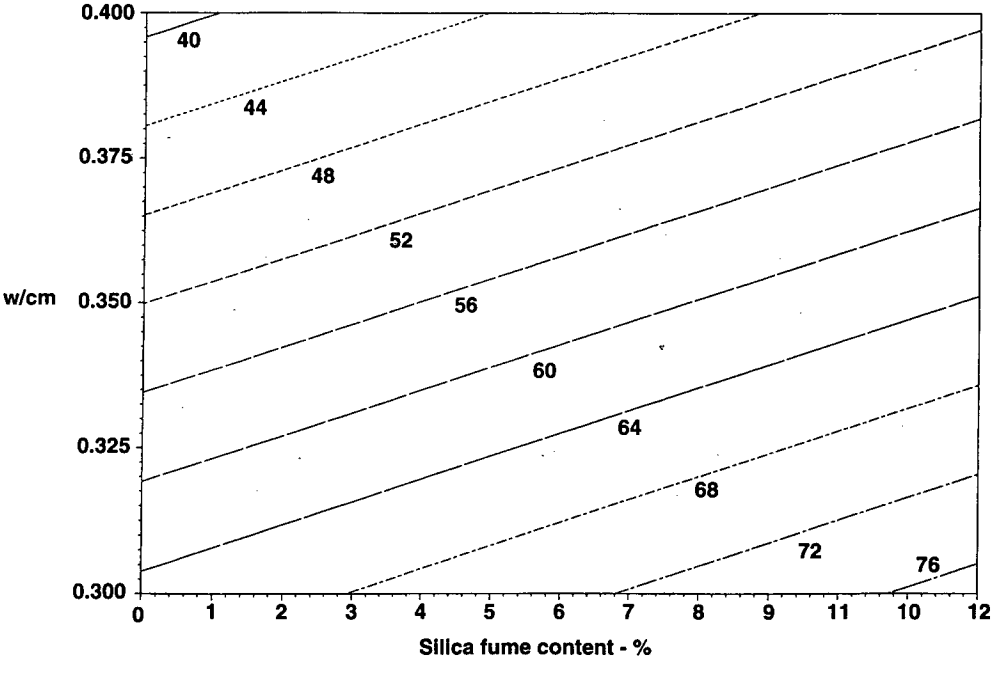

Figure 12. Contour plots for 28-day compressive strength of overlay concrete mixtures.

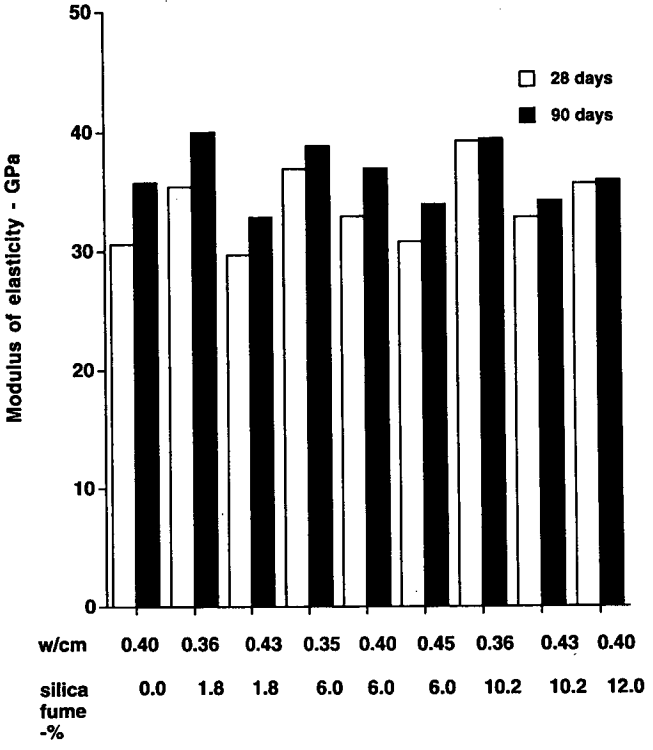

Figure 13. Elastic modulus of full-depth concrete mixtures.

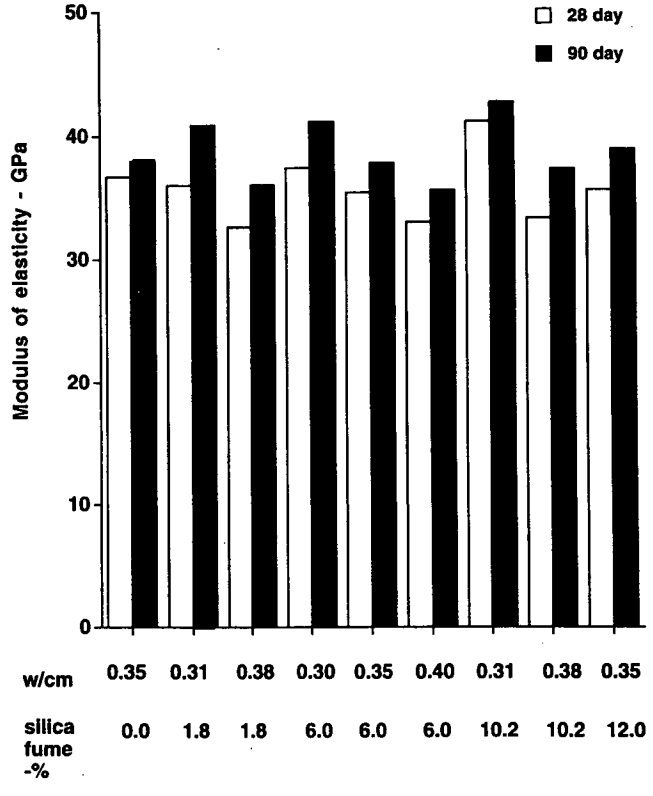

Figure 14. Elastic modulus of overlay concrete mixtures.

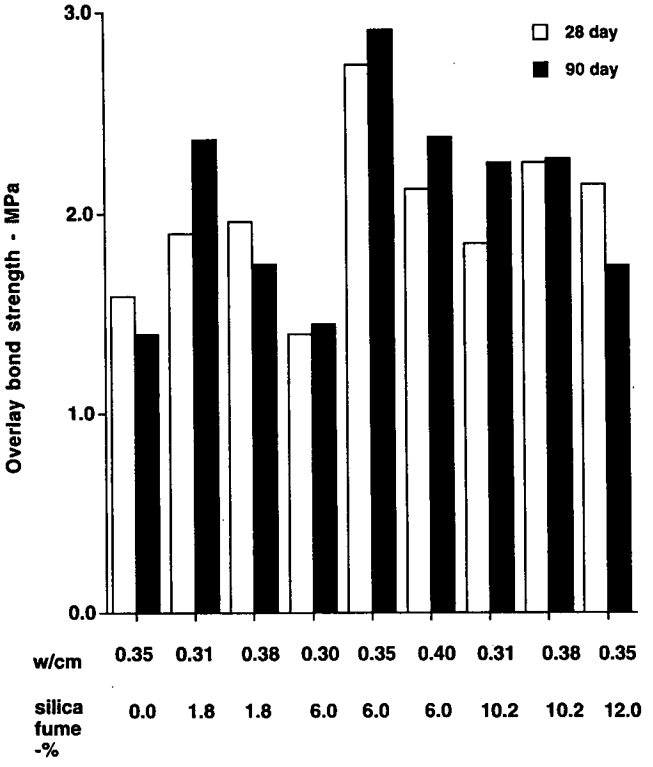

Figure 15. Bond strength of overlay concrete mixtures.

thermal expansion coefficient for the silica fume mixes, results are still within a narrow range as compared to expected variation of CTE for conventional concretes, which ranges *(20)* from 7 to 14 × 10^{-6}/°C (4 to 8 × 10^{-6}/°F), depending primarily on the particular type of aggregate used.

TABLE 3 Coefficient of thermal expansion (CTE) for full-depth mixtures

Specimen	% Silica Fume	w/cm	CTE, °C^{-1}
1FA	0	0.40	13.7E-06
4FA	6	0.35	14.0E-06
6FA	6	0.45	13.8E-06
9FA	12	0.40	13.3E-06

Note: °C^{-1} = 0.556 °F^{-1}

TABLE 4 Coefficient of thermal expansion (CTE) for overlay mixtures

Mix	% Silica Fume	w/cm	CTE, °C^{-1}
1O	0	0.35	13.9E-06
4O	6	0.30	13.3E-06
6O	6	0.40	13.0E-06
9O	12	0.35	13.1E-06

Note: °C^{-1} = 0.556 °F^{-1}

CHAPTER 3

INTERPRETATION, APPRAISAL, AND APPLICATION

INTERPRETATION

The results of this study indicate that there are no fundamental reasons why use of silica fume concrete in bridge-deck applications should not continue to grow as "high-performance concretes" become an increasingly important part of bridge construction. Use of silica fume concretes allows placement of materials with very low permeabilities and high strengths, which protect reinforcing steel from corrosion and lead to a longer lasting and more durable structure. Recent work (*21*) indicates that the properties of silica fume concretes can be further enhanced through combination with fly ash and other pozzolans. Work is continuing in these areas and further advances are to be expected.

One of the primary reasons for initiating this study was concern raised with respect to possible tendencies of silica fume concrete to exhibit higher shrinkage and cracking in bridge-deck applications. Multivariate models developed under this research study indicate that silica fume has little effect on long-term shrinkage of concrete. At early ages, however, shrinkage is affected by silica fume content, though at this point the absolute values of shrinkage are small. What is significant, however, is that shrinkage shows an increased sensitivity to changes in w/cm as the silica fume content is increased. This is especially important with regard to construction practice, as deliberate or inadvertent addition of water to the mixture will raise w/cm, and if this is done in mixtures containing high levels of silica fume, drying shrinkage may increase significantly.

The cracking tendency of mixtures evaluated under this study was found to be highly sensitive to the length of curing time. For concretes given only 1 day of moist curing, the amount of silica fume in the mix has a significant effect on cracking tendency. However, by curing concretes for 7 days or more, this effect is substantially reduced, and cracking is not related to the amount of silica fume used in the concrete. The amount of cement contained in the mix also influences cracking. Mixtures having high cement contents contain greater amounts of paste (the sum of cement and water), which is the component of concrete that undergoes shrinkage and leads to cracking. Concretes used for bridge-deck overlays have typically been designed with rather high cement contents and are susceptible to such problems. A lower shrinkage, less crack-prone overlay can be obtained by reducing the amount of cement and still maintaining specified performance characteristics. Use of Type K (shrinkage-compensating) cement may help to alleviate some of these problems, as no cracking was observed in any of the Type K concretes produced in this study.

To achieve optimum results, and avoid some of the aforementioned problems, the amount of silica fume used in the concrete should be limited. For many of the physical properties investigated in this study, little practical improvement was obtained by increasing content of silica fume above a range of 6 to 8 percent by mass of cementitious material in the concrete. Unless there is a specific reason for use of high levels of silica fume, a range of 6 to 8 percent should yield the desired levels of performance. Silica fume can be used in either dry-densified or wet slurry formulations; there is little significant difference in performance between the two forms of silica fume.

APPRAISAL

Shrinkage and Cracking Tendency of Silica Fume Concretes

At early ages, inadequate curing, high w/cm, and/or high cement factors can increase shrinkage up to 40 percent in silica fume concrete mixtures typical of those used for bridge-deck placement. Because cracking problems have recently been observed at early ages in the lives of decks, shrinkage may be the primary cause of the cracking in silica fume mixtures. Direct testing of cracking under restrained conditions, however, shows that silica fume concretes tend to crack only when they are insufficiently moist-cured. If silica-fume concrete mixtures are given 7 days of continuous moist curing, there is then no association between silica fume content and cracking. Therefore, agencies must ensure that this minimum recommended moist curing period is specified for all bridge-deck construction projects where silica fume concrete is to be used.

Use of shrinkage-compensating cement (Type K) will also help reduce the potential for cracking of silica fume concrete. However, this material is currently produced at only 1 location in the eastern United States, and availability may be limited in other areas.

Effect of Silica Fume on Other Properties of Concrete

The effects of silica fume on a variety of other properties of concrete were also investigated under this project. These included chloride diffusivity, compressive strength, modulus of elasticity, bond strength, and coefficient of thermal expansion. Common to most of the relationships between silica fume and physical properties was the existence of a point of "diminishing returns" beyond which little practical benefit is realized from increasing the amount of silica fume. This point appears to occur between 6 and 8 percent silica fume by mass of cementitious materials. For instance, replacing 6 percent of the cement with silica fume in a mixture having w/cm of 0.4 may reduce chloride diffusivity by a factor of 3, but adding an additional 4 percent (for a total of 10 percent silica fume) increases the factor to only 3.5. Thus, almost 70 percent more silica fume is needed to reduce the diffusivity an additional 15 percent. Similar trends are seen with respect to compressive strength; here the w/cm of the mix has more of an influence than does silica fume content. At constant w/cm, use of 6 percent silica fume can increase strength almost 25 percent over mixtures with no silica fume. Using 8 percent silica fume or more adds little more to strength for the particular mixtures included in this study. Silica fume also affects elastic modulus. The effect is more pronounced at earlier ages (28 days) as opposed to later ages and reflects the beneficial effects of silica fume on densification of the paste/aggregate transition zone. The percentage increase is much less than for compressive strength; therefore it is unlikely that the relatively small increases in elastic modulus would contribute to increased brittleness in silica fume as opposed to conventional concrete for the particular mixtures investigated in this study. Silica fume had little discernible effect on the strength of bond to underlying concrete, although scatter in test results may have obscured any real trends. Finally, the data obtained from this study suggest that there is little, if any, effect of silica fume on coefficient of thermal expansion, this property being controlled mainly by aggregate type and content.

APPLICATION

Guidelines for Field Use of Silica Fume Concrete

As this study was confined to laboratory measurements, no direct investigation of field practices was undertaken. However, the strong influence of moist-curing time on tendency to cracking of silica fume concretes requires agencies and contractors to pay very close attention to curing practices when using these materials for bridge-deck placement. Curing should be initiated as soon as practicable. Often, this requires that burlap matting be prewetted and ready to place on the newly finished concrete surface as soon as placement, consolidation, and finishing of concrete are complete. The time between initial exposure of the finished concrete to the environment and the application of soaked burlap must be minimized. The burlap should then be covered with plastic sheeting to prevent evaporation of the curing water. If at all possible, additional curing water should be applied through soaker hoses running under the protective plastic sheeting so that the burlap is kept continuously wetted throughout the period of cure. A minimum cure time of 7 days is recommended on the basis of the results of this investigation. Though not included in this study, supplemental membrane curing after termination of the moist curing would also be beneficial, a practice which has been adopted by a number of agencies.

Recommended Changes to Specifications

As noted, in specifications for silica fume concrete to be used for bridge-deck placements it is recommended that a minimum of 7 days continuous moist curing be specified. Thus, special provisions for silica fume concrete placement should include reference to Section 8.11 "Curing Concrete" of the AASHTO *Standard Specifications for Highway Bridges* (22), and specify that silica fume concrete shall be cured in accordance with Section 8.11.3.2 "Water Method" for a minimum of 7 days. If possible, this should be followed by a membrane cure in accordance with Section 8.11.3.3. Section 8.11.4 "Bridge Decks" should be modified when silica fume concrete is placed so that the water cure is applied immediately after finishing is complete and maintained for 7 days, and the membrane is then applied immediately after the water cure is completed. Additionally, consideration should be given to limitation of silica fume contents to a range of 6 to no more than 8 percent by mass of cementitious materials. This limitation would need to be included in special provisions for each silica fume concrete placement, the exact proportions being selected with consideration of the characteristics of local materials. While results of this study do not indicate that amounts in excess of this range are harmful, they do not appear to be cost-effective for the particular applications for which silica fume concrete is currently employed by highway agencies.

CHAPTER 4

CONCLUSIONS AND SUGGESTED RESEARCH

CONCLUSIONS

On the basis of the work carried out under this project, the following conclusions can be stated:

1. Cracking tendency of concrete is influenced by the addition of silica fume only when the concrete is improperly cured. When concrete is cured for 7 days under continuously moist conditions, there is no statistically significant effect of silica fume on the tendency of the concrete to exhibit early-age cracking. It is recommended that specifications for silica fume concretes in bridge-deck construction include a provision for 7-day continuous moist curing of exposed surfaces.
2. Silica fume has little effect on the ultimate (long-term) shrinkage of concrete; that is, concretes containing silica fume do not shrink more than otherwise identical concretes without silica fume. At early ages, however, silica fume concrete mixes show somewhat higher shrinkages then their conventional counterparts. Concrete containing silica fume is more sensitive to changes in water-to-cementitious materials ratio (w/cm) than conventional concrete in terms of the shrinkage which develops at early ages.
3. Use of silica fume results in dramatic reductions in chloride diffusivity. Chloride diffusivity may be reduced by a factor of three or more over conventional concretes not containing silica fume. Most of the reduction occurs as silica fume content is increased from 0 to the 6 to 8 percent range. Further addition of silica fume provides little additional benefit.
4. Use of silica fume can also increase compressive strength at constant w/cm. Strength increases up to 25 percent can be obtained with 6 percent silica fume. As with chloride diffusivity, there is little benefit to be gained in use of silica fume contents over about 8 percent.
5. In general, an increased level of silica fume will result in a higher elastic modulus, as would be expected from the increase in compressive strength. The effect is more pronounced at 28 days of age than at later ages.

SUGGESTED RESEARCH

The present study was confined to laboratory preparation of concrete mixtures and determination of physical properties of the resultant concretes. As all concretes were prepared under controlled conditions, the effects of construction variables could not be included. While it would not be practicable to include the entire set of laboratory concretes in a field study, it would certainly be possible to include selected mixes in a controlled field study where test sections could be monitored over an extended time period. An outline of such a study is included as Appendix D of this report.

Another area in which further research is warranted are the blends of silica fume with other pozzolans, such as fly ash, ground-granulated blast furnace slag, and other forms of silica such as metakaolin. Such concretes are often referred to as "ternary" mixtures. More information is needed on optimal blend proportions, and total amounts of the blended material to be used in concretes for highway applications. The effects of such materials on the properties included in the current research program should be studied in any future research effort.

REFERENCES

1. Malhotra, V.M., Ramachandran, V.S., Feldman, R.F., and Aitcin, P.C., "Specific Surface Area," *Condensed Silica Fume in Concrete*, CRC Press, Boca Raton, FL (1987), pp. 13–15.
2. Bernhardt, C.J., "SiO_2 Dust As an Admixture to Cement," *Betongen Idag*, Vol. 17, No. 2 (1952), pp. 29–33.
3. Bunke, D., "ODOT Experience with Silica-Fume Concrete," *Transportation Research Record 1204*, Transportation Research Board, Washington, DC (1988), pp. 27–35.
4. Luther, M.D., "Silica Fume (Microsilica) Concrete in Bridges," *Concrete International*, Vol. 15, No. 4 (April 1993), pp. 29–33.
5. Ozyildirim, C., "High Performance Concrete for Transportation Structures," *Concrete International*, Vol 15, No. 1 (January 1993), pp. 33–38.
6. Holland, T.C., "Practical Considerations for Using Silica Fume in Concrete," *Transportation Research Record 1204* , Transportation Research Board, Washington, DC (1988), pp. 8–10.
7. Weil, T.G., "Addressing Parking Garage Corrosion with Silica Fume," *Transportation Research Record 1204*, Transportation Research Board, Washington, DC (1988), pp. 27–35.
8. American Concrete Institute, "Guide for the Use of Silica Fume in Concrete," ACI 234R-96, Farmington Hills, MI (1996), 51 pp.
9. Powers, T.C., and Brownyard, T.L., "Studies of the Physical Properties of Hardened Portland Cement Paste—Part 5. Studies of the Hardened Paste by Means of Specific-Volume Measurements," *Proceedings of the American Concrete Institute*, Vol. 43 (1947), pp. 669–712.
10. Paillere, A.M., Buil, M., and Serrano, J.J., "Effect of Fiber Addition on the Autogeneous Shrinkage of Silica Fume Concrete," *ACI Materials Journal*, Vol. 86, No. 2 (March–April 1989), pp. 139–144.
11. McDonald, J.E., "Properties of Silica Fume Concrete," US Army Waterways Experiment Station Technical Report REMR-CS-32, Vicksburg, MS (1991), 43 pp.
12. Krauss, P.D., and Rogalla, E.A., "Transverse Cracking in Newly Constructed Bridge Decks," *NCHRP Report 380*, Transportation Research Board, Washington, DC (1996), 126 pp.
13. *AASHTO Standard Specifications—Part II Tests*, "Standard Method of Test for Resistance of Concrete to Chloride Ion Penetration," American Association of State Highway and Transportation Officials, Washington, DC (1995), pp. 648–649.
14. American Concrete Institute, "Standard Practice for the Use of Shrinkage-Compensating Concrete," ACI 223–93, ACI Manual of Concrete Practice—Part 2, American Concrete Institute, Farmington Hills, MI (1996).
15. Detwiler, R.J., Kojundic, T., and Fidjestøl, P., "Evaluation of Staunton, Illinois, Bridge Deck Overlays," *Concrete International*, Vol. 19, No. 8 (August 1997), pp. 43–45.
16. Crank, J., *The Mathematics of Diffusion*, 2nd. ed., Clarendon Press, Oxford, England (1975).
17. American Concrete Institute, "Use of Epoxy Compounds with Concrete (Appendix A—Test Methods)," ACI 503R-93, ACI Manual of Concrete Practice—Part 5, American Concrete Institute, Farmington Hills, MI (1996).
18. Whiting, D., Nagi, M., Okamoto, P., Yu, T., Peshkin, D., Smith, K., Darter, M., Clifton, J., and Kaetzel, L., *Optimization of Highway Concrete Technology*, Report No. SHRP-C-373, Strategic Highway Research Program, Washington, DC (1994).
19. Knab, L.I., Sprinkel, M.M., and Lane, O.J. Jr., *Preliminary Performance Criteria for the Bond of Portland-Cement and Latex-Modified Concrete Overlays*, NISTIR 89-4156, US Department of Commerce, Gaithersburg, MD (1989).
20. Neville, A.M., *Properties of Concrete*, 2nd. ed., Pitman Publishing, New York, NY (1975).
21. Streeter, D.A., "Developing High Performance Concrete Mix for New York State Bridge Decks," *Transportation Research Record 1532, Transportation Research Board, Washington, DC* (1996), pp. 60–65.
22. *AASHTO Standard Specifications for Highway Bridges—Fifteenth Edition*, American Association of State Highway and Transportation Officials, Washington, DC (1992), pp. 492–494.
23. Pettersson, K., *The Effect of Different Factors on Chloride Diffusion in Concrete Structures* [In Swedish], CBI Report 4:94, Cement och Betong Institutet, Stockholm, Sweden (1994), 37 pp.
24. Whiting, D., Nagi, M., and Broomfield, J.P., *Evaluations of Sacrificial Anodes for Cathodic Protection of Reinforced Concrete Bridge Decks*, Report No. FHWA-RD-95-041, Federal Highway Administration, Washington, DC (1995), 110 pp.
25. *Handbook for Cement and Concrete, Vol. I*, CRD- C 39-81 "Test Method for Coefficient of Linear Thermal Expansion of Concrete," US Army Engineer Waterways Experiment Station, Vicksburg, MS (August 1949 with quarterly supplements).
26. Hunter, W.G., Hunter, J.J., and Box, G.E.P., *Statistics for Experimenters*, Wiley & Sons, New York, NY (1978).
27. Neter, J., Wasserman, W., and Kutner, M.H., *Applied Linear Statistical Models*, Irwin Publications, Boston, MA (1990).

APPENDIX A

CONCRETE BATCH MATERIALS, PROPORTIONS, AND PREPARATION

MATERIALS

Cement

Three lots of cement were used in the research program. Cement A, a Type I/II portland cement, was used to prepare all specimens in Phase I of the program. Cement B was approximately a 65:35 blend of the remainder of the stock of Cement A and a new supply of the same type of cement obtained from the same mill as Cement A approximately one year later. Cement B was used to prepare all specimens in Phase II of the program. Cement C was a shrinkage compensating Type K cement. All cements were obtained in 42 kg (94 lb) plastic-lined bags and all bags in a given shipment were thoroughly blended to obtain a uniform test lot of cement. The chemical compositions and physical properties of the cements are given in Table A-1.

Silica Fume

The majority of the work in Phase I and all work in Phase II was carried out using a densified silica fume supplied in 23 kg (50 lb) bags. The chemical composition and physical characteristics are given in Table A-2. For a portion of the work in Phase I, a slurry (55 percent solids) of the same silica fume was obtained in 19 L (5 gal) pails.

Aggregates

A highly siliceous, rounded river gravel was used as the coarse aggregate in all mixes. Material was received in separate size fractions and recombined to produce the desired gradation. Gradations having maximum sizes of 19 mm (0.75 in) and 9.5 mm (0.375 in) were used to produce the "full-depth" and "overlay" mixtures, respectively. Natural sand from the same source was used as fine aggregate in the as-received gradation. The gradations and physical characteristics of the aggregates are given in Table A-3. All aggregates were available from the supplier in bags as clean, washed materials.

Admixtures

An air-entraining agent based on neutralized Vinsol® resin with a solids content of 8 percent was used in all mixtures. A high-range water reducer, based on the sodium salt of the sulfonated condensation product of naphthalene-formaldehyde with a solids content of 40 percent, was used in all silica fume mixtures.

PROPORTIONING, MIXING, AND SPECIMEN PREPARATION

Mixture Proportions

As silica fume has been used for the construction of both full-depth bridge decks and relatively thin (less than 50 mm [2 in]) concrete deck overlays, two separate mixtures were developed for this research program. Current AASHTO specifications *(22)* indicate that a minimum cement content of 363 kg/m^3 (611 lb/yd^3) is recommended for the Class AE concretes typically used for bridge decks. In order to be consistent with current practice and AASHTO specifications, a cementitious materials content of approximately 368 kg/m^3 (620 lb/yd^3) was selected as a target for the full-depth mixtures. This includes both the hydraulic cement content and the silica fume. For the overlay mixtures, inspection of special overlay provisions of a number of highway agencies indicated that cement contents used in overlays differed among agencies. Comparative studies carried out for SHRP *(18)* utilized a cementitious content of 415 kg/m^3 (700 lb/yd^3) in silica fume bridge deck overlays. As bridge deck overlay concretes have traditionally employed relatively high cement contents, a cementitious materials content of 415 kg/m^3 (700 lb/yd^3) was selected.

With cementitious materials contents selected, the water-to-cementitious materials ratio (w/cm) was varied over the ranges associated with typical practice, 0.35 to 0.45 for full-depth mixtures and 0.30 to 0.40 for overlay mixtures. Silica fume content (percent by mass of the total cementitious materials content) varied from 0 to 12 percent in Phase I of the study and 0 to 9 percent in Phase II (extension of the cracking tendency testing). The silica fume contents and w/cms used in the actual test batches were determined by the central composite design for the experiment (see Appendix C).

The actual mixture proportions and properties of the fresh concretes for Phase I of the study are given in Tables A-4 and A-5 for the full-depth and overlay mixtures, respectively. In addition, Tables A-6 and A-7 give the proportions and properties of the mixtures prepared using the slurry form of silica fume and Type K shrinkage-compensating cement, respectively. Tables A-4 through

A-7 show the mean value of each characteristic for the three rounds of concrete prepared for each mixture.

For Phase II of the study only full-depth mixtures were prepared, as the intent of this additional work was to investigate the tendency towards cracking of mixtures typically used in full-depth bridge deck placement. The actual mixture proportions and properties (means of 5 separate rounds of concrete) of these concretes are given in Table A-8. The silica fume contents and w/cms were based on a full factorial experimental design using three silica fume contents and three levels of w/cm.

A final set of mixtures was prepared for placement on reinforced concrete base slabs, and subsequent determination of tensile bond strengths through "pull-off" testing. These duplicated the mixture proportions used for the nine original overlay mixtures. The actual batch proportions and characteristics of fresh concrete are shown in Table A-9. A description of the specimen preparation and testing for this series is included in Appendix B.

Batching and Mixing

Coarse aggregate was weighed into batching containers to the desired gradation and inundated with potable water 18 to 24 hours before mixing. Immediately before mixing, a measured amount of water was drained from each container such that the water remaining would satisfy the absorption of the coarse aggregate plus the net amount of water required for the batch. The portion of the remaining water not absorbed into the aggregate was then drained into a separate container and added during the mixing process. Fine aggregate was placed into a laboratory mixer and sufficient water added to bring its moisture content into the range of 1.5 to 2.5 percent (slightly above SSD condition for the aggregate used). This supply of fine aggregate was then stored in a sealed container until just prior to mixing. Moisture content was determined by oven during and used to correct the SSD batch quantities and added batch water.

All mixing was carried out in a 0.06 m^3 (2.0 ft^3) counter-current pan mixer. Coarse aggregate, sand, and approximately 50 percent of the mix water were added first to the mixer, the mixer started, and the silica fume then added to the revolving mix of aggregates to ensure uniform distribution in the batch. The cement and HRWR were then added along with the remainder of the mix water, and mixing was continued until a uniform consistency was observed. The air-entraining agent was then added and mixing continued for exactly 3 minutes. The batch was then allowed to rest for 3 minutes, followed by a final 2 minutes of mixing. In most cases, a second

increment of HRWR was added during this final mixing period to bring the slump into the desired range (over 75 mm [3 in]) and to allow the mix to remain workable during preparation of test specimens.

Specimen Preparation and Curing

After concrete mixing was complete, tests for slump (AASHTO T 119), air content (AASHTO T 152), and unit weight (AASHTO T 121) were carried out on the fresh concrete. All unit weight measurements were made using a 0.014 m^3 (0.5 ft^3) container. Concrete was accepted for specimen preparation if the measured slump was equal to or greater than 75 mm (3 in), and the air content was within the range of 6 ± 1.5 percent for mixes containing 19 mm (0.75 in) maximum size coarse aggregate and 7.5 ± 1.5 percent for mixes containing 9.5 mm (0.375 in) maximum size coarse aggregate. Test specimens were prepared following AASHTO T 126 procedures. With the exception of additional external vibration used on cracking tendency test specimens, all specimens were consolidated by rodding. Exposed surfaces were finished with a magnesium trowel and covered with wet burlap and polyethylene sheeting to prevent evaporation of water from the concrete during the first 18-24 hours after casting. The specimens were then demolded and placed in the appropriate curing environment. This was either a moist room maintained at 23 ± 1.7 °C (73.4 ± 3°F), or a tank of lime-saturated water maintained at the same temperature, depending on the particular test to be carried out (see Appendix B for details of curing specific to the individual test procedures).

Workability and Finishability

The workability and finishing characteristics of concrete are best evaluated at the jobsite on full-scale production mixes. However, as a large number of specimens was being prepared under this test program, some preliminary observations could be made regarding the ease with which the concrete could be worked and its action under the use of hand-held trowels. It is recognized that such characteristics may be different during actual bridge deck placements where mechanical vibration is used to consolidate the concrete and where a large part of the finishing is done by machine. The observations are shown in Table A-10. Qualitative assessments were made by ACI-certified field technicians. As might be expected when dealing with mixtures having relatively high cementitious materials contents and low w/cm, a number of the mixes exhibited less than desirable workability as well as problems with finishing. It should be noted that "workability" in this instance refers primarily to the ability of the technician to consolidate the mix by hand. In those cases (mixes 2F and 3F) where "needs vibration" was noted in Table A-10, the mixes would most

likely have consolidated with no additional effort if internal vibration were used (this was impractical with the small size of the molds used to prepare laboratory specimens). Mixes denoted as "stiff" or "stiffening" lost slump relatively quickly and therefore were somewhat more difficult to consolidate into the molds. Many of the mixes were sticky and caused the trowel to "drag" across the surface of the concrete. In three cases (mix 3O, 7O and 9S) this resulted in tearing of the surface under the trowel. Again, it is not clear if such problems would occur under actual field placement conditions where mechanical finishing equipment is primarily used. As such problems have been noted with regard to finishing of silica fume concretes *(4)*, the minimum amount of finishing effort needed to adequately close the concrete surface should be employed.

Table A-1a. Chemical compositions of cements.

Chemical Analysis	Value Percent		
	Cement A Type I/II	Cement B Type I/II	Cement C Type K
Silicon dioxide (SiO_2)	21.00	20.93	18.60
Aluminum oxide, (Al_2O_3)	4.06	4.40	5.41
Ferric oxide (Fe_2O_3)	3.25	2.94	2.31
Calcium oxide (CaO)	63.52	63.36	61.29
Magnesium oxide (MgO)	2.28	2.66	3.92
Sulfur trioxide (SO_3)	2.66	2.62	5.97
Loss on ignition	1.58	1.35	2.20
Insoluble residue	0.20	0.28	0.35
Tricalcium silicate (C_3S)	57	55	
Dicalcium silicate (C_2S)	18	19	
Tricalcium aluminate (C_3A)	6	8	
Tetracalcium aluminoferrite (C_4AF)	10	9	
Alkalies (Na_2O equivalent)	0.43	0.53	0.65

1MPa = 145 lbf/in^2

Table A-1b. Physical properties of cements

Physical Properties	Value		
	Cement A Type I/II	Cement B Type I/II	Cement C Type K
Specific Surface, Blaine, m^2/kg	391	365	453
Soundness, autoclave expansion, %	0.00	0.02	111
Time of setting: Vicat, min	178	172	103
1 day Compressive strength, MPa	MPa		
1 day	13.2	12.3	14.8
3 day	27.0	25.2	28.5
7 day	31.0	29.5	31.9
28 day	41.0	40.1	37.6
Air content: percent by volume	7.9	9.0	10.8
Specific gravity	3.15	3.15	3.08

1MPa = 145 lbf/in^2

Table A-2. Chemical composition and physical properties of silica fume.

Chemical Analysis	Value Percent	Physical Properties	Value
Silicon dioxide (SiO_2)	95.74	Surface area, m^2/kg	23,710
Aluminum oxide, (Al_2O_3)	0.39	Density, Mg/m^3	2.12
Ferric oxide (Fe_2O_3)	0.13	% Retained, 45 µm sieve	0.9
Calcium oxide (CaO)	0.29		
Magnesium oxide (MgO)	0.30		
Loss on ignition	2.53		
Alkalies (Na_2O equivalent)	0.38		

Table A-3. Gradations and characteristics of aggregates.

FINE AGGREGATE

Mixes	Grading, % Retained on Sieve Size Indicated					
	4.75 mm	2.36 mm	1.18 mm	600 µm	300 µm	150 µm
All	3	14	28	54	86	98

Fineness Modulus	Bulk Specific Gravity, SSD	Absorption, % by Mass
2.82	2.64	0.52

COARSE AGGREGATE

	Grading, % Retained on Sieve Size Indicated				Bulk Specific Gravity, SSD	Absorption % by Mass
	19 mm	9.5 mm	4.75 mm	2.36 mm		
Full-Depth	0	60	100	100	2.68	1.22
Overlay	0	0	80	100	2.68	1.38

Table A-4. Mixture proportions and properties for full-depth mixtures (1).

Material		Quantities (kg/m^3)								
(SSD Basis)	% fume	0	1.8		6.0			10.2		12
	w/cm	0.40	0.36	0.43	0.35	0.40	0.45	0.36	0.43	0.40
Mix Designation		1F	2F	3F	4F	5F	6F	7F	8F	9F
Cement		369	364	360	343	342	341	331	328	321
Silica Fume		0	7	7	22	22	21	37	37	44
Fine Agg.		733	751	716	743	722	699	742	708	720
Coarse Agg.		1071	1097	1046	1085	1055	1020	1084	1034	1052
Water		148	133	158	128	146	163	132	157	146
HRWR-mL/kg		4.3	8.7	3.0	12.6	9.8	7.3	15.7	9.4	13.8
AEA-mL/kg		1.9	2.0	2.0	3.7	3.4	3.2	3.9	3.9	5.0
Properties										
Slump - mm		104	124	114	112	127	142	109	107	117
Air Content - %		5.7	5.4	6.4	6.6	6.8	7.3	5.9	6.8	6.7
Unit Weight- kg/m^3		2321	2376	2308	2352	2313	2278	2350	2289	2307

(1) Quantities shown are means of three rounds
1 lb/yd^3 = 0.5933 kg/m^3
1 lb/ft^3 = 16.018 kg/m^3
1 fl.oz./cwt. = 0.652 mL/kg

Table A-5. Mixture proportions and properties for overlay mixtures [1].

Material		Quantities (kg/m^3)								
(SSD Basis)	% fume	0	1.8		6.0			10.2		12
	w/cm	0.35	0.31	0.38	0.30	0.35	0.40	0.31	0.38	0.35
Mix Designation		1O	2O	3O	4O	5O	6O	7O	8O	9O
Cement		414	407	408	386	387	392	370	373	363
Silica Fume		0	8	8	24	25	25	42	42	49
Fine Agg.		852	874	839	869	843	826	871	832	840
Coarse Agg.		865	887	852	882	856	839	876	845	853
Water		145	129	158	123	144	167	128	158	144
HRWR-mL/kg		10.7	14.6	8.1	20.6	14.3	8.5	21.9	14.3	19.5
AEA-mL/kg		1.7	1.9	1.9	3.3	3.0	2.4	3.5	3.5	4.5
Properties										
Slump - mm		124	114	140	132	145	114	107	127	137
Air Content - %		5.7	5.4	6.4	6.6	6.8	7.3	5.9	6.8	6.7
Unit Weight- kg/m^3		2303	2326	2284	2310	2281	2278	2324	2276	2268

(1) Quantities shown are mean of three rounds
1 lb/yd^3 = 0.5933 kg/m^3
1 lb/ft^3 = 16.018 kg/m^3
1 fl.oz./cwt. = 0.652 mL/kg
1 inch = 25.4 mm

Table A-6. Mixture proportions and properties for silica fume slurry overlay mixtures (1).

Material		Quantities (kg/m^3)								
(SSD Basis)	% fume	0	1.8		6.0			10.2		12
	w/cm				0.35			0.31	0.38	0.35
Mix Designation					5S			7S	8S	9S
Cement					386			370	376	367
Silica Fume					24			42	42	50
Fine Agg.					842			872	837	852
Coarse Agg.					855			877	849	864
Water					144			128	159	146
HRWR-mL/kg					14.1			22.7	14.5	20.1
AEA-mL/kg					3.3			4.0	3.9	4.6
Properties										
Slump - mm					173			122	112	148
Air Content - %					6.8			5.9	6.8	6.7
Unit Weight- kg/m^3					2271			2315	2289	2303

(1) Quantities shown are means of three rounds
1 lb/yd^3 = 0.5933 kg/m^3
1 lb/ft^3 = 16.018 kg/m^3
1 fl.oz./cwt. = 0.652 mL/kg
1 inch = 25.4 mm

Table A-7. Mixture proportions and properties for Type K cement mixtures (1).

Material		Quantities (kg/m^3)								
(SSD Basis)	% fume	0	1.8		6.0			10.2		12
	w/cm	0.40	0.36	0.43	0.35	0.40	0.45	0.36	0.43	0.40
Mix Designation		1K			4K		6K			9K
Cement		367			342		344			320
Silica Fume		0			22		22			43
Fine Agg.		729			739		705			717
Coarse Agg.		1065			1081		1030			1048
Water		147			127		164			145
HRWR-mL/kg		8.9			18.2		8.4			20.1
AEA-mL/kg		2.2			3.1		2.4			4.4
Properties										
Slump - mm		114			140		104			145
Air Content - %		5.7			6.6		7.3			6.7
Unit Weight- kg/m^3		2340			2352		2295			2302

(1) Quantities shown are means of three rounds
1 lb/yd^3 = 0.5933 kg/m^3
1 lb/ft^3 = 16.018 kg/m^3
1 fl.oz./cwt. = 0.652 mL/kg
1 inch = 25.4 mm

Table A-8. Mixture proportions and properties for Phase II full-depth mixtures (1).

Material		Quantities (kg/m^3)								
(SSD Basis)	% fume	0			6.0			9.0		
	w/cm	0.35	0.40	0.45	0.35	0.40	0.45	0.35	0.40	0.45
Mix Designation		1	2	3	4	5	6	7	8	9
Cement		369	369	367	347	344	346	336	336	335
Silica Fume		0	0	0	22	22	22	33	33	33
Fine Agg.		735	716	693	732	706	692	733	712	699
Coarse Agg.		1119	1090	1055	1115	1075	1054	1116	1083	1065
Water		129	148	165	129	146	166	129	148	159
HRWR-mL/kg		10.2	4.1	1.1	14.6	9.2	4.8	16.5	11.3	9.0
AEA-mL/kg		1.8	1.6	1.5	2.6	2.5	2.0	2.8	2.7	2.5
Properties										
Slump - mm		164	130	178	128	131	126	118	123	137
Air Content - %		5.7	5.4	6.4	6.6	6.8	7.3	5.9	6.8	6.7
Unit Weight- kg/m^3		2354	2335	2278	2350	2300	2291	2355	2322	2301

(1) Quantities shown are means of five rounds
1 lb/yd^3 = 0.5933 kg/m^3
1 lb/ft^3 = 16.018 kg/m^3
1 fl.oz./cwt. = 0.652 mL/kg

Table A-9. Mixture proportions and properties for overlay mixtures used for bond testing (1).

Material		Quantities (kg/m^3)								
(SSD Basis)	% fume	0	1.8		6.0			10.2		12
	w/cm	0.35	0.31	0.38	0.30	0.35	0.40	0.31	0.38	0.35
Mix Designation		1B	2B	3B	4B	5B	6B	7B	8B	9B
Cement		412	403	412	383	385	394	368	375	363
Silica Fume		0	8	8	24	25	25	42	42	49
Fine Agg.		847	865	845	862	840	831	867	837	841
Coarse Agg.		860	878	858	875	853	844	872	849	853
Water		144	127	159	122	143	168	127	159	144
HRWR-mL/kg		12.8	16.5	11.6	20.8	17.8	11.9	26.8	15.5	20.3
AEA-mL/kg		2.3	2.6	2.3	4.2	3.6	3.0	4.4	4.4	5.2
Properties										
Slump - mm		157	224	152	211	236	147	114	163	160
Air Content - %		5.7	5.4	6.4	6.6	6.8	7.3	5.9	6.8	6.7
Unit Weight- kg/m^3		2289	2317	2308	2281	2264	2301	2295	2287	2267

(1) Quantities shown are for single mixes
1 lb/yd^3 = 0.5933 kg/m^3
1 lb/ft^3 = 16.018 kg/m^3
1 fl.oz./cwt. = 0.652 mL/kg
1 inch = 25.4 mm

Table A-10. Workability and finishability characteristics of concrete mixtures.

Mix	Workability (1)	Comments	Finishability (1)	Comments
1F	G		G	
2F	G	needs vibration	G	slight drag
3F	G	needs vibration	G	
4F	G		G	slight sticky
5F	G		G	little sticky
6F	G		G	
7F	G		G	light drag
8F	G		G	
9F	G		G	slight drag
1O	P	stiff	G	
2O	G		G	
3O	G		F	surface tears
4O	F	stiffening	G	
5O	G		G	
6O	G		G	
7O	F	stiff	F	does not close
8O	G		G	
9O	G		F	sticky
5S	G		G	
7S	F	stiffening	G	
8S	G		G	
9S	G		F	some tearing
1K	G		G	
4K	F	needs vibration	F	
6K	F	stiff	F	
9K	F	stiffening	F	sticky

(1) E-excellent; G-good; F-fair; P-poor

APPENDIX B

LABORATORY TEST RESULTS

The results of all laboratory testing carried out under this research program are presented in this Appendix. A limited interpretation of the data gathered is also presented. More detailed statistical analyses and models are presented in Appendix C for most of these data. Further interpretation of the practical significance of the data may be found in Chapter Three of this report.

DRYING SHRINKAGE

Drying shrinkage was measured according to AASHTO T 160, Length Change of Hardened Hydraulic Cement Mortar and Concrete, except that the overlay concrete specimens were cured in 23 ± 1.7°C (73.4 ± 3°F) limewater for 3 days and the full-depth concrete specimens for 7 days, after which both sets were stored at 23 ± 1.7°C (73.4 ± 3°F), 50 ± 4 % R.H. The lengths were measured at 4, 7, 14, and 28 days, and 8, 16, 44, and 64 weeks. Triplicate 75 x 75 x 285 mm (3 x 3 x 11-1/4 in) specimens were prepared for each mix.

The results for all full-depth mixes are shown in Table B-1 and plotted in Figure B-1. The only evident trend seems to be a tendency towards lower shrinkage for those mixes produced at lower w/cm. This is to be expected, as shrinkage depends primarily on the water content of a concrete mix.

The results for the overlay mixes are shown in Table B-2 and plotted in Figure B-2. The shrinkage is generally greater for these mixes, presumably due to the higher paste contents of the overlay concrete. Again, the mixes with lowest w/cm appear to have somewhat less shrinkage than the others.

The results for the silica fume slurry mixes (overlay mix design and curing regimen) are as shown in Table B-3 and plotted in Figure B-3. There is virtually no difference between comparable mixes: the values for the concretes made with densified silica fume (Table B-2) are much the same as for the comparable concretes made with silica fume slurry (Table B-3) at the same ages.

Finally, the results for the Type K cement mixes are shown in Table B-4 and plotted in Figure B-4. There appears to be a difference between the shrinkage of the Type K concretes and that of

comparable mixes using Type I /II cement (Figure B-1). This is actually not surprising, as the initial expansion of concrete produced using Type K cement generally occurs within the first 24 hours after casting. Beyond this point the unrestrained drying shrinkage of Type K concretes may be comparable to or greater than that of conventional concretes. The benefit of Type K cement is that its initial expansion induces compressive stresses in the concrete member due to the restraint imposed by the reinforcement; these compressive stresses must subsequently be overcome by drying shrinkage before crack-inducing tensile stresses can develop.

CRACKING TENDENCY

Phase I

Cracking tendency was measured according to a method utilized under NCHRP Project 12-37 (*12*), in which early cracking of full-depth concrete bridge decks was investigated. This method involves casting a 75 mm (3 in) thick, 150 mm (6 in) high ring of concrete around the outside of a steel cylinder with an outside diameter of 300 mm (12 in) and 19 mm (3/4 in) thick walls. Good correlation between the results of this test and actual cracking of bridge decks under field conditions was achieved in Project 12-37. Details of the specimen configuration are shown in Figures B-5 and B-6. This geometry provides essentially complete restraint against shrinkage while still producing measurable strains (0 to -1×10^{-4} mm/mm, or 0 to -100 μin/in). The inside of the steel ring was instrumented with four strain gages placed at the quarter points around the ring which were recorded every 30 minutes by a data acquisition system. The strain gages were affixed to prepared points on the interior surface with epoxy strain gage adhesive and coated with a waterproof sealant. Fresh concrete was placed into the annular space in three equal layers, each of which was consolidated by a combination of rodding and external vibration using a small hand-held vibrator. The concrete was finished at a level approximately 6 mm (0.25 in) below the top surface of the mold using a specially designed trowel which conformed to the inside surface of the form. This created a reservoir on top of the concrete into which a saturated limewater solution was placed. The entire mold was then covered with polyethylene sheeting. After the specified period of moist curing the limewater was removed and the exterior form stripped from the specimen. The top surface of the concrete was then covered with a polyethylene sheet affixed to the concrete with silicone sealant. Drying then occurred from the exposed sides of the concrete specimen.

Use of this technique allowed for easy detection of cracking, as a crack suddenly reduced the stress locally, resulting in a local decrease in strain. An example of a plot obtained from one of the test specimens (Mix 4O, Specimen B) is shown in Figure B-7. It can be seen that strain was

instantaneously released from all gages 8 days after the initiation of drying. An example of a somewhat different pattern of strain release is shown in Figure B-8. Here two of the strain gages released most of their strain starting at 42 days after the initiation of drying, indicating a crack located between these two gages. Strain was maintained in the steel at the other two gage locations in this instance. In other specimens only one gage showed a release of strain; this typically happened when the crack was in the immediate vicinity of that gage. For any given specimen, only the time to first crack was recorded. Duplicate specimens were cast from all of the full-depth and Type K mixes, and overlay mixes 1, 4, 6, and 9, representing the extremes of w/cm and silica fume content for the overlay mixtures.

The times to first crack for the specimens cast from the Phase I full-depth mixes are given in Table B-5. The time was measured from the end of the 7-day moist curing period. The control mix (without silica fume) had an average time to first crack of 35 days. Mixes 2, 3, and 4 cracked somewhat later, while Mix 6, which had the highest w/cm ratio, cracked considerably sooner. Mixes 7, 8, and 9 did not crack within the test period. It should be noted that it is the nature of fracture data to give a wide scatter. This is because fracture is sensitive to the presence, size, type, and location of flaws in the material. Hence, the occurrence of such data as for Mixes 2 and 4, where one of the duplicate specimens cracked and the other did not. In addition, this is an experimental technique, not a standard method. Thus it is not known how many replicate specimens are needed to produce enough data to provide definitive results.

The times to first crack for the overlay mixes are given in Table B-6. The time was measured from the end of the 3-day moist curing period. All of the overlay concrete specimens tested eventually cracked. The silica fume mixes cracked before the control mix.

There was no cracking in any of the Type K mixes (Table B-7). The best comparisons are between Mix 1 with Type K vs. Type I/II (Table B-5) where neither of the Type K specimens cracked but both of the Type I/II specimens cracked. For Mix 6 similar results are seen. Neither the TypeI/II nor the Type K concretes cracked for Mix 9. For Mix 4 the results are difficult to interpret due to the inconsistent behavior of the duplicates for the Type I/II in Table B-5.

The following general conclusions can be drawn from these results.

- Those mixtures most susceptible to cracking have high paste (cementitious materials plus water) contents. This is typical of the overlay mixtures used in this program.

  All of the overlay mixtures exhibited cracking, while not all of the full-depth mixtures (which were prepared at lower paste contents) cracked.

- Within a given type of mix (and the full-depth series of mixes offers the only comparisons in this Phase) the tendency to cracking does not appear to be related to silica fume content. In fact, the three mixes of highest silica fume content in the full-depth series did not exhibit cracking, while all mixes at the lowest levels of silica fume cracked.

- The use of Type K (shrinkage compensating) cement appears to be effective in reducing the tendency to crack in such concretes. For those full-depth mixes which exhibited cracking, the substitution of Type K cement for Type I/II cement appeared to have eliminated the tendency to cracking. However, as the overlay mixtures were not prepared with Type K cement, a comparison in this case was not possible.

Because of the limited data obtained in Phase I, no statistical analyses of these data were performed. ANOVA and further analyses were performed on the Phase II data (see below) and are described in Appendix C of this report.

Phase II

Because of the scatter of the data from Phase I of the cracking tendency testing, an additional phase of the study was undertaken. As in Phase I, the test variables consisted of the water/cementitious materials ratio (w/cm), silica fume content, and curing period. The plan consisted of a full factorial experiment over three w/cms (0.35, 0.40, and 0.45), three silica fume contents (0, 6, and 9 percent) and two curing regimes (1- and 7-day moist cure). The range of w/cms selected represents that typically specified by state highway agencies. The 6 and 9% silica fume contents were selected to bracket the most commonly used dosages of silica fume for this type of application, and 0% silica fume was included as a control. One day of curing represents a "worst case" scenario in which proper curing procedures are not adhered to, possibly due to the accidental drying out of the burlap over a weekend. Seven days of curing represents normal practice for this application, and is typical of many state highway agency specifications. Five replicate specimens were prepared for each condition, as the two replicates used previously had not produced definitive results. All specimen details and casting procedures remained the same as for the Phase I work, except that Cement B (a blend of the remaining stock of Cement A with a new supply of the same type of cement obtained from the same source approximately one year later)

was used to make the concretes. The chemical composition and physical properties of this cement are given in Tables A-1a and A-1b, respectively.

A summary of time to first crack (days from time of stripping) of the specimens cured for one and seven days is shown in Tables B-8 and B-9. The time to first crack is given for each individual specimen, with the five replicates of each concrete mix reported as a set. It can be seen that for the specimens cured for one day, the silica fume concretes of a given w/cm cracked sooner than the control specimens of the same w/cm. This result is consistent with observations of concretes in the field, where silica fume concretes have proved to be more sensitive to poor curing practices. For the concretes cured 7 days, a lower w/cm appears to result in longer times to first crack. For a given w/cm, the 6% silica fume concrete specimens appear to crack more readily than either the 9% silica fume mixes or the controls. More detailed statistical analyses of these data can be found in Appendix C.

Tables B-10 and B-11 report the compressive strengths of companion cylinders broken at one and seven days, respectively. Each number represents the mean of five rounds of concrete, three cylinders being cast for each round, resulting in an aggregate of 15 tests for each number reported in the tables. Tables B-12 and B-13 report the modulus of elasticity as determined for the same set of cylinders; two tests were run on each of 10 cylinders to obtain each reported quantity. As expected, for any given level of silica fume, there is a significant increase in the compressive strength as the w/cm decreases. There does not appear to be a consistent relationship between silica fume content and compressive strength at either test age. The same trends are evident in the elastic moduli (Tables B-12 and B-13). In general, increased compressive strength corresponds with increased tensile strength to resist cracking. However, the modulus of elasticity, which generally also increases with increasing strength, will reduce the tendency of the concrete to deform rather than crack. For these mixes, the modulus of elasticity and compressive strength both appear to have been primarily a function of w/cm rather than of silica fume content.

CHLORIDE ION INGRESS

Chloride ion ingress was evaluated according to AASHTO T 259, Resistance of Concrete to Chloride Ion Penetration, which is commonly known as the "90-day ponding test." Some modifications were used to provide additional information about the diffusivity of high-quality concrete to chloride ions. Concretes having low w/cm and/or high silica fume contents generally have very low diffusivities. Thus, it can be difficult to obtain meaningful data about them or to provide good comparisons among them using standard test methods. The first modification was

an extension of the test period to 180 days to provide more time for the chloride ions to migrate into the concrete. The second modification was to obtain chloride ion concentrations at closely spaced intervals (approximately 1 mm [0.04 in]) rather than at the 12 mm (0.5 in) intervals specified by T 259. Closely spaced sampling intervals are particularly useful in tests of low-diffusivity concretes, as the chloride ions penetrate the concrete only to a shallow depth. The technique has been used previously in observing chloride ion migration in cores taken from a bridge deck in Illinois (*15*) where two high-quality concretes (one with and one without silica fume) were used. In the current study, this approach was used to plot chloride ion concentration profiles at 1 mm (0.04 in) intervals and to calculate apparent diffusivities for the different concretes.

Triplicate 305 x 305 x 75 mm (12 x 12 x 3 in) specimens were prepared from each mix. The full-depth and Type K mixtures were cured for an initial moist period of 7 days. The overlay and silica fume slurry mixtures were moist cured for an initial period of 3 days. All curing was carried out in a moist room conforming to AASHTO M 201, Moist Cabinets, Moist Rooms, and Water Storage Tanks Used in the Testing of Hydraulic Cements and Concretes. The specimens were then stored in a drying room maintained at 23 ± 1.7°C (73.4 ± 3°F), 50 ± 4 % R.H. for a period of 28 days. Dikes fabricated from foamed polystyrene were then placed around the top surface of each specimen and bonded to the surface with silicone sealant. All slabs were then dried for an additional 13 days prior to ponding. They were then ponded with a 3 percent sodium chloride solution for a period of 180 days. Two of each of these sets were used to extract 100 mm (4 in) nominal diameter cores from the center of each test slab for the profiling. The third was retained as a spare. Any cores which could not be sampled immediately were stored in a freezer at -18°C (0 °F) to prevent further diffusion.

Samples were obtained by milling on a lathe at approximately 1 mm (0.04 in) increments from the finished surface of each slab, up to about 10 mm (0.40 in) from the surface, then at wider intervals as the profiles became less steep. Each sampling increment was approximately 1 mm (0.04 in) thick. The dust from each layer was analyzed separately for acid-soluble chloride according to ASTM C1152, Acid-Soluble Chloride in Mortar and Concrete. As an example, Figure B-9 shows profiles obtained from specimens taken from full-depth mixes 1, 5, and 9, which contain a w/cm of 0.40 and 0, 6, and 12 percent silica fume, respectively. The effect of silica fume on the ingress of chloride into the slabs is clear, especially when comparing the 6 and 12 percent silica fume concretes with the control. It is also interesting to note the small difference between the profiles for the 6 and 12 percent silica fume concretes, indicating a point of diminishing returns for silica fume content as regards the ability to reduce chloride ingress. This is

also apparent from an examination of the results generated by the statistical models presented in Appendix C.

The effect of w/cm on the chloride profiles for mixes 4, 5, and 6 is seen in Figure B-10. Here all profiles are for full-depth mixes with silica fume contents of 6 percent and w/cm of 0.35, 0.40, and 0.45, respectively. Again, one can see a difference in the chloride profiles as w/cm is decreased. The effect of w/cm does not seem to be as dramatic as that of silica fume content in Figure B-9.

For each profile, the data were fitted to the following solution to Fick's Second Law of diffusion (*16*). This solution is valid for a semi-infinite flat plate where D_c and C_0 (defined below) are not functions of time.

$$C_x = C_0\left(1 - \text{erf}\left[\frac{x}{2\sqrt{D_c \cdot t}}\right]\right) \qquad \text{(B.1)}$$

where C_x = chloride level at depth x (m)
C_0 = near-surface chloride concentration (taken as the chloride content in the first sampling increment)
D_c = coefficient of diffusion (m^2/sec)
t = time (sec)

While this equation "fits" the data well mathematically, it is not strictly valid from the standpoint of the physical and chemical processes that take place when chloride ions migrate into concrete. Fick's Second Law is actually a simplification of a more generalized model of diffusion. It is based on three assumptions:

1. The material in which diffusion takes place must be permeable and homogeneous.
2. The diffusion properties of the material must not change either with time or with the concentration of the diffusant.
3. There can be no chemical reaction or physical binding between the diffusant and the material.

In the case of chloride ion transport through concrete, each of these assumptions is violated:

1. Concrete is permeable but not homogeneous. The presence of interconnected pores, cracks, microcracks, and aggregate particles will affect the ability of the chloride ions to migrate into the concrete.
2. The diffusion properties of concrete in most practical cases will change with time as hydration proceeds. They may also be affected by the chloride ion concentration.
3. The hydration products of the aluminates in the cement and/or supplementary cementing materials bind chloride ions, preventing their migration.

In addition, there is more than one mechanism of chloride ion transport through concrete in a ponding test. Capillary action undoubtedly plays a much more significant role near the concrete surface when the concrete has been allowed to dry for a period of time, as is the case in AASHTO T 259. Pettersson (*23*) reports that for a 0.40 water-cement ratio concrete dried at room temperature and 60% RH, the effect of capillary action was at least 20 times as great as that of diffusion.

However, recognizing the limitations of the analysis, keeping the conditions of exposure constant, and using the numerical data for comparison purposes within the same study only, the data can be useful. In order to emphasize the point that what has been calculated is not strictly a diffusion coefficient, the term "apparent diffusion coefficient" is used in this report. Apparent diffusion coefficients were obtained by least-squares fitting of the profiles to the above equation using a commercial nonlinear curve-fitting software package for a desktop computer. The values obtained are shown in Tables B-14 through B-17. Values were found to be within the range of published literature data (*19*) for bridge deck quality concrete (w/c from 0.40 to 0.45) and silica fume concrete.

Response surface statistical models for full-depth and overlay mixtures, as well as comparison analyses between TypeI/II and Type K mixtures and between slurry and densified forms of silica fume, are presented in Appendix C.

COMPRESSIVE STRENGTHS

The compressive strength was measured according to AASHTO T 22, Compressive Strength of Cylindrical Concrete Specimens. For each mix, 100 x 200 mm (4 x 8 in) cylinders were cast for curing to each of four test ages: 7, 28, 56, and 90 days. Curing was carried out in a moist room conforming to AASHTO M 201, and maintained at 23 ± 1.7°C (73.4 ± 3°F), 100% R.H. Triplicate specimens were cast for each test age.

Table B-18 shows the test results for the full-depth mixes. As might be expected, there are considerable differences between the mixes. Both silica fume content and w/cm appear to have significant influences on the compressive strength, although the influence of the latter is more consistent. For instance, while at a w/cm of 0.40 there is a consistent trend of increasing strength with increasing percentage silica fume replacement, the increase is much greater when going from 0% silica fume to 6% than from 6 to 12%. For w/cm in the 0.43 to 0.45 range, there is essentially no difference in strength between the concretes containing 1.8% and 6% silica fume. In contrast, at all silica fume contents a decrease in w/cm invariably results in an increase in strength. It can also be seen from the data in Table B-18 that the greatest strength gain for the silica fume concretes occurs between ages 7 and 28 days. The amount of this strength gain generally increases with an increase in silica fume content. This is also not unexpected, considering the pozzolanic nature of silica fume. The main pozzolanic activity of silica fume takes place between ages 7 and 28 days, although it may start earlier when the alkali content of the cement is high.

Table B-19 shows the compressive strength data for the overlay mixes. A similar pattern can be seen in that the silica fume concretes show their greatest strength gain between ages 7 and 28 days. A comparison of the later age strengths suggests the existence of a point of diminishing returns, rather than linearly increasing benefits, with increasing silica fume content.

Table B-20 shows the results for the silica fume slurry concretes, which are directly comparable to those for the overlay concretes, as the only difference between them was the form in which the silica fume was added to the mix. It is clear that the strengths at all ages are very similar, indicating that the form of the silica fume admixture does not affect the strength provided that mixing is adequate.

Table B-21 shows the compressive strengths for the Type K mixes. A comparison of the results for the Type K and Type I/II cements indicates a similar pattern in terms of strength gain over time and the effects of w/cm and silica fume content. However, the use of Type K cement was found to result in a significantly higher compressive strengths at all test ages.

Response surface statistical models for compressive strength of full-depth and overlay mixtures at 28 and 90-days age, as well as comparison analyses between TypeI/II and Type K mixtures and between the slurry and densified forms of silica fume at all test ages, are presented in Appendix C.

MODULUS OF ELASTICITY

The modulus of elasticity was measured according to ASTM C 469, Static Modulus of Elasticity and Poisson's Ratio of Concrete in Compression, on the same specimens used for the compressive strength measurements, except that the modulus of elasticity was measured only at 28 and 90 days of age. Duplicate specimens were tested for each mix.

The moduli of elasticity for the full-depth mixes are given in Table B-22. The same basic trends as seen for compressive strength for these mixes are evident. There is a gradual increase in modulus with increasing silica fume content, but the largest increases are seen when the w/cm is decreased. All of the values obtained (25 to 40 GPa{4 to 6 million psi}) are typical of concretes in this strength class.

The moduli of elasticity of the overlay mixes are given in Table B-23. On the whole, there is no significant change with increasing silica fume content. As for strength, the effect of w/cm predominates.

The moduli of elasticity of the slurry and Type K mixes are presented in Tables B-24 and B-25, respectively. There is no consistent effect of the slurry form of silica fume on the modulus of elasticity as compared with that of dry densified fume. Likewise, there is no consistent difference between Type K cement on the modulus of elasticity as compared with Type I/II concretes for comparable mixes.

Response surface statistical models for the modulus of elasticity of the full-depth and overlay mixtures at 28 and 90 days' age, as well as comparison analyses between the TypeI/II and Type K mixtures and between the slurry and dry densified forms of silica fume at these test ages, are presented in Appendix C.

OVERLAY BOND STRENGTHS

Reinforced concrete slabs 500 x 1000 x 180 mm (20 x 40 x 7 in) that had previously been overlaid and used for the testing of experimental cathodic protection (CP) systems for bridge decks were used as substrates for the application of silica fume concrete overlays. Descriptions of the concrete mixtures, reinforcement details, and curing and environmental storage procedures for these slabs are given in an FHWA report (*24*). The old overlay material was removed with a small chipping hammer, being careful not to damage the underlying concrete surface. As the old

overlays had been cast with "free-draining" concretes, they were rather weakly bonded to the substrate and were easy to remove with the small hammer. The surfaces were then sandblasted with coarse blast grit so as to expose the coarse aggregate and obtain a good surface on which to bond the overlay. A total of five such slabs was prepared. An environmental room was then set to 35 °C (95°F) and the base slabs and all concrete materials (except batch water and chemical admixtures) were moved into the room the day before batching to allow them to come to temperature. Mix designs were identical to those used for the previous overlay batch series (mixes 1O through 9O), which had been cast at approximately 23°C (73°F). A total of nine overlays was planned, each base slab being used to accommodate two separate sections, with a bulkhead placed transversely between the sections.

The concrete mixer pan was stored at 35 °C (95°F) prior to mixing the concretes. All materials and the pan were then transported the short distance to the mixing lab and the concrete was mixed using the standard AASHTO T 126 3-3-2 minute mixing cycle. The slump, air content, unit weight, and concrete temperature were measured on each batch. The characteristics of the fresh concretes are presented in Table A-11 (see Appendix A of this report). The concrete was then returned to the heated room, where the 40 mm (1-1/2 in) thick overlays were placed on top of the slabs. Due to the time required to transport the heated materials and cast the overlays, castings were done on two separate days. Mixes 3, 5, 7,and 8 were cast on the first day, cured under wet burlap overnight, and moved outdoors the next day. Mixes 1, 2, 4, 6, and 9 were cast on the third day, cured identically to the first set, and moved outdoors on the fourth day. After each day's casting was complete, the heater in the environmental room was turned off and the room allowed to cool in order to simulate the cooling that takes place overnight after a hot summer day. By the next morning the temperature of the room was approximately 30°C (85°F), with the slab surface temperatures (under the curing mats) approximately 33°C (92 °F).

Immediately after setting up the slabs outdoors, foamed polystyrene dikes were placed around the periphery of each slab and approximately 25 mm (1 in) of curing water placed within the dike after curing of the dike adhesive was complete. This condition was maintained for 2 days so as to obtain a total of 72 hours of moist curing for each specimen. The dikes were then removed and the slab surfaces exposed to ambient conditions. Temperatures over the period from placement of the slabs outdoors to coring for bond testing at 28 days were typical of summer in the Chicago area, with daily highs from 26 to 32°C (80 to 90 °F) and lows from 20 to 24°C (68 to 75 °F). There was little rainfall during the period, with only occasional thundershowers, the rainfall from which quickly evaporated off the surfaces of the slabs. Ambient humidities, however, were higher than normal for the region during this period.

At 28 days' age, 50 mm (2 in) cores were drilled at three locations on each overlay section through each overlay and into approximately 19 mm (3/4 in) of the underlying base concrete. A 50 mm (2 in) diameter steel dolly was then bonded to the top surface of each core position. A reaction frame and calibrated load cell were then used to measure direct tensile strength of the overlay bond by slowly pulling the dolly. The test method is similar to the field test for surface soundness and adhesion described in ACI 503R-89, Use of Epoxy Compounds with Concrete (Appendix A – Test Methods). The tests were repeated at 90 days. The results are presented in Tables B-26 and B-27. It should be noted that failure will occur at the weakest plane in the core. This is not necessarily fully along the overlay/substrate interface. Most of the results, therefore, can be looked on as lower bounds to the "true" bond strength. In all cases the mean values significantly exceed the value of 0.7 MPa (100 psi) specified by SHRP (*18*) for minimum tensile bond strength of concrete overlays as well as the criterion of 1.4 MPa (200 psi) established by NIST (*19*) for bond testing of concrete overlays in shear, which typically yields higher results than testing under uniaxial tension. From examination of the data it is also apparent that there is a wide variation between replicate tests, reflecting the variability typically encountered in pull-off bond testing. A simple one-way analysis of variance performed on the data indicated that this was indeed the case, there being no significant difference detectable between the data sets, at least within the inherent precision of the measurements. Additionally, paired t-testing of the 28- and 90- day test results indicated no significant effect of age.

COEFFICIENT OF THERMAL EXPANSION

The coefficient of thermal expansion was measured following CRD-C 39, Coefficient of Linear Thermal Expansion of Concrete (*25*), adapted for testing of air-dry specimens. The specimens were triplicate 75 x 75 x 285 mm (3 x 3 x 11-1/4 in) prisms previously used for the drying shrinkage tests. The specimens were heated to 60 °C (140 °F) for 48 hours in a laboratory oven before measurement of the lengths by comparator. The specimens were then cooled to 4 °C (40 °F) for an additional 48 hours and a second comparator reading obtained. The difference in length was divided by the difference in temperature to obtain the coefficient of thermal expansion in $°C^{-1}$ ($°F^{-1}$).

The results for the full-depth and overlay mixtures are shown in Tables B-28 and B-29. There appears to be no substantial effect of either silica fume content or w/cm on the test results. Data in the literature indicate that the coefficient of thermal expansion is determined primarily by the characteristics and volume proportion of the aggregate used in the concrete.

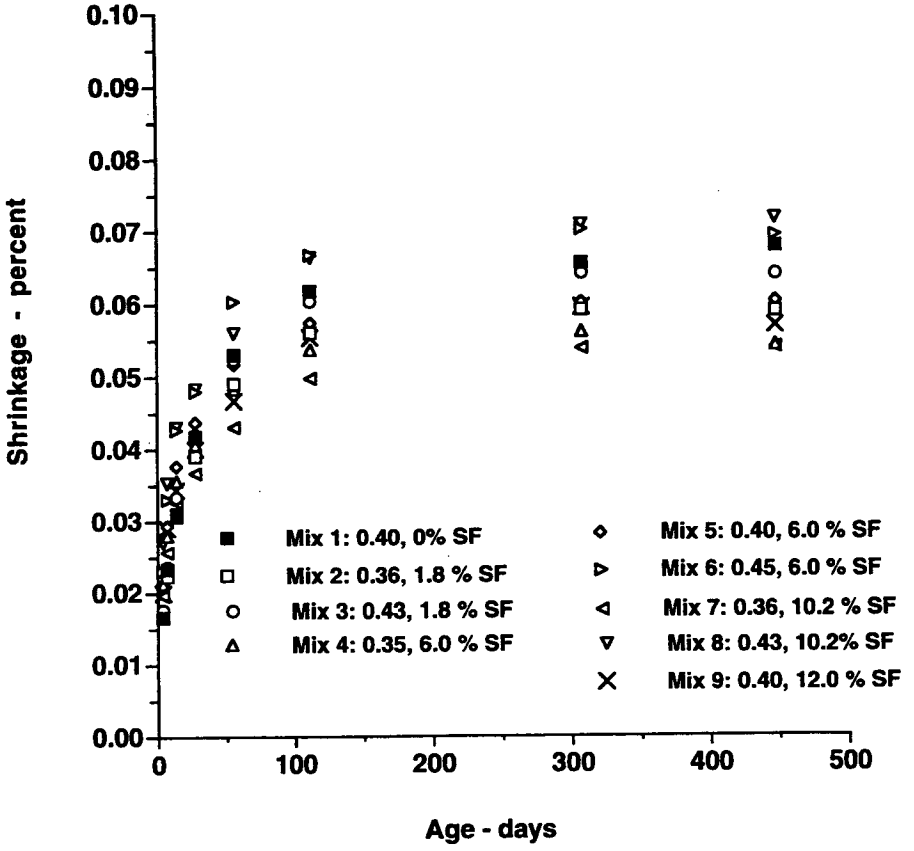

Figure B-1. Shrinkage of full depth mixtures through 64 weeks.

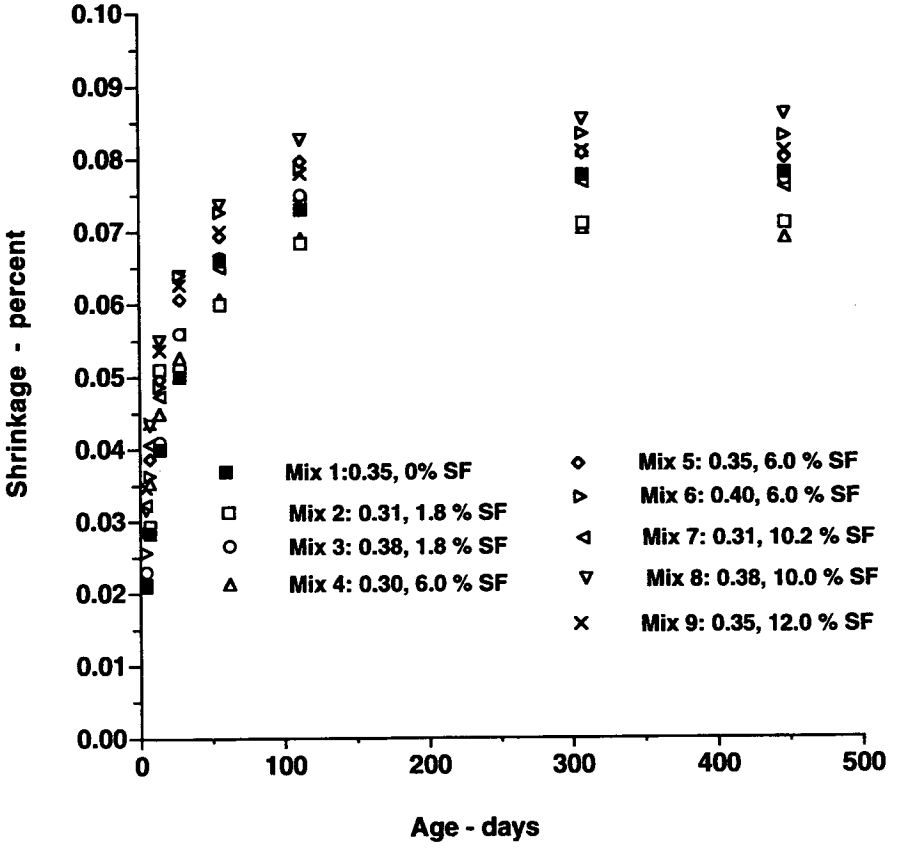

Figure B-2. Shrinkage of overlay mixtures through 64 weeks.

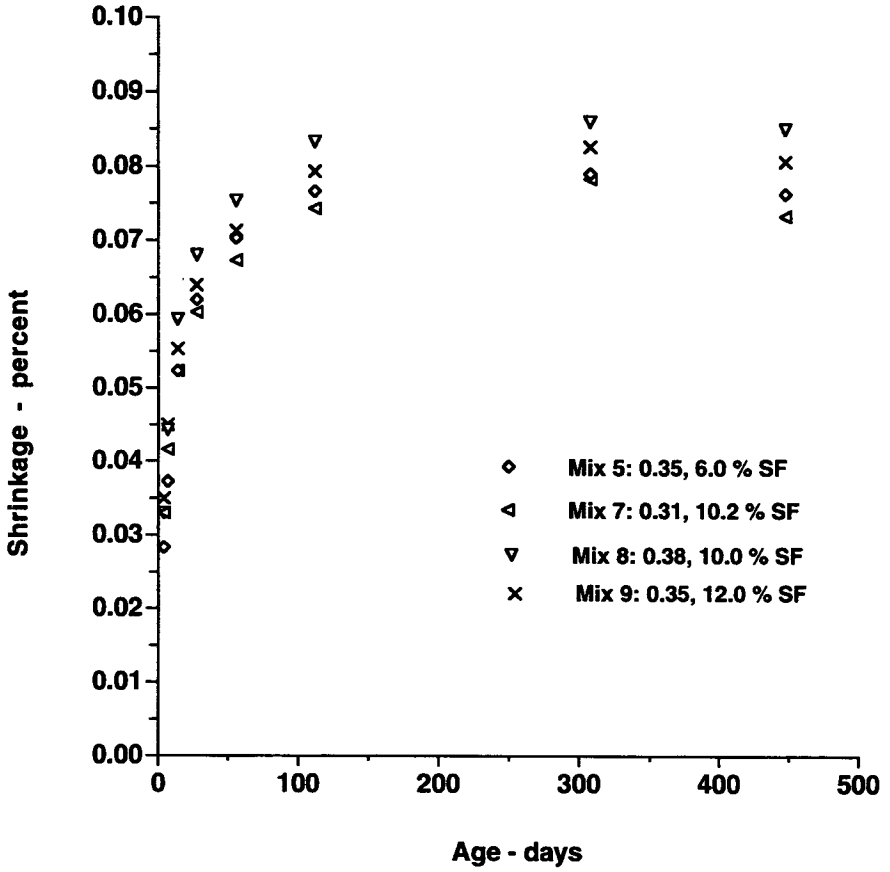

Figure B-3. Shrinkage of slurry mixtures through 64 weeks.

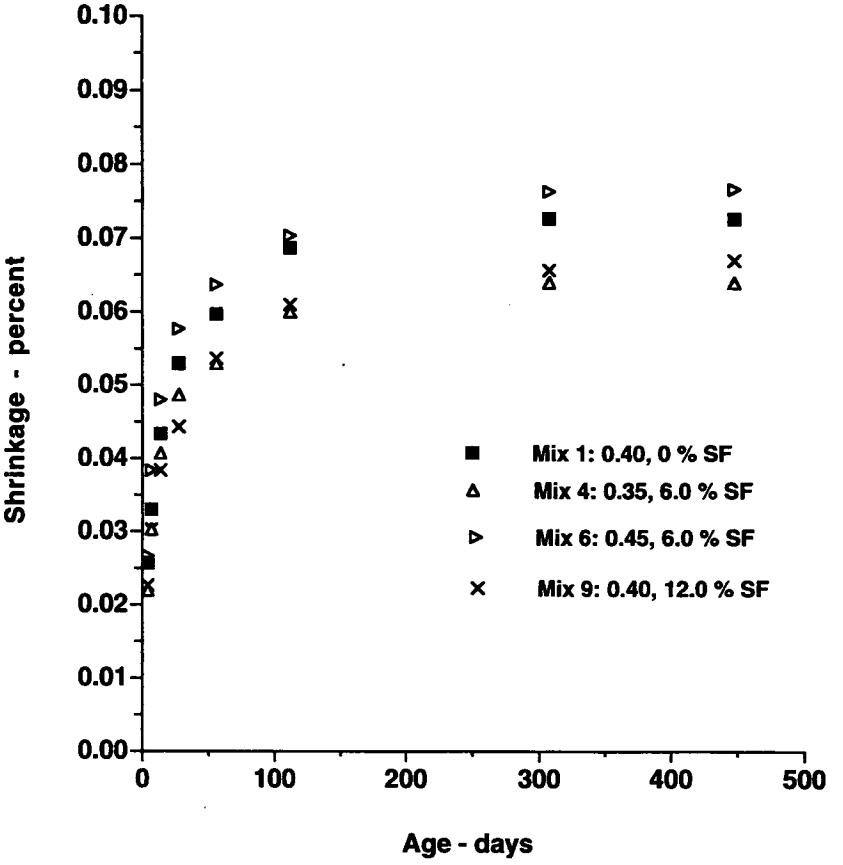

Figure B-4. Shrinkage of Type K mixtures through 64 weeks.

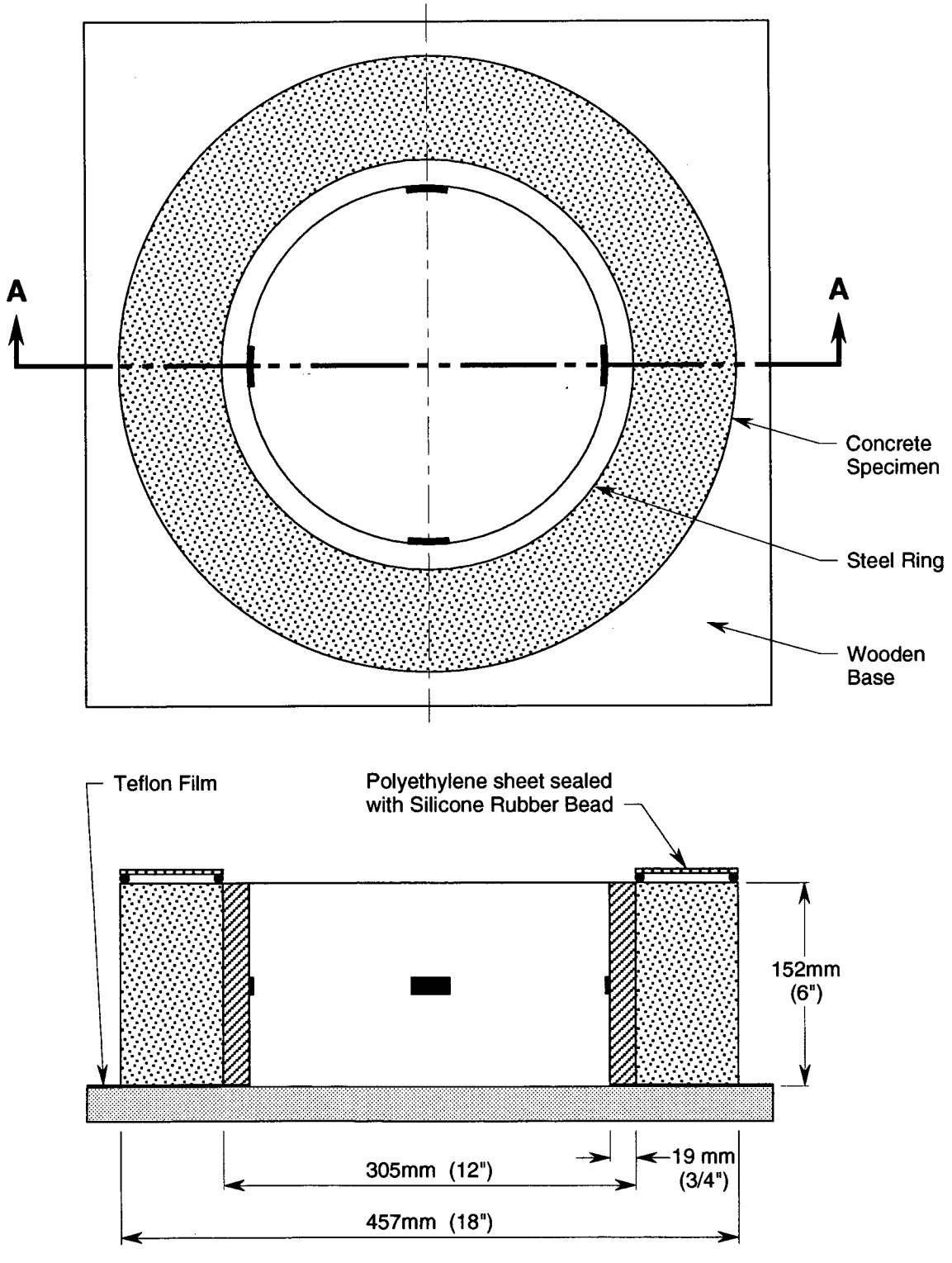

Figure B-5 Specimen configuration for cracking tendency tests.

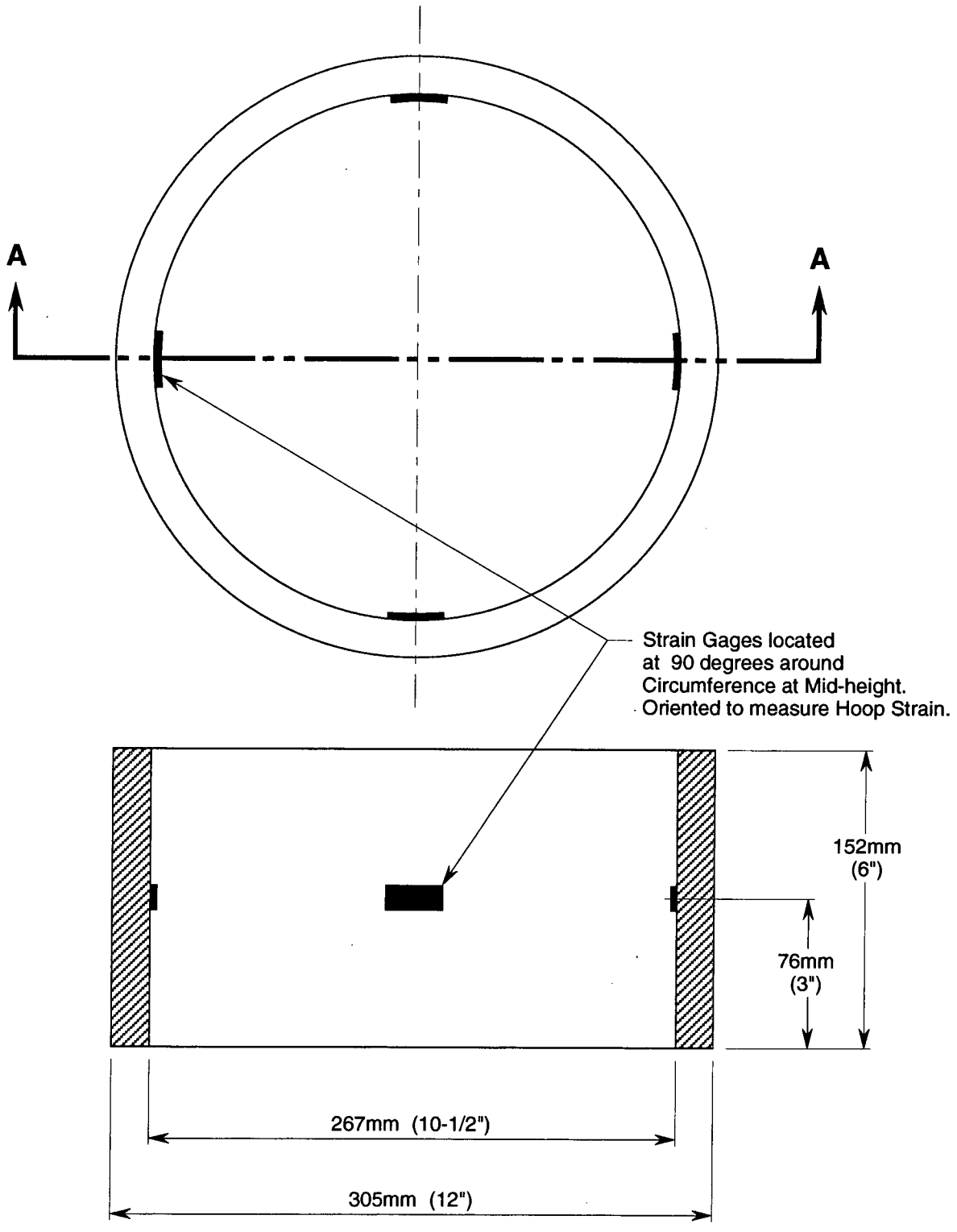

Figure B-6 Strain gage placement details for cracking tendency tests.

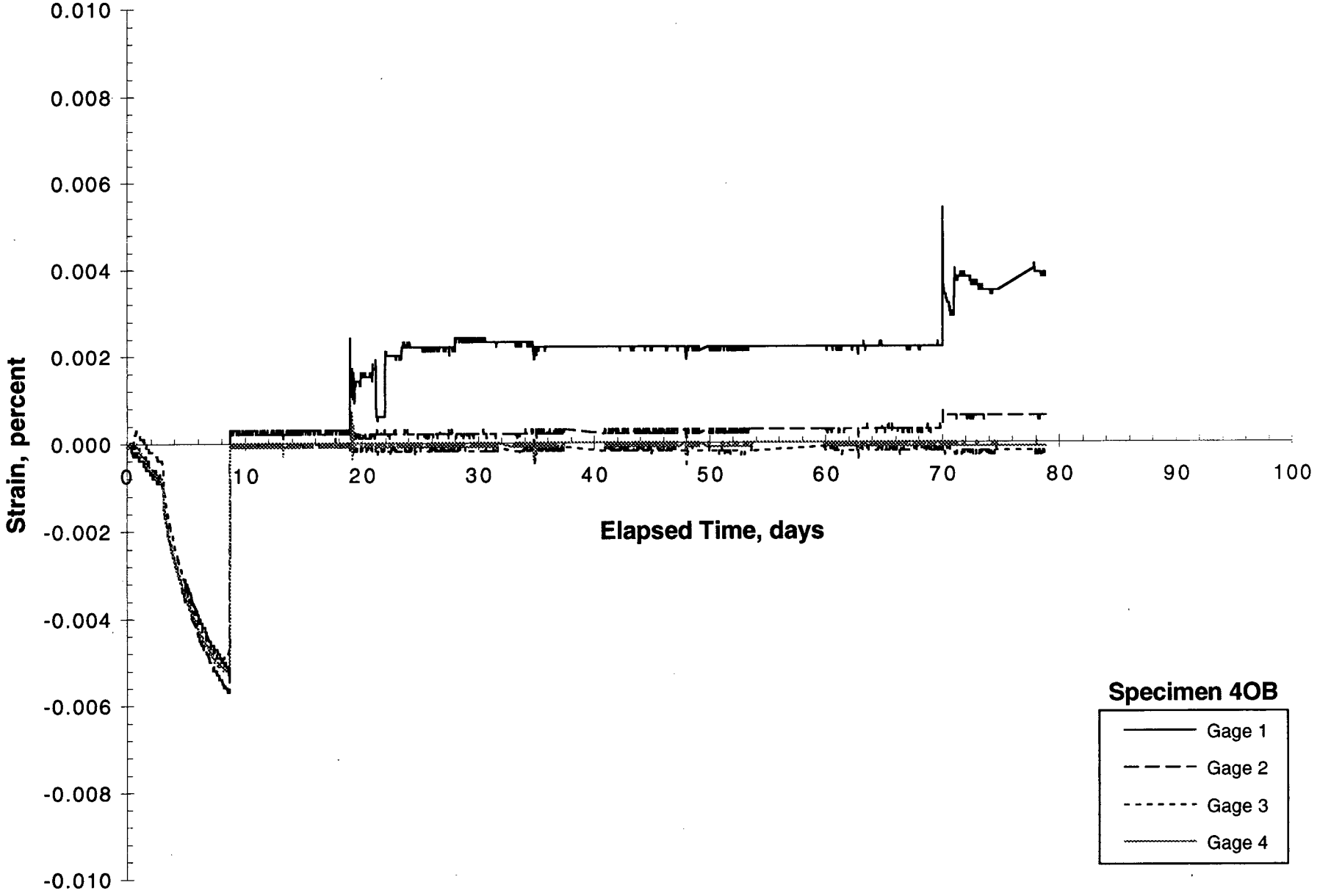

Figure B-7 Example of strain release pattern for cracking tendency test.

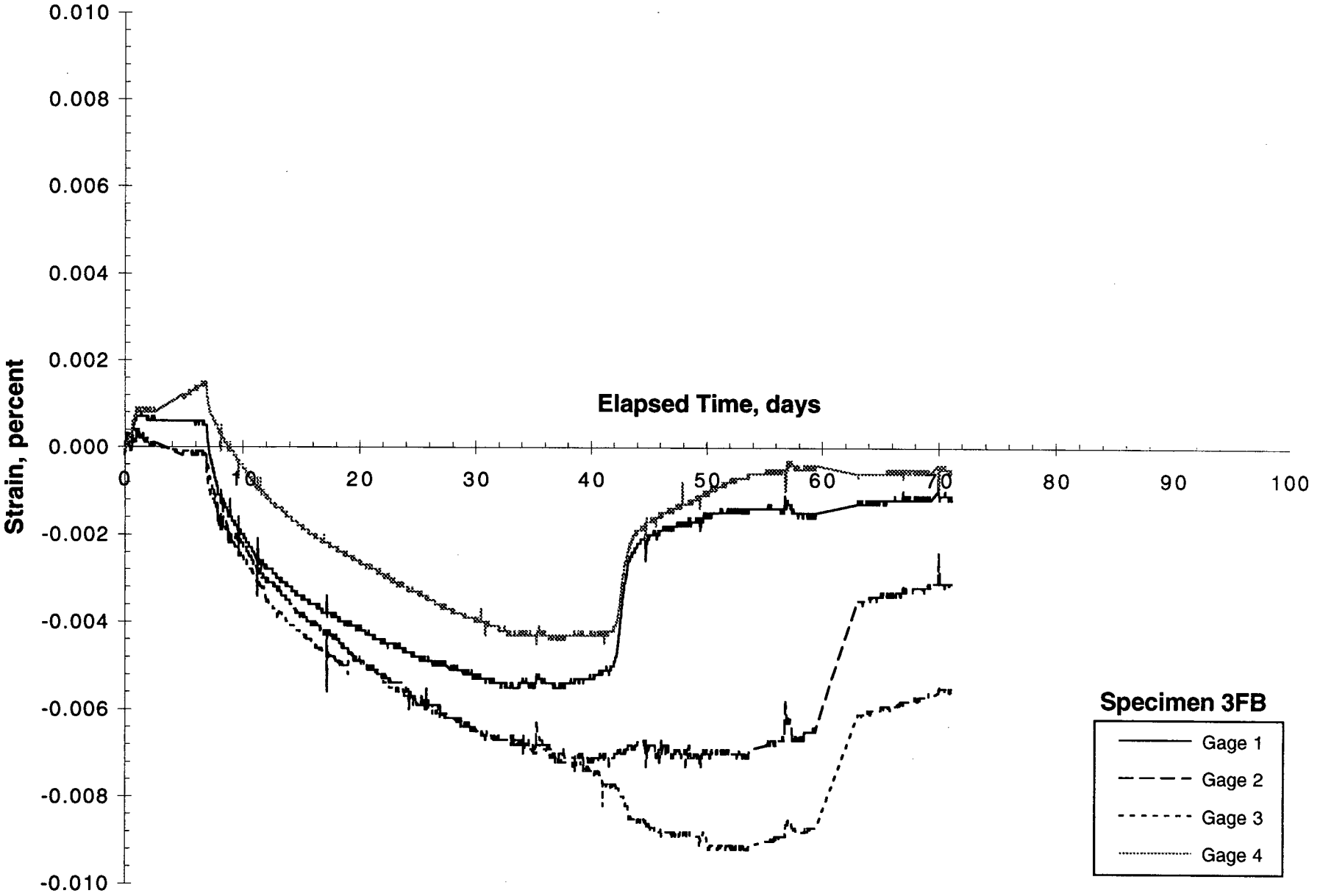

Figure B-8 Strain release pattern for cracking located between gages 1 and 4.

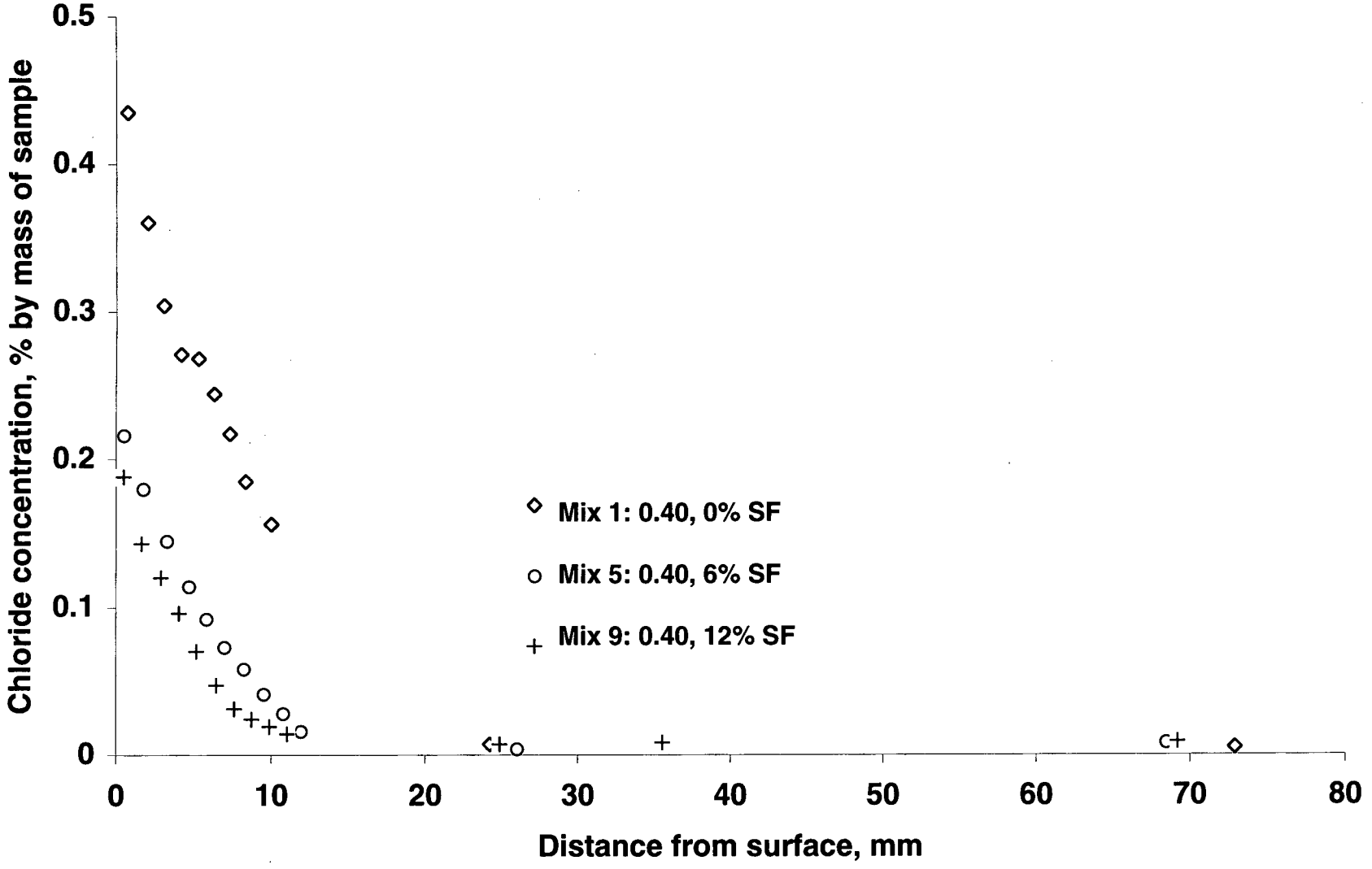

Figure B-9. Acid-soluble chloride profiles for full-depth concretes: Mixes 1,5, and 9.

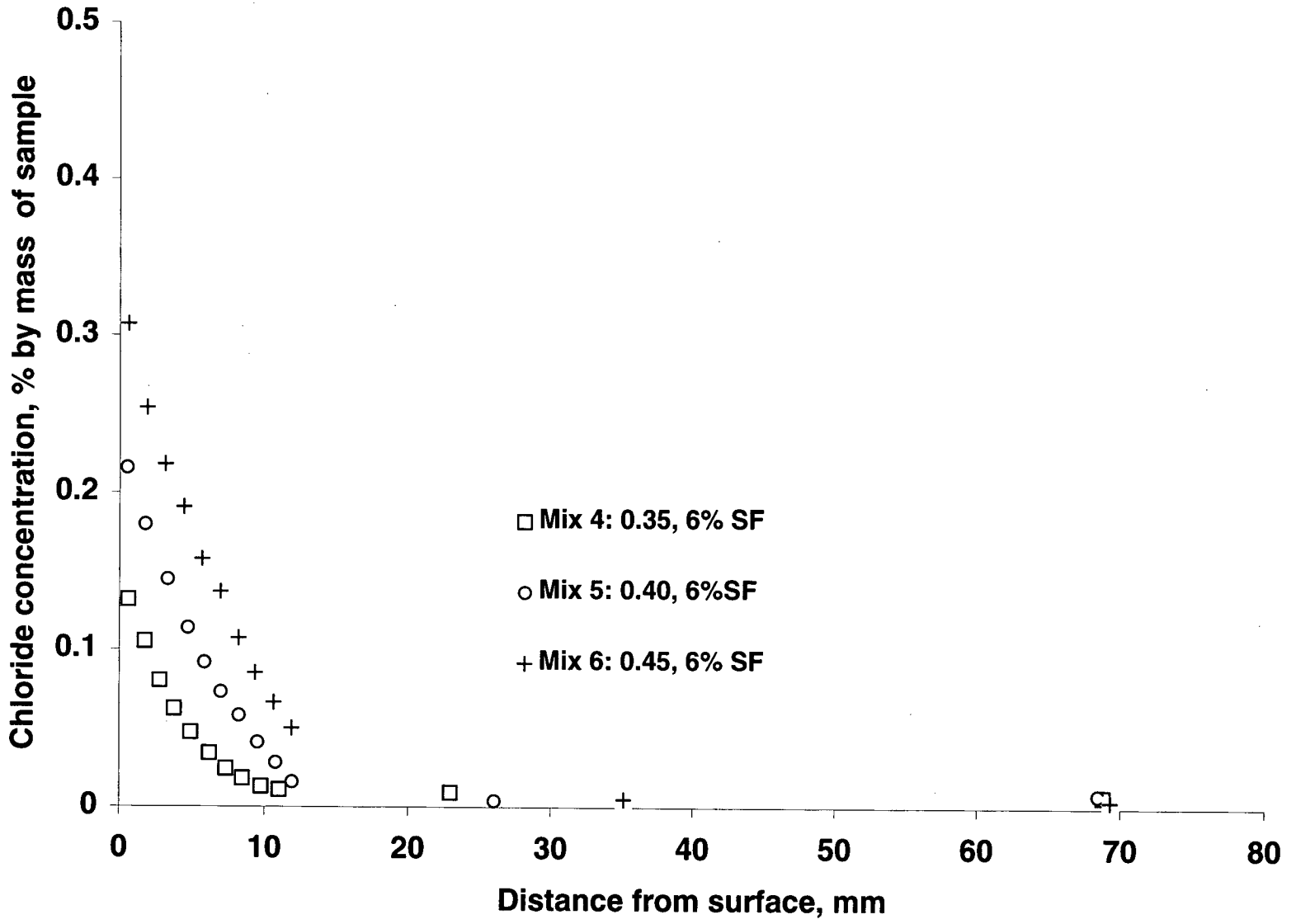

Figure B-10. Acid-soluble chloride profiles for full-depth concretes: Mixes 4, 5, and 6.

Table B-1. Length change data, %, for full-depth mixes cured 7 days.

Mix	Curing	4 days	7 days	14 days	28 days	8 weeks	16 weeks	44 weeks	64 weeks
0.40, 0% SF	0.006	-0.017	-0.023	-0.031	-0.042	-0.053	-0.062	-0.065	-0.068
0.36, 1.8% SF	0.003	-0.017	-0.022	-0.031	-0.039	-0.049	-0.056	-0.059	-0.059
0.43, 1.8% SF	0.009	-0.018	-0.024	-0.033	-0.042	-0.052	-0.060	-0.064	-0.064
0.35, 6.0% SF	0.001	-0.021	-0.028	-0.036	-0.041	-0.048	-0.054	-0.056	-0.054
0.40, 6.0% SF	0.002	-0.021	-0.029	-0.038	-0.044	-0.052	-0.057	-0.060	-0.060
0.45, 6.0% SF	0.005	-0.023	-0.033	-0.043	-0.048	-0.060	-0.067	-0.070	-0.069
0.36, 10.2% SF	0.007	-0.020	-0.026	-0.033	-0.037	-0.043	-0.050	-0.054	-0.054
0.43, 10.2% SF	0.004	-0.027	-0.035	-0.043	-0.048	-0.056	-0.066	-0.071	-0.071
0.40, 12% SF	0.006	-0.020	-0.029	-0.034	-0.040	-0.047	-0.055	-0.059	-0.057

Table B-2. Length change data, %, for overlay mixes cured 3 days.

Mix	Curing	4 days	7 days	14 days	28 days	8 weeks	16 weeks	44 weeks	64 weeks
0.35, 0% SF	0.004	-0.021	-0.028	-0.040	-0.050	-0.066	-0.073	-0.078	-0.078
0.31, 1.8% SF	0.001	-0.021	-0.029	-0.051	-0.051	-0.060	-0.068	-0.071	-0.071
0.38, 1.8% SF	0.002	-0.023	-0.028	-0.041	-0.056	-0.066	-0.075	-0.078	-0.077
0.30, 6.0% SF	0.004	-0.029	-0.035	-0.045	-0.053	-0.061	-0.069	-0.070	-0.069
0.35, 6.0% SF	0.003	-0.028	-0.039	-0.050	-0.061	-0.069	-0.080	-0.081	-0.080
0.40, 6.0% SF	0.000	-0.026	-0.036	-0.049	-0.064	-0.073	-0.079	-0.083	-0.083
0.31, 10.2% SF	0.003	-0.032	-0.041	-0.047	-0.056	-0.065	-0.074	-0.077	-0.076
0.38, 10.2% SF	0.004	-0.032	-0.043	-0.055	-0.064	-0.074	-0.083	-0.085	-0.086
0.35, 12% SF	0.005	-0.035	-0.044	-0.054	-0.063	-0.070	-0.078	-0.081	-0.081

Table B-3. Length change data, %, for slurry mixes cured 3 days.

Mix	Curing	4 days	7 days	14 days	28 days	8 weeks	16 weeks	44 weeks	64 weeks
0.35, 6.0% SF	0.004	-0.028	-0.037	-0.052	-0.062	-0.070	-0.077	-0.079	-0.076
0.31, 10.2% SF	0.001	-0.033	-0.042	-0.052	-0.060	-0.067	-0.074	-0.078	-0.073
0.38, 10.2% SF	0.005	-0.033	-0.044	-0.059	-0.068	-0.075	-0.083	-0.086	-0.085
0.35, 12% SF	0.007	-0.035	-0.045	-0.055	-0.064	-0.071	-0.079	-0.083	-0.081

Table B-4. Length change data, %, for Type K mixes cured 7 days.

Mix	Curing	4 days	7 days	14 days	28 days	8 weeks	16 weeks	44 weeks	64 weeks
0.40, 0% SF	0.016	-0.026	-0.033	-0.043	-0.053	-0.060	-0.069	-0.073	-0.073
0.35, 6.0% SF	0.020	-0.022	-0.030	-0.041	-0.049	-0.053	-0.060	-0.064	-0.064
0.45, 6.0% SF	0.013	-0.027	-0.038	-0.048	-0.058	-0.064	-0.070	-0.076	-0.077
0.40, 12% SF	0.016	-0.023	-0.030	-0.038	-0.044	-0.054	-0.061	-0.066	-0.067

Table B-5. Time to first crack, days, for full-depth mixes (Phase I).

Mix	Specimen 1	Specimen 2	Average
1: 0.40, 0% SF	32	37	35
2: 0.36, 1.8% SF	42	no crack	42*
3: 0.43, 1.8% SF	42	42	42
4: 0.35, 6.0% SF	51	no crack	51*
5: 0.40, 6.0% SF	no crack	no crack	no crack
6: 0.45, 6.0% SF	18	23	21
7: 0.36, 10.2% SF	no crack	no crack	no crack
8: 0.43, 10.2% SF	no crack	no crack	no crack
9: 0.40, 12% SF	no crack	no crack	no crack

Table B-6. Time to first crack, days, for overlay mixes (Phase I).

Mix	Specimen 1	Specimen 2	Average
1: 0.35, 0% SF	25	20	23
4: 0.30, 6.0% SF	8	11	10
6: 0.40, 6.0% SF	13	14	14
9: 0.35, 12% SF	7	11	9

Table B-7. Time to first crack, days, for Type K mixes (Phase I).

Mix	Specimen 1	Specimen 2	Average
1: 0.35, 0% SF	no crack	no crack	no crack
4: 0.30, 6.0% SF	no crack	no crack	no crack
6: 0.40, 6.0% SF	no crack	no crack	no crack
9: 0.35, 12% SF	no crack	no crack	no crack

Table B-8. Time to first crack, days, for full-depth concretes cured for 1 day (Phase II).

w/cm	Silica Fume Content 0%	6%	9%
0.45	33	19	17
	36	14	18
	27	17	11
	27	13	16
	22	23	20
0.40	24	17	30
	26	12	17
	22	23	11
	24	18	22
	31	10	14
0.35	35	13	11
	43	12	23
	22	14	18
	24	28	28
	35	17	21

Table B-9. Time to first crack, days, for full-depth concretes cured for 7 days (Phase II).

w/cm	Silica Fume Content 0%	6%	9%
0.45	33	25	30
	35	20	46
	38	19	28
	40	20	28
	33	16	31
0.40	36	49	51
	24	18	14
	34	25	34
	18	21	55
	50	56	52
0.35	53	29	67
	29	57	32
	32	17	53
	28	37	66
	32	64	30

Table B-10. Compressive strengths, MPa, for Phase II concretes at 1 day.

	Silica Fume Content		
w/cm	0%	6%	9%
0.45	11.4	14.7	12.3
0.40	15.3	16.4	18.3
0.35	23.0	24.5	23.1

1MPa = 145 lbf/in^2

Table B-11. Compressive strengths, MPa, for Phase II concretes at 7 days.

	Silica Fume Content		
w/cm	0%	6%	9%
0.45	24.1	28.6	27.0
0.40	30.8	30.9	35.5
0.35	42.2	41.6	43.8

1MPa = 145 lbf/in^2

Table B-12. Modulus of elasticity, GPa, for Phase II concretes at 1 day.

	Silica Fume Content		
w/cm	0%	6%	9%
0.45	18.4	20.7	18.3
0.40	21.8	22.2	23.0
0.35	26.9	27.1	27.4

1GPa = 0.145 lbf/in^2

Table B-13. Modulus of elasticity, GPa, for Phase II concretes at 7 days.

	Silica Fume Content		
w/cm	0%	6%	9%
0.45	26.9	29.9	27.0
0.40	31.1	29.9	31.5
0.35	35.0	34.8	35.5

1GPa = 0.145 lbf/in^2

Table B-14. Apparent diffusion coefficients for full-depth mixes.

Specimen	% Silica Fume	w/cm	Apparent Diffusion Coefficient, (m^2/sec)
1F-A	0	0.40	4.80E-12
1F-B	0	0.40	3.42E-12
2F-A	1.8	0.36	6.28E-12
2F-B	1.8	0.36	2.94E-12
3F-A	1.8	0.43	7.19E-12
3F-B	1.8	0.43	3.73E-12
4F-A	6	0.35	9.22E-13
4F-B	6	0.35	9.98E-13
5F-A	6	0.40	1.61E-12
5F-B	6	0.40	1.71E-12
6F-A	6	0.45	2.49E-12
6F-B	6	0.45	2.45E-12
7F-A	10.2	0.36	1.22E-12
7F-B	10.2	0.36	8.63E-13
8F-A	10.2	0.43	1.35E-12
8F-B	10.2	0.43	1.34E-12
9F-A	12	0.40	1.07E-12
9F-B	12	0.40	1.09E-12

1 m^2/sec = 10.76 ft^2/sec

Table B-15. Apparent diffusion coefficients for overlay mixes.

Specimen	% Silica Fume	w/cm	Apparent Diffusion Coefficient, (m^2/sec)
1O-A	0	0.35	6.26E-12
1O-B	0	0.35	7.26E-12
2O-A	1.8	0.31	2.31E-12
2O-B	1.8	0.31	2.05E-12
3O-A	1.8	0.38	4.59E-12
3O-B	1.8	0.38	8.07E-12
4O-A	6	0.30	8.92E-13
4O-B	6	0.30	9.45E-13
5O-A	6	0.35	1.20E-12
5O-B	6	0.35	1.53E-12
6O-A	6	0.40	1.86E-12
6O-B	6	0.40	4.09E-12
7O-A	10.2	0.31	6.82E-13
7O-B	10.2	0.31	1.08E-12
8O-A	10.2	0.38	1.50E-12
8O-B	10.2	0.38	1.15E-12
9O-A	12	0.35	5.19E-13
9O-B	12	0.35	7.81E-13

1 m^2/sec = 10.76 ft^2/sec

Table B-16. Apparent diffusion coefficients for slurry mixes.

Specimen	% Silica Fume	w/cm	Apparent Diffusion Coefficient, (m^2/sec)
5SA	6	0.35	1.24E-12
5SB	6	0.35	1.11E-12
7SA	10.2	0.31	8.07E-13
7SB	10.2	0.31	7.71E-13
8SA	10.2	0.38	1.15E-12
8SB	10.2	0.38	1.03E-12
9SA	12	0.35	8.57E-13
9SB	12	0.35	5.61E-13

1 m^2/sec = 10.76 ft^2/sec

Table B-17. Apparent diffusion coefficients for Type K mixes.

Specimen	% Silica Fume	w/cm	Apparent Diffusion Coefficient, (m^2/sec)
1KA	0	0.4	5.78E-12
1KB	0	0.4	3.54E-12
4KA	6	0.35	1.32E-12
4KB	6	0.35	9.41E-13
6KA	6	0.45	2.14E-12
6KB	6	0.45	2.44E-12
9KA	12	0.4	8.72E-13
9KB	12	0.4	9.17E-13

1 m^2/sec = 10.76 ft^2/sec

Table B-18. Compressive strengths of full-depth bridge deck mixes, MPa.

Mix	7-day	28-day	56-day	90-day
1: 0.40, 0% SF	28.9	33.2	40.7	41.9
2: 0.36, 1.8% SF	37.0	44.0	49.3	51.1
3: 0.43, 1.8% SF	27.4	34.5	36.0	40.3
4: 0.35, 6.0% SF	39.9	53.9	59.3	61.1
5: 0.40, 6.0% SF	33.4	43.4	46.6	49.2
6: 0.45, 6.0% SF	25.7	34.8	38.9	40.5
7: 0.36, 10.2% SF	40.8	55.5	58.2	57.6
8: 0.43, 10.2% SF	28.3	39.1	42.7	43.2
9: 0.40, 12% SF	33.5	45.4	44.8	48.3

1MPa = 145 lbf/in^2

Table B-19. Compressive strengths of overlay bridge deck mixes, MPa

Mix	7-day	28-day	56-day	90-day
1: 0.35, 0% SF	43.5	53.2	57.1	59.0
2: 0.31, 1.8% SF	50.5	61.8	68.7	71.9
3: 0.38, 1.8% SF	36.5	44.7	50.2	51.4
4: 0.30, 6.0% SF	52.8	72.7	76.7	79.7
5: 0.35, 6.0% SF	44.2	57.3	58.8	67.3
6: 0.40, 6.0% SF	35.7	48.2	52.5	53.3
7: 0.31, 10.2% SF	54.6	74.8	76.7	81.2
8: 0.38, 10.2% SF	36.9	52.5	58.2	58.6
9: 0.35, 12% SF	48.2	62.9	62.4	65.7

1MPa = 145 lbf/in^2

Table B-20. Compressive strengths of silica fume slurry concretes, MPa.

Mix	7-day	28-day	56-day	90-day
5: 0.35, 6.0% SF	42.0	58.4	64.2	63.3
7: 0.31, 10.2% SF	53.2	63.5	80.3	76.9
8: 0.38, 10.2% SF	41.5	57.8	63.5	61.4
9: 0.35, 12% SF	45.8	63.2	71.3	71.4

1MPa = 145 lbf/in^2

Table B-21. Compressive strengths of Type K mixes, MPa.

Mix	7-day	28-day	56-day	90-day
1: 0.40, 0% SF	35.4	42.1	47.3	47.4
4: 0.35, 6.0% SF	44.6	58.5	63.7	64.5
6: 0.45, 6.0% SF	29.4	40.8	44.2	45.0
9: 0.40, 12% SF	37.7	50.6	52.2	52.4

1MPa = 145 lbf/in^2

Table B-22. Modulus of elasticity for full depth mixes, GPa.

Mix	28 days	90 days
1: 0.40, 0% SF	30.6	35.7
2: 0.36, 1.8% SF	35.4	40.0
3: 0.43, 1.8% SF	29.7	32.8
4: 0.35, 6.0% SF	36.9	38.8
5: 0.40, 6.0% SF	32.9	36.9
6: 0.45, 6.0% SF	30.8	33.9
7: 0.36, 10.2% SF	39.2	39.4
8: 0.43, 10.2% SF	32.8	34.2
9: 0.40, 12% SF	35.6	35.9

1GPa = 0.145 lbf/in^2

Table B-23. Modulus of elasticity for overlay mixes, GPa.

Mix	28 days	90 days
1: 0.35, 0% SF	36.7	38.0
2: 0.31, 1.8% SF	36.0	40.9
3: 0.38, 1.8% SF	32.6	36.0
4: 0.30, 6.0% SF	37.4	41.2
5: 0.35, 6.0% SF	35.4	37.8
6: 0.40, 6.0% SF	33.0	35.6
7: 0.31, 10.2% SF	41.2	42.7
8: 0.38, 10.2% SF	33.3	37.3
9: 0.35, 12% SF	35.6	38.9

1GPa = 0.145 lbf/in^2

Table B-24. Modulus of elasticity for silica fume slurry mixes, GPa.

Mix	28 days	90 days
5: 0.35, 6.0% SF	34.1	38.8
7: 0.31, 10.2% SF	38.3	41.6
8: 0.38, 10.2% SF	35.0	36.9
9: 0.35, 12% SF	36.9	37.8

1GPa = 0.145 lbf/in^2

Table B-25. Modulus of elasticity for Type K mixes, GPa.

Mix	28 days	90 days
1: 0.40, 0% SF	33.8	36.5
4: 0.35, 6.0% SF	34.5	38.3
6: 0.45, 6.0% SF	33.0	32.4
9: 0.40, 12% SF	35.0	36.9

1GPa = 0.145 lbf/in^2

Table B-26. 28-Day bond strengths for overlay mixtures.

Mix	Specimen	Bond, MPa	Failure Zone
1: 0.35, 0% SF	Core 1	1.19	80% parent
	Core 2	1.87	50% parent
	Core 3	1.73	50% parent
	Mean	1.59	
2: 0.31, 1.8% SF	Core 1	1.78	60% parent
	Core 2	1.82	50% parent
	Core 3	2.11	80%parent
	Mean	1.90	
3: 0.38, 1.8% SF	Core 1	2.15	65% parent
	Core 2	1.93	100% overlay
	Core 3	1.80	40% parent
	Mean	1.96	
4: 0.30, 6.0% SF	Core 1	0.97	70% parent
	Core 2	0.92	60% parent
	Core 3	2.30	90% parent
	Mean	1.40	
5: 0.35, 6.0% SF	Core 1	3.07	70% parent
	Core 2	2.35	80% parent
	Core 3	2.81	100% overlay
	Mean	2.74	
6: 0.40, 6.0% SF	Core 1	1.95	100% overlay
	Core 2	1.49	80% parent
	Core 3	2.94	60% parent
	Mean	2.12	
7: 0.31, 10.2% SF	Core 1	2.15	65% parent
	Core 2	0.48	45% parent
	Core 3	2.92	100% parent
	Mean	1.85	
8: 0.38, 10.2% SF	Core 1	2.33	80% parent
	Core 2	1.67	100% parent
	Core 3	2.74	50% parent
	Mean	2.25	
9: 0.35, 12% SF	Core 1	1.73	100% parent
	Core 2	2.77	70% parent
	Core 3	1.93	80% parent
	Mean	2.14	

1MPa = 145 lbf/in^2

Table B-27. 90-day bond strengths for overlay mixtures.

Mix	Specimen	Bond, MPa	Failure Zone
1: 0.35, 0% SF	Core 1	2.88	30% parent
	Core 2	0.66	30% parent
	Core 3	0.66	30% parent
	Mean	1.40	
2: 0.31, 1.8% SF	Core 1	2.50	50% parent
	Core 2	2.66	50% parent
	Core 3	1.95	60%parent
	Mean	2.37	
3: 0.38, 1.8% SF	Core 1	1.69	25% parent
	Core 2	1.72	100% overlay
	Core 3	1.84	20% parent
	Mean	1.75	
4: 0.30, 6.0% SF	Core 1	3.01	60% parent
	Core 2	0.31	10% parent
	Core 3	1.03	50% parent
	Mean	1.45	
5: 0.35, 6.0% SF	Core 1	3.14	60% parent
	Core 2	3.23	100% parent
	Core 3	2.37	90% parent
	Mean	2.91	
6: 0.40, 6.0% SF	Core 1	2.66	25% parent
	Core 2	2.39	25% parent
	Core 3	2.08	50% parent
	Mean	2.38	
7: 0.31, 10.2% SF	Core 1	2.15	60% parent
	Core 2	2.26	75% parent
	Core 3	2.32	100% parent
	Mean	2.25	
8: 0.38, 10.2% SF	Core 1	2.11	100% overlay
	Core 2	2.08	100% parent
	Core 3	2.61	60% parent
	Mean	2.27	
9: 0.35, 12% SF	Core 1	1.49	80% parent
	Core 2	1.89	70% parent
	Core 3	1.84	100% parent
	Mean	1.74	

1MPa = 145 lbf/in^2

Table B-28. Coefficient of thermal expansion (CTE) for full-depth mixes.

Specimen	% Silica Fume	w/cm	CTE, °C^{-1}
1FA	0	0.40	1.29E-05
1FB	0	0.40	1.37E-05
1FC	0	0.40	1.42E-05
		Mean	1.37E-05
4FA	6	0.35	1.29E-05
4FB	6	0.35	1.40E-05
4FC	6	0.35	1.49E-05
		Mean	1.40E-05
6FA	6	0.45	1.31E-05
6FB	6	0.45	1.37E-05
6FC	6	0.45	1.46E-05
		Mean	1.38E-05
9FA	12	0.40	1.28E-05
9FB	12	0.40	1.40E-05
9FC	12	0.40	1.33E-05
		Mean	1.33E-05

1 °C^{-1} = 0.556 °F^{-1}

Table B-29. Coefficient of thermal expansion (CTE) for overlay mixes.

Specimen	% Silica Fume	w/cm	CTE, °C^{-1}
1OA	0	0.35	1.42E-05
1OB	0	0.35	1.33E-05
1OC	0	0.35	1.42E-05
		Mean	1.39E-05
4OA	6	0.3	1.35E-05
4OB	6	0.3	1.31E-05
4OC	6	0.3	1.33E-05
		Mean	1.33E-05
6OA	6	0.4	1.30E-05
6OB	6	0.4	1.31E-05
6OC	6	0.4	1.26E-05
		Mean	1.30E-05
9OA	12	0.35	1.39E-05
9OB	12	0.35	1.33E-05
9OC	12	0.35	1.22E-05
		Mean	1.31E-05

1 °C^{-1} = 0.556 °F^{-1}

APPENDIX C

STATISTICAL ANALYSIS AND MODELING

In this Appendix, the design of the experiments and the results of statistical analyses of the data found in Appendix B are presented. From these analyses, statistical models were constructed using response surface methodology. The models are intended to illustrate the significance of the major variables (i.e. silica fume content and w/cm) and trends in physical properties of concrete with respect to the major variables studied. The models are not meant as predictors of actual values of physical properties to be expected for in-service concretes. Statistical analyses were carried out on drying shrinkage, Phase II cracking data, apparent diffusivity coefficients for chloride ions, compressive strength, and modulus of elasticity. For data which were inconsistent or subject to wide variability, such as the Phase I cracking and the overlay bond strengths, no formal statistical analyses were performed. In cases where only limited data were obtained, comparison analyses were performed.

EXPERIMENTAL DESIGN

Introduction

One of the major advantages in the statistical design of experimental programs is the more efficient use of resources in providing valid results (*26*). Traditionally, experimenters hold all test conditions constant except the one factor they are examining. The variables are tested in sequence rather than in combination. This is rather inefficient and sometimes misleading when testing such materials as concrete, where many mixes would have to be prepared to obtain information on the effects of a single independent variable on the property of interest (response variable). Also, this type of experimental design may obscure interactions among variables. The statistical design of an experimental program employs statistics from the outset. Blocking allows the experimenter to eliminate known and controllable sources of error. Randomization reduces the contaminating effects of uncontrolled (perhaps uncontrollable) sources of error. Designs such as the factorial design or the central composite design allow the examination of combinations of variables which may interact; in the present case, the w/cm and the silica fume content. Once the results are obtained, they can be analyzed and graphically displayed to illustrate the effects of simultaneous changes in the variables on the response. Thus, a statistical approach yields more reliable data while making more efficient use of the resources available.

Response Surfaces and the Central Composite Design

For the analysis of the data generated under this research program, the central composite design was chosen to study the effects of silica fume content and w/cm on the various physical properties of the concrete mixtures. The central composite design is well suited to what is termed "response surface methodology." In this approach, a multivariate relationship between the independent variables and the response variable is developed from multiple regression analysis of the data. Response surface designs are most useful when the factors examined are known to be important, and interest centers on understanding the relationship of a property to these factors and on optimizing these factors. The relationship usually takes the form of a quadratic (i.e. second order) equation. These designs permit efficient estimation of quadratic models and so can identify an optimal condition if it is located inside the experimental region. If it is outside the experimental region, the response surface will identify a direction in which to move in search of the optimal condition. For the case of two independent variables, the model will usually take the form

$$Y = b_0 + b_1 X_1 + b_2 X_2 + b_3 X_1 X_2 + b_4 X_1^2 + b_5 X_2^2 \qquad (C.1)$$

where:

Y = dependent (response) variable

$b_0, b_1, b_2, b_3, b_4, b_5, \ldots$ = regression constants

X_1 = first independent variable

X_2 = second independent variable

It may not be necessary to use all of the terms in the model to explain the relationship adequately. In some cases, transformation of variables (e.g. logarithmic or exponential) may permit better fitting of the data. A three-step iterative process is used to identify an appropriate model for the data by: 1) specifying a model, 2) fitting the model by least-squares techniques, and 3) checking the accuracy of the model. Scatter plots (exploratory data analysis) are examined to specify a model. Typically, model specification proceeds from the simplest to the most complex. At stage one, the most important variable enters the model linearly. The model is then fitted from the data by least-squares regression. Residuals (i.e. the difference between the raw response data and those predicted by the model) are computed and plotted to check the accuracy of the fitted model. If any symmetric structure remains in the residuals, the model is modified by including an additional term, and the procedure is then repeated. More details can be found in Neter et al. (*27*). After a satisfactory equation has been developed, the results are displayed graphically using contour plots. The response variable can be easily viewed as increasing (or decreasing) contours in the region of interest.

Figures C-1a and C-1b illustrate the central composite design for the full-depth and overlay mixtures, respectively. For both figures, the range of silica fume contents is from 0 to 12 percent. For the full-depth mixtures, the range of w/cm is 0.35 to 0.45. For the overlays, the range of w/cm is 0.30 to 0.40. This design has nine points. Four are on the axes; one is at the center; and the remaining four points, which are not on the central axes, are factorial (2^2 full factorial). While the latter points are not integral values of silica fume content, they are required for the design selected from statistical tables (*26)* based on the number of independent observations for the central composite design. For each of the nine points, a different concrete mixture was prepared, with three replicate batches prepared for each mixture. The efficiency of this design can been seen from the fact that if a full factorial were to be performed, then 25 mixes (5 silica fume contents x 5 w/cms) would need to be prepared for each type of concrete. The central composite design was selected instead of the full factorial design because: 1) factorial designs are best used for screening important factors from a large list of candidate factors; here, the two factors are known to be important; and 2) the central composite design has the advantage of constant precision of the fitted response surface regardless of direction; this is not true of the full factorial design. It should be noted that in Phase II of the cracking tendency study, a full factorial design was selected, as it was critical that data be obtained for particular combinations of silica fume content and w/cm in the range of interest.

Comparison Analyses

In the present study, two sets of comparison analyses were performed. In the first set, Type I/II and Type K cements were compared for the full-depth mixtures 1, 4, 6, and 9. In the second set the slurry and dry-densified forms of silica fume were compared for the overlay mixtures 5, 7, 8, and 9. To formally test whether the mean response differs for the two types in each set, an ANOVA was performed and confidence intervals constructed for the difference in mean response. The ANOVA is performed to test whether interaction is present between cement type (or form of silica fume) and mix, i.e., whether the difference in mean response depends on the mix under examination. If this interaction is not statistically significant, one can conclude that interaction is not present and that the difference in mean response is independent of mix. The data are then averaged across the mixes, and a 95% confidence interval for the difference in mean response is constructed. If this interval contains zero, then the mean response does not differ between type of cement (or silica fume). If the interval does not contain zero, then one can conclude that the mean response does differ, and the interval will contain the true difference with 95% confidence. If

interactions between type of cement (or silica fume) are present, 95% confidence intervals may be constructed separately for each mix.

DRYING SHRINKAGE

Shrinkage after 4 Days

Full-Depth Mixtures

Data obtained after 4 days of drying at 23 ± 1.7°C (73.4 ± 3°F) and 50 ± 4 % R.H. were used to develop a statistical model for the relationship among shrinkage, w/cm, and silica fume content for the full-depth mixtures. Results of what are termed "exploratory data analyses" for the full-depth set are presented in Figures C-2a through C-2f. This figure consists of six views of the data which can be used to determine whether there are any trends or anomalies within the data sets. The first view is used to examine the reproducibility of the results and determine whether examination of the data for statistical outliers is warranted. In this case, Figure C-2a shows 4-day shrinkage (SHR4D) for each of the rounds for all 9 mixes. With the possible exception of the last two mixes, the reproducibility is good. Though there appears to be a higher degree of scatter in the values for mixes 8 and 9, the difference between the extreme values and the mean in both cases is within the limit of precision of the method (1S = 0.0084%). Thus there are no outliers. The next two views serve as guidance to the statistician as to which terms to include in the model. Figure C-2b shows shrinkage versus silica fume content for all of the batches. There appears to be a relationship between silica fume content and shrinkage. Figure C-2c shows w/cm on the x-axis. There is less of a clear trend in this case, but the influence of w/cm is such that inclusion in the model is warranted. Figure C-2d shows the central composite design and the shrinkage associated with each mix. The axes of the model can be examined to obtain an estimate of behavior at fixed values of w/cm and silica fume content, these being at w/cm = 0.400 and 6 percent silica fume. Figure C-2e compares the shrinkages for each round of mixes. Examination of this view can be used to determine whether any differences which occurred between the rounds (e.g., change of operators or conditions) had a significant influence on the results. In this case, the means (represented by the tie-line running across the view) are within the expected reproducibility (d2s = 0.014%), and the ranges for all three rounds are comparable. Figure C-2f is used to establish whether there is any trend in the data relating to order of casting. There appears to be no association between shrinkage and the order of casting for these data.

The data were subjected to multiple regression analysis and a statistical model was developed. The model is given as Equation C.2, and the response surface contours are shown in Figure C-3.

$$SHR4D = 0.02336 - 0.00217sf - 0.02006w/cm + 0.00972sf*w/cm - 0.00010sf^2 \quad (C.2)$$

where:

SHR4D = percent shrinkage at 4 days
0.02336 = regression constant
sf = silica fume content, % by mass of cementitious material
w/cm = water-to-cementitious materials ratio

The first two terms are linear in silica fume content and w/cm, the third is an interaction term between silica fume content and w/cm, and the fourth is a quadratic silica fume content term. The model demonstrates that at a fixed w/cm, the shrinkage increases with increasing silica fume content. The model also illustrates an increased sensitivity to changes in the silica fume content at lower silica fume contents. At levels above about 6 percent silica fume, the contours "flatten out" with a slight upwards bend, so increases in the silica fume content have only a minor effect on shrinkage. At silica fume contents up to about 5 percent, there is little influence of w/cm on shrinkage. For higher silica fume contents, shrinkage increases with increasing w/cm.

Overlay Mixtures

Data obtained after four days of drying at 23 ± 1.7°C (73.4 ± 3°F) and 50 ± 4 % R.H. were used to develop a statistical model for the relationship among shrinkage, w/cm, and silica fume content for the overlay mixtures. The results of the exploratory data analyses for this set are presented in Figures C-4a through C-4f. Figure C-4a shows the 4-day shrinkage (SHR4D) for each of the rounds for all nine mixes. With the possible exception of mix 5, the reproducibility is good. As before, the difference between the extreme values and the mean for mix 5 is within the limit of precision of the method (1S = 0.0084%). In addition, statistical testing indicated no outliers. Figure C-4b shows the shrinkage versus silica fume content for all of the batches. There is a fairly strong relationship between silica fume content and shrinkage. Figure C-4c shows w/cm on the x-axis. There is little association indicated between the variables. Figure C-4d shows the central composite design and the shrinkage associated with each mix. While there is a trend across silica fume content at any fixed value of w/cm, there is no clear trend with respect to w/cm at any given silica fume content. Figure C-4e compares the shrinkages for each round of mixes. As for the full-depth set, the ranges are comparable, and there is little difference in overall means between

the rounds. Figure C-4f indicates no association between shrinkage and order of casting for these data.

The data were subjected to multiple regression analysis, and a statistical model was developed. The model is given as Equation C.3; the response surface contours are shown in Figure C-5.

$$SHR4D = 0.02051 + 0.00116sf \quad (C.3)$$

where:

SHR4D = percent shrinkage at 4 days
0.02051 = regression constant
sf = silica fume content, % by mass of cementitious material

This model is much simpler than that for the full-depth mixes, and contains only one term (plus the constant). The single term is linear in silica fume. The response surface contours are given in Figure C-5. Interpretation is straightforward; as the silica fume content is increased at any given w/cm, the shrinkage will increase. There is no effect of w/cm on shrinkage.

Shrinkage after 16 Weeks

Full-Depth Mixtures

Data obtained after 16 weeks of drying at 23 ± 1.7°C (73.4 ± 3°F) and 50 ± 4 % R.H. were used to develop a statistical model for the relationship among shrinkage, w/cm, and silica fume content for full-depth mixtures. Results of exploratory data analyses for the full-depth set are presented in Figures C-6a through C-6f. Figure C-6a shows 16-week shrinkage for each of the rounds for all 9 mixes. No outliers were evident. Figure C-6b shows shrinkage versus silica fume content for all of the batches. There does not appear to be a consistent relationship. Figure C-6c is the same view, this time with w/cm on the x-axis. A trend of increasing shrinkage with increasing w/cm is evident. Figure C-6d shows the central composite design and the shrinkage associated with each mix. Figure C-6e compares the shrinkages for each round of mixes. The ranges are comparable, and means for both rounds are close. Figure C-6f shows no association between strength and casting order.

The data were subjected to multiple regression analysis, and a statistical model was developed. The model is given as Equation C.4, and response surface contours are shown in Figure C-7.

$$SHR16W = 0.05120 - 0.00806sf + 0.02261w/cm + 0.01957sf*w/cm \quad (C.4)$$

where:

SHR16W = percent shrinkage at 16 weeks
0.05120 = regression constant
sf = silica fume content, % by mass of cementitious material
w/cm = water-to-cementitious materials ratio

The model contains three terms (plus the constant). The first two terms are linear in silica fume and w/cm, the third is an interaction term between silica fume and w/cm. The model demonstrates that at a fixed silica fume content the shrinkage increases with increasing w/cm. The model also illustrates an increased sensitivity to w/cm changes at higher silica fume contents. For instance, for a silica fume content of 4 percent, an increase of w/cm of 0.08 is required to change the shrinkage by 0.01%. However, for a silica fume content of 10 percent, the same change in shrinkage occurs with half this much change in w/cm (0.04).

Overlay Mixtures

Data obtained after 16 weeks of drying at 23 ± 1.7°C (73.4 ± 3°F) and 50 ± 4 % R.H. were used to develop a statistical model for the relationship among shrinkage, w/cm, and silica fume content for the overlay mixtures. The results of exploratory data analyses for this set are presented in Figures C-8a through C-8f. Figure C-8a shows 16-week shrinkage for each of the rounds for all 9 mixes. For these data, the ranges between replicate results appear to be generally higher than for the full-depth case; however, no outliers were evident. Figure C-8b shows shrinkage versus silica fume percentage for all the batches. No consistent trend is apparent. Figure C-8c is the same view, this time with w/cm on the x-axis. A nonlinear trend of increasing shrinkage with increasing w/cm is seen. Figure C-8d shows the central composite design and the shrinkage associated with each mix. Figure C-8e compares shrinkages for each round of mixes. The ranges are comparable, and the means for both rounds are fairly close. Figure C-8f shows no association between strength and order of casting.

The data were subjected to multiple regression analysis and a statistical model was developed. The model is given as Equation C.5 and response surface contours are shown in Figure C-9.

$$SHR16W = 0.10707 + 0.00062sf + 0.93486w/cm - 1.19893(w/cm)^2 \quad (C.5)$$

where:

SHR16W = percent shrinkage at 16 weeks
0.10707 = regression constant
sf = silica fume content, % by mass of cementitious material
w/cm = water-to-cementitious materials ratio

The model contains three terms (plus the constant). The first two terms are linear in silica fume content and w/cm; the third is a quadratic term in w/cm. As was seen for the full-depth case, this model demonstrates that at a fixed silica fume content the shrinkage increases with increasing w/cm. The trend of increasing sensitivity towards shrinkage for increasing silica fume content, however, is not seen in this model. What is different is the apparent increase with shrinkage as the silica fume content increases for a given w/cm. However, it should be noted that in most cases only three contours are intercepted as one proceeds from low to high silica fume content. This would represent a change of only 0.006% shrinkage, which is close to the range seen between replicates for most of the mixes. Therefore, for the overlay concrete at 16 weeks' age, it is difficult to attach much significance to the effect of silica fume content on shrinkage based on these data.

Shrinkage after 64 Weeks

Full-Depth Mixtures

After 64 weeks of drying at 23 ± 1.7°C (73.4 ± 3°F) and 50 ± 4 % R.H., the testing was terminated and the final data were used to develop a statistical model for the relationship among shrinkage, w/cm, and silica fume content for the full-depth mixtures. Results of exploratory data analyses for the full-depth set are presented in Figures C-10a through C-10f. As before, this consists of six views of the data to determine if there are any trends or anomalies within the sets. Figure C-10a shows the 64-week shrinkage for each of the rounds for all 9 mixes. With the possible exception of the mixes 1 and 6, the reproducibility is good for all replicates. No statistical outliers were found. Figure C-10b shows shrinkage versus silica fume content for all of the batches. There does not appear to be a relationship between silica fume content and shrinkage. Figure C-10c is the same view, this time with w/cm on the x-axis. There is more of a trend in this case. Figure C-10d shows the central composite design and the shrinkage associated with each mix. Figure C-10e compares shrinkages for each round of mixes. The ranges and means for the three rounds vary, but the differences are within the known precision of the testing. Figure C-10f shows no consistent association between shrinkage and order of casting.

The data were subjected to multiple regression analysis, and a statistical model was developed. The model is given as Equation C.6, and response surface contours are shown in Figure C-11.

$$SHR64W = 0.0486 - 0.0081sf + 0.0346w/cm + 0.0199sf*w/cm \quad (C.6)$$

where:

SHR64W = percent shrinkage at 64 weeks
0.0486 = regression constant
sf = silica fume content, % by mass of cementitious material
w/cm = water-to-cementitious materials ratio

The model contains three terms (plus the constant). The first two terms are linear in silica fume content and w/cm; the third is an interaction term between silica fume content and w/cm. This model takes the same form as that for the 16-week shrinkage of the full-depth mixtures (Eqn. C.4). As seen from the contours in Figure C-11, the model demonstrates that at a fixed level of w/cm the dependence of shrinkage on increasing silica fume content is not sharp. This can be compared with the contours for the 4-day shrinkage model (see Figure C-3), which showed a much stronger dependence of shrinkage on silica fume content. Finally, in 4-day, 16-week, and 64-week models, shrinkage increases with increasing w/cm, especially at the higher silica fume contents.

Overlay Mixtures

After 64 weeks of drying at 23 ± 1.7°C (73.4 ± 3°F) and 50 ± 4% R.H., the testing was terminated and the final data were used to develop a statistical model for the relationship among shrinkage, w/cm, and silica fume content for the overlay mixtures. The results of exploratory data analyses for the full-depth set are presented in Figures C-12a through C-12f. Figure C-12a shows the 16-week shrinkage for each of the rounds for all 9 mixes. The reproducibility appears good for all mixes, and there were no outliers. Figure C-12b shows the shrinkage versus silica fume content for all of the batches. As for the full-depth concrete, there does not appear to be a strong relationship between silica fume content and shrinkage. Figure C-12c is the same view, this time with w/cm on the x-axis. There is somewhat more of a trend in this case. Figure C-12d shows the central composite design and the shrinkage associated with each mix. Figure C-12e compares the shrinkages for each round of mixes. The ranges are comparable, and the means for the three rounds are close. Figure C-12f shows no association between shrinkage and order of casting.

The data were subjected to multiple regression analysis, and a statistical model was developed. The model is given as Equation C.7, and response surface contours are shown in Figure C-13.

$$SHR64W = -0.10608 + 0.00053sf + 0.92045w/cm - 1.14241(w/cm)^2 \quad (C.7)$$

where:

SHR64W = percent shrinkage at 64 weeks
- 0.10608 = regression constant
sf = silica fume content, % by mass of cementitious material
w/cm = water-to-cementitious materials ratio

The model contains three terms (plus the constant). The first term is linear in silica fume content, the second linear in w/cm, and the final term is a quadratic in w/cm. This model is qualitatively identical to the 16-week overlay shrinkage model (eqn. C.5), with a stronger dependence of shrinkage on w/cm than on silica fume content.

In summary, the early-age (4-day) shrinkage models show a much stronger association with silica fume content than do the later age (i.e., 16-week and 64-week) models. If ultimate shrinkage is a design concern, then the effect of silica fume content is expected to be relatively minor (as compared with w/cm). However, at early ages (especially if concretes are not properly cured), concretes containing silica fume may exhibit greater levels of shrinkage as the silica fume content is increased. This may help to explain concern with silica fume mixes early in the life of the concrete with respect to those parameters which contribute to cracking. Behavior with respect to cracking under conditions of restraint is discussed later in this Appendix

Comparison Analyses of Drying Shrinkage

Type I/II vs. Type K Cement Concretes

Analyses of variance were carried out on the shrinkage data for the TypeI/II and Type K mixes from age 4 days to 64 weeks. Only mixes 1, 4, 6, and 9 from the full-depth set were subjected to the analyses, as Type K cement concretes were prepared only at the extremes of the two independent variables, and using only the full-depth concrete mix design. First, the results indicated no dependence of shrinkage difference on the particular mix used. That is, the same direction of difference was noted for all mixtures. Secondly, the use of Type K cement was found to result in a significantly higher shrinkage at all test ages. The mean difference between Type K

and Type I/II cement mixes (shown as Type K-Type I/II) as well as the 95% confidence interval about the mean, are given in Table C-1. As noted previously, if application of the confidence interval to the mean difference does not change the sign of the difference, then the difference can be considered to be significant at the confidence limit chosen (95% in this case). It is seen that even at the negative end of the confidence interval the difference is still positive, indicating that for all of these mixes we can be 95% certain that Type K will yield a shrinkage greater than Type I/II cement. On first inspection, this appears to be in conflict with the use of Type K cement as a "shrinkage compensating" product, and with the cracking tendency test data (Phase I) for Type K mixes, where no cracking was found in any of the specimens prepared with the Type K cement. However, while there is an initial expansion of concrete made with Type K cement, this occurs generally within the first 24 hours after casting. Beyond this point, the unrestrained drying shrinkage (measured starting at 24 hours) of Type K concretes is comparable to that of conventional concretes. The benefit of Type K cement is that its initial expansion induces compressive stresses in the concrete member due to restraint of reinforcement, so that these compressive stresses must subsequently be overcome by drying shrinkage before crack-producing tensile streses can develop. Thus, Type K cement concrete can actually show a higher unrestrained drying shrinkage, and, because of the initial expansion, still function as intended.

Dry Densified vs. Slurry Forms of Silica Fume

Analyses of variance were carried out on the shrinkage data for concretes made with dry-densified and slurry forms of silica fume for ages ranging from 4 days to 64 weeks. Only mixes 5, 7, 8, and 9 of the overlay concretes (i.e., those having the highest silica fume contents) were subjected to the analyses, as it was felt that if no differences were found with these mixtures, there would be no reason to expect differences for mixtures having lower silica fume contents. As for the previous analysis, the results indicated no dependence of shrinkage difference on the particular mix used. Secondly, for all test ages (except 2 weeks) there was no significant difference in shrinkage between the two forms of silica fume. The mean difference between slurry and densified silica fume mixes (shown as Slurry-Densified) as well as the 95% confidence interval about the mean, are given in Table C-2. It is seen that for all ages (except 2 weeks) the confidence interval exceeds the mean value of the difference, indicating that for all of these mixes we can be 95% certain that no difference exists. Since there is no physical reason why a difference should be significant at 2 weeks and not at earlier or later ages, this can be treated as an anomaly.

CRACKING TENDENCY (PHASE II STUDY)

As a first step in analyzing the data from Phase II of the cracking study, the data in Tables B-8 and B-9 were combined to form a full data set containing the results obtained at both 1 and 7 days of curing. This full data set consists of 18 "conditions," that is, 3 w/cms x 3 silica fume contents x 2 curing times. As noted in Appendix B, there were five replicate specimens for each condition studied. As was done for many of the statistical analyses in this study, a log transformation of the data was carried out. This helped to stabilize the variance and make the data more normally distributed, it being an assumption of ANOVA that the variance is constant and the data are normally distributed. Results are shown in Table C-3, which shows the ANOVA statistics for this analysis. A level of significance of 95% ($\alpha = 0.05$) was selected to establish significance of the factors. If the probability statistic (P_r) shown in the table is less than 0.05, there is a low probability that the effect would have occurred purely by chance, and one may conclude that the factor is significant. From the F value and P_r for the ANOVA as a whole, it may be concluded that the "null hypothesis" (i.e., all 18 conditions produce the same mean days to cracking) is rejected and that one or more factors are significant. The three factors significant at the 95% confidence level ($P_r < 0.05$), in order of decreasing significance, are curing time, silica fume content, and the interaction between curing time and silica fume content. For the mixtures cured for one day, the mean time for days-to-cracking was 21 days. Conversely, for the mixtures cured for seven days, the mean time-to-cracking was 36 days. As the effect of curing time was highly influential, and as the interaction of silica fume content and curing time was also significant, separate analyses were then carried out on the separate data sets for each curing time.

Mixtures Given One Day of Moist Curing

ANOVA results for the specimens given one day of curing are shown in Table C-4. Again, as for the full data set, a 95% confidence level was selected as the significance criterion. From examination of the results, the only significant factor appears to be the silica fume content of the concrete. The data were then further analyzed to determine for which pairs of the means (i.e., 0 % - 6%, 0% - 9%, and 6% - 9%) was the difference between the two means significant. To carry out these multiple comparisons, Tukey's Studentized Range Test (27) was performed. This test can be used for both hypothesis testing of the simple difference between the means, and to construct confidence limit estimates for the difference. The latter is more instructive, and results are presented in Table C-5. Shown are the mean differences and the confidence interval ($\pm$ 0.263 for all cases). If the confidence interval does not contain zero, it may be concluded that a significant difference exists between the two means under examination. This is true for the 0% - 6% and 0% -

9% cases. The 6% - 9% comparison does include zero when the confidence limit of ± 0.263 is applied to the mean of 0.0956; therefore, there is no significant difference in this case. We may conclude that the addition of 6 or 9 percent silica fume to a non-silica fume mix will effect a significant reduction in days-to-cracking for mixtures cured for one day, but increasing the silica fume content to 9 percent starting with a mix already containing 6 percent silica fume will not appreciably decrease the time-to-cracking.

Mixtures Given Seven Days of Moist Curing

ANOVA results for the specimens given seven days of moist curing are shown in Table C-6. Again, as for the full data and one-day cure data sets, a 95% confidence level was selected as the significance criterion. The P_r value for the model is not sufficiently low (< 0.05) to reject the null hypothesis, so we may conclude that the mean time-to-cracking after seven days of curing is not significantly different. This is verified by examination of the P_r values for each of the factors, none of which is significant at the 95% confidence level.

To summarize, results of the more extensive series of restrained cracking tendency tests carried out in Phase II of this study reinforce the widely recognized belief that proper curing is essential to obtain acceptable concrete performance. The mean time-to-cracking of the test specimens was delayed by over 2 weeks when curing was extended from one to seven days. After one day of curing, the tendency of the concretes to crack is sensitive to the silica fume content, and cracking occurs at earlier ages when the concrete contains silica fume. After seven days of moist curing, there is no assignable effect of any of the factors studied on time-to-cracking.

CHLORIDE DIFFUSIVITY

Full-Depth Mixtures

Data obtained from concrete slabs using exposure and sampling procedures described in Appendix B for the chloride ion diffusivity testing were used to develop a statistical model for the relationship among chloride ion diffusivity, w/cm, and silica fume content for the full-depth mixtures. Results of exploratory data analyses for the full-depth set are presented in Figures C-14a through C-14f. The nature of diffusivity data, which can span a number of orders of magnitude, indicated a logarithmic transform of the data to be appropriate prior to modeling. Accordingly, the apparent diffusivity coefficients are presented as their $\log_{10}$ counterparts in Figure C-14. While not immediately obvious from a cursory examination of the data in Figure C-14a, mix 2 round A

and mix 3 round A were found to represent outlier values. This was discovered after initial construction of linear models and obtaining the standardized difference in the fitted values for fits including and excluding data points using a "dffits" procedure (*27*). The final models were then developed excluding these data points. Figure C-14b shows log D_c versus silica fume content for all of the batches. There is a consistent trend of decreasing diffusivity with increasing silica fume content. Figure C-14c is the same view, this time with w/cm on the x-axis. There is no clear trend in this case. Figure C-14d shows the central composite design and the apparent diffusivity coefficient associated with each mix. Figure C-14e compares the apparent diffusivities for each round of mixes. The fact that the ranges are comparable and means for both rounds are close indicates that there was no trend which occurred over the two weeks when the specimens were cast. Figure C-14f reinforces this, as it shows no association between strength and order of casting.

The data were subjected to multiple regression analysis, and a statistical model was developed. The model is given as Equation C.8, and the response surface contours are shown in Figure C-15.

$$LOG_{10}DC = 0.4559 - 0.0923sf + 2.9474w/cm + 0.0036sf^2 \qquad (C.8)$$

where:

$LOG_{10}DC$ = base 10 logarithm of apparent diffusivity coefficent to chloride ions
0.4559 = regression constant
sf = silica fume content, % by mass of cementitious material
w/cm = water-to-cementitious materials ratio

A model linear in silica fume content and w/cm with a single quadratic term in silica fume content was found to provide an adequate representation of these data. The model yields D_c in log form, the anti-logarithm being taken to construct the surface contours shown in Figure C-15. This model graphically illustrates the effect of silica fume on chloride diffusivity. For any given w/cm ratio, as silica fume content is increased the apparent diffusivity drops. The most sensitive region is in the lower range of silica fume contents. Here the contour lines are "tighter" and, much like a topographical map, indicate that the slope is steeper. That is, the apparent diffusivity changes at a faster rate as the silica fume content is increased. At silica fume contents over 4 to 6 percent, it takes a much greater addition to effect a large change in apparent diffusivity. A point of diminishing returns may be reached at silica fume contents over about 6 percent. In fact, at the lower w/cm values, the apparent diffusivity is relatively insensitive to increases in the silica fume content above 6 percent. From the contour plot it can also be seen that the effect of w/cm is much less than that of silica fume content. The effect of

w/cm is strongest at very low silica fume contents. For any fixed silica fume content, the effect of w/cm on apparent diffusivity coefficient is more linear. That is, we find approximately the same change in apparent diffusivity coefficient at any given value of w/cm. Again, however, at lower silica fume contents, the contours are much tighter, a larger range of diffusivity being encompassed by the same range of w/cm. For silica fume contents over 5 percent, there is only a small effect of w/cm on D_c.

Overlay Mixtures

The overlay diffusivity model was somewhat more direct than the full-depth model, as no outliers were detected and no quadratic term was necessary. The results of an exploratory data analysis for the overlay set are presented in Figures C-16a through C-16f. As for the full-depth concretes, a log transformation of the data was used. Figure C-16a shows the apparent diffusivity coefficient (on a log scale) for each of the rounds for all 9 mixes. Figure C-16b shows log D_c versus silica fume content for all of the batches. There is a consistent trend of decreasing apparent diffusivity coefficient with increasing silica fume content. Figure C-16c is the same view, this time using w/cm on the x-axis. The trends are less clear in this case. Figure C-16d shows the central composite design and the apparent diffusivity coefficient associated with each mix. Figure C-16e compares the apparent diffusivities for each round of mixes. The fact that the ranges are comparable and means for both rounds are close indicates that there was no trend which occurred over the two weeks when the specimens were cast. Figure C-16f reinforces this, as it shows no association between apparent diffusivity coefficient and order of casting.

The data were subjected to multiple regression analysis, and a statistical model was developed. The model is given as Equation C.9, and response surface contours are shown in Figure C-17.

$$LOG_{10}DC = 0.1241 - 0.0756sf + 4.5629w/cm \qquad (C.9)$$

where:

$LOG_{10}DC$ = base 10 logarithm of apparent diffusivity coefficent
0.1241 = regression constant
sf = silica fume content, % by mass of cementitious material
w/cm = water-to-cementitious materials ratio

A model linear in silica fume content and w/cm was found to provide an adequate representation of these data. With the exception of the curvature induced by the quadratic term in the full-depth model, the contour plots (Figure C-17) for the overlay model follow a trend

similar to that seen for the full-depth mixtures. The overlay mixes are more sensitive overall to the effects of silica fume; the range of apparent diffusivity coefficients encompassed by the contours from 0 to 12 percent fume is 75 x 10^{-13} m^2/sec vs approximately 50 x 10^{-13} m^2/sec for the full-depth mixes. For any given w/cm ratio, as the silica fume content is increased, the apparent diffusivity coefficient decreases. The most sensitive region is in the lower range of silica fume contents. Here the contour lines are "tighter" and, much like a topographical map, indicate that the slope is steeper. That is, the apparent diffusivity coefficient changes at a faster rate as the silica fume content is increased. At silica fume contents over 4 to 6 percent, it takes a much greater addition to effect a large change in the apparent diffusivity coefficient. For any fixed silica fume content, the apparent diffusivity coefficient increases with an increase in w/cm. This is especially apparent at the lowest levels of silica fume (4 percent or less). At higher silica fume contents, there is only a one- or two-step increase in apparent diffusivity coefficient over the entire range of w/cm included in the study.

Comparison Analyses of Chloride Diffusivities

Type I/II vs. Type K Cement Concretes

Analyses of variance were carried out on mixes 1, 4, 6, and 9 from the full-depth set where comparisons could be made between the Type I/II and Type K cements. Statistical techniques employed were identical to those used for the drying shrinkage comparisons. First, the results indicated no dependence of difference between apparent diffusivity coefficients on the particular mix used. Since specimens were tested at only one age (180 days), only a single comparison is made. The mean difference between Type K and Type I/II cement mixes is 0.89 (Type K-Type I/II). The 95% confidence interval (obtained from the statistical analysis) is $\pm$ 7.72. As the confidence interval encompasses zero, it can be concluded that there is no significant difference between diffusivity coefficients of similar Type I/II and Type K mixes. This means that use of Type K cement will not offer any significant advantages (or disadvantages) over Type I/II cement with regards to chloride diffusivity.

Dry-Densified vs. Slurry Forms of Silica Fume

Analyses of variance were also carried out on chloride diffusivity data for concretes (mixes 5, 7, 8, and 9) produced with dry-densified and slurry forms of silica fume. As for the full-depth concretes, the results indicated no dependence of diffusivity difference on the particular mix used. Secondly, there was no significant difference in diffusivity between the two forms of silica fume.

The mean difference between densified and slurry mixes was -1.14 (slurry-densified). The 95% confidence interval (obtained from statistical analysis) is ± 2.19. As the confidence interval encompasses zero, it can be concluded that there is no significant difference between apparent diffusivity coefficients of similar densified and slurry silica fume mixes.

COMPRESSIVE STRENGTH

28-Day Results

Full-Depth Mixtures

Data obtained after 28 days of moist curing were used to develop a statistical model for the relationship among compressive strength, w/cm, and silica fume content for the full-depth mixtures. The results of exploratory data analyses for the full-depth set are presented in Figures C-18a through C-18f. Figure C-18a shows 28-day strength (STR28) for each of the rounds for all 9 mixes. With the possible exception of mix 8, the reproducibility is good. All three rounds of mix 8 were retained for the analysis, as the criteria for statistical outliers were not met. Figure C-18b shows the strength versus silica fume content for all of the batches. There does appear to be a relationship between silica fume content and strength. Figure C-18c shows w/cm on the x-axis. There is a fairly clear trend in this case, an increase in w/cm leading to a decrease in strength, as would be expected. Figure C-18d shows the central composite design and the strength associated with each mix. Figure C-18e compares the strength for each round of mixes. The fact that the ranges are comparable and the means for each round are close indicates that there was no trend which occurred over the three weeks when the specimens were cast. Figure C-18f reinforces this, as it shows no association between strength and order of casting.

The data were subjected to multiple regression analysis, and a statistical model was developed. The model is given as Equation C.10, and response surface contours are shown in Figure C-19.

$$STR28 = 153.07686 + 6.08635sf - 479.562w/cm - 11.40409sf*w/cm - 0.10734(sf)^2 + 453.93748(w/cm)^2 \quad (C.10)$$

where:

STR28 = 28-day compressive strength (MPa)
153.07686 = regression constant
sf = silica fume content, % by mass of cementitious material

w/cm = water-to-cementitious materials ratio

The model contains five terms (plus the constant). The first term is linear in silica fume content, the second is linear in w/cm, the third term is a cross product, and the fourth and fifth terms are quadratic in silica fume content and w/cm, respectively. It may be seen from Figure C-19 that at any given w/cm ratio, as the silica fume content increases the strength increases. This is strictly true, however, only at the lowest w/cm ratios included (below about 0.375). For higher ratios, a plateau effect can be seen. For instance, at a w/cm of 0.400, 34 MPa (~5000 lbf/in^2) can be obtained with a very low silica fume content; 38 MPa (5500 lbf/in^2) is obtained at a silica fume content between 1 and 2 percent, and 42 MPa (6,100 lbf/in^2) at a silica fume content between 4 and 5 percent. To obtain 44 MPa (6,500 lbf/in^2), however, requires a silica fume content of nearly 8 percent. Further increases in silica fume content beyond that point offer little additional increase in strength. As w/cm is increased above 0.400, the "ultimate" strength which can be achieved decreases. There is no such "plateau" effect seen for w/cm. At any given silica fume content, an increase in w/cm will lead to a decrease in strength. Strength is somewhat more sensitive to changes in w/cm at the lower levels of w/cm, but not dramatically so. Finally, at silica fume contents over 8 percent, the strength is more sensitive to changes in w/cm.

Overlay Mixtures

Data obtained after 28 days of moist curing were used to develop a statistical model for the relationship among compressive strength, w/cm, and silica fume content for the overlay mixtures. The results of exploratory data analyses for the full-depth set are presented in Figures C-20a through C-20f. Figure C-20a shows the 28-day strength (STR28) for each of the rounds for all 9 mixes. No statistical outliers were detected. The remaining views are similar to those for the full-depth set. As for the full-depth mixes, the ranges and means for the three rounds are comparable, and there is no trend of strength with order of casting, so the data appear to be well behaved.

The data were subjected to multiple regression analysis and a statistical model was developed. The model is given as Equation C.11 and the response surface contours are shown in Figure C-21.

$$STR28 = 143.24269 + 1.02732sf - 260.7901w/cm \quad (C.11)$$

where:

STR28 = 28-day compressive strength (MPa)

143.24269 = regression constant
sf = silica fume content, % by mass of cementitious material
w/cm = water-to-cementitious materials ratio

The model contains two linear terms (plus the constant), and therefore represents a plane in three dimensional space. Hence, the contour plots in Figure C-21 are a series of parallel straight lines. For any given w/cm ratio, the strength increases linearly with silica fume content. Likewise, for any given silica fume content, the w/cm ratio increases linearly with decreasing strength. In contrast to the full-depth mixture model, there is no plateau effect. However, the contours are rather shallow, and at any given level of w/cm, the difference over the entire range of silica fume is not greater than 10 MPa (1,500 lbf/in^2).

90-Day Results

Full-Depth Mixtures

Data obtained after 90 days of moist curing were used to develop a statistical model for the relationship among compressive strength, w/cm, and silica fume content for the full-depth mixtures. The results of exploratory data analyses for the full-depth concretes are presented in Figures C-22a through C-22f. Figure C-22a shows the 90-day strength for each of the rounds for all 9 mixes. It was observed that the variance tended to increase with an increase in mean value. For this reason, a log transformation was made in the subsequent analyses to satisfy the assumption of constant variance for regression modeling. Figure C-22b shows the strength versus silica fume content for all of the batches. Figure C-22c is the same view, this time with w/cm on the x-axis. Figure C-22d shows the central composite design and the strength associated with each mix. Figure C-22e compares the strengths for each round of mixes. The fact that the ranges are comparable and the means for each round are close indicates that there was no trend which occurred over the three weeks when the specimens were cast. Figure C-22f reinforces this, as it shows no association between strength and casting order.

The data were subjected to multiple regression analysis, and a statistical model was developed. The model is given as Equation C.12, and response surface contours are shown in Figure C-23.

$$LnSTR90 = 5.25823 + 0.04534sf - 3.81934w/cm - 0.00284(sf)^2 \quad (C.12)$$

where:

LnSTR90 = natural logarithm of 90-day compressive strength

5.25823 = regression constant
sf = silica fume content, % by mass of cementitious material
w/cm = water-to-cementitious materials ratio

The model contains three terms (plus the constant). Two terms are linear, one each for silica fume content and w/cm; the third is a quadratic silica fume content term. The model is similar to that for the 28-day full-depth strength, although the 90-day model uses fewer terms. The plateau effect is again demonstrated; that is, strength increases up to a certain silica fume content beyond which further additions have little effect. As would be expected, at any given silica fume content, an increase in w/cm results in a decrease in strength.

Overlay Mixtures

Data obtained after 90 days of moist curing were used to develop a statistical model for the relationship among compressive strength, w/cm, and silica fume content for overlay mixtures. The results of exploratory data analyses for the full-depth set are presented in Figures C-24a through C-24f. The first view shows the 90-day strengths (STR90) for each of the rounds for all 9 mixes. No statistical outliers were detected, and logarithms were taken for subsequent analyses. The remaining views are similar to those for the full-depth concretes.

The data were subjected to multiple regression analysis, and a statistical model was developed. The model is given as Equation C.13, and response surface contours are shown in Figure C-25.

$$LnSTR90 = 5.61945 + 0.03180sf - 4.47741w/cm - 0.00177(sf)^2 \quad (C.13)$$

where:

LnSTR90 = natural logarithm of 90-day compressive strength
5.61945 = regression constant
sf = silica fume content, % by mass of cementitious material
w/cm = water-to-cementitious materials ratio

The model contains three terms (plus the constant) and is qualitatively identical to that for the 90-day full-depth mixtures. Two terms are linear, respectively, in silica fume content and w/cm; the third is a quadratic silica fume content term. The model is qualitatively similar to that for the 28-day strength for the full-depth concretes, although the 90-day model uses fewer terms. The plateau effect is again demonstrated; that is, the strength increases up to a certain silica fume content, beyond which further increases have little effect. As would be expected, at a given silica

fume content, an increase in w/cm results in a decrease in strength. This model differs from the 28-day model for strength of overlay concrete in that the plateau effect was not seen in the 28-day model, but is present in the 90-day model. It is difficult to assign any particular physical cause to explain the difference between these two models for strength of overlay concrete. It is likely that the extra term simply improves the mathematical fit of the data, although a plateau effect is a reasonable outcome.

In summary, the strength models show the expected association of both w/cm and silica fume content with compressive strength. In all of the models, the strength increases with a decrease in w/cm. In one case (28-day full-depth concrete), there is an increased sensivity of strength to changes in w/cm at higher silica fume contents. In the remaining three cases modeled, the sensitivity was fairly constant across the range of silica fume contents studied. Likewise, in three out of the four models, a plateau effect was seen as the silica fume content increased. That is, beyond silica fume contents of about 6 percent, there was much less of an increase in strength as silica fume content was increased. Therefore, there is a point of diminishing returns at a silica fume content of approximately 6 percent.

Comparison Analyses of Compressive Strength

Type I/II vs. Type K Cement Concretes

Analyses of variance were carried out on the compressive strength data for the TypeI/II and Type K mixes for test ages of 7, 28, 56, and 90 days. As for the previous comparisons, only mixes 1, 4, 6, and 9 of the full-depth concretes were subjected to the analyses, as Type K cement concretes were prepared only at the extremes of the two independent variables, and using only the full-depth concrete mix design. First, results indicated no dependence of compressive strength difference on the particular mix used. That is, the same direction of difference was noted for all mixtures. Secondly, the use of Type K cement was found to result in a significantly higher compressive strength at all test ages. The mean difference between Type K and Type I/II cement mixes (shown as Type K-Type I/II) as well as the 95% confidence interval about the mean, are given in Table C-7. It is seen that even at the negative end of the confidence interval the difference is still positive, indicating that for all of these mixes we can be 95% certain that Type K will yield a strength greater than Type I/II cement. Average difference over all ages and mixtures is 5.4 MPa (783 lbf/in.^{2}).

Dry Densified vs. Slurry Forms of Silica Fume

Analyses of variance were carried out on the compressive strength data for the concretes produced with dry densified and slurry forms of silica fume for test ages of 7, 28, 56, and 90 days. Only mixes 5, 7, 8, and 9 of the overlay concretes (i.e., those having the highest silica fume contents) were subjected to the analyses, as it was felt that if no differences were found with these mixtures, there would be no reason to expect differences for mixtures having lower silica fume contents. Results for the analysis of the slurry and dry densified forms of silica fume were not clear cut with respect to strength at all test ages. ANOVA indicated no significant mean differences between the two forms of fume at 7, 28, and 90 days. However, the analysis indicated that at 56 days there was a significant mean difference. This is illustrated in Table C-8, which shows the same statistics for this comparison as for the previous comparisons of Type K and Type I/II. It can be seen that for the 7, 28, and 90 day results the sign of the mean difference changes when the confidence interval is added to (or subtracted from) the mean difference. Thus, there is no significant difference between the two forms of silica fume in these cases. However, for the 56 day results, when the confidence interval (4.37 MPa[633 lbf/in^2]) is subtracted from the mean (5.83 MPa [845 lbf/in^2]) the result (i.e. 1.46 MPa [212 lbf/in^2]) is still a positive difference, indicating that the slurry form of silica fume results in a higher compressive strength at this test age. While this was the case for all of the 56-day mixtures, it is difficult to identify a physical explanation for this result.

ELASTIC MODULUS

28-Day Results

Full-Depth Mixtures

Data obtained after 28 days of moist curing were used to develop a statistical model for the relationship among modulus of elasticity, w/cm, and silica fume content for full-depth mixtures. The results of exploratory data analyses for the full-depth concretes are presented in Figures C-26a through C-26f. Trends are evident with respect to w/cm and silica fume content, and there are no anomalies in the data. The regression model is given as Equation C.14, and the response surface contours are shown in Figure C-27.

$$MOD28 = 60.61691 + 0.41312sf - 73.65846w/cm \qquad (C.14)$$

where:

MOD28 = 28-day elastic modulus (GPa)
60.61691 = regression constant
sf = silica fume content, % by mass of cementitious material
w/cm = water-to-cementitious materials ratio

The model contains two linear terms (plus the constant), and represents a plane in three dimensional space. Hence, the contour plots in Figure C-27 are a series of parallel straight lines. For any given w/cm ratio, the modulus of elasticity increases linearly with silica fume content. Likewise, for any given silica fume content, the modulus of elasticity increases linearly with decreasing w/cm.

Overlay Mixtures

Data obtained after 28 days of moist curing were used to develop a statistical model for the relationship among modulus of elasticity, w/cm, and silica fume content for the overlay mixtures. The results of exploratory data analyses for the overlay concretes are presented in Figures C-28a through C-28f. The trends are less evident with respect to silica fume content, but the w/cm still shows a strong effect. No outliers were discovered in the data. The regression model is given as Equation C.15, and the response surface contours are shown in Figure C-29.

$$MOD28 = 142.17252 + 2.29306sf - 567.7978w/cm - 4.97355sf*w/cm - 0.02848(sf)^2 + 731.93044(w/cm)^2 \quad (C.15)$$

where:

MOD28 = 28-day modulus of elasticity (GPa)
142.17252 = regression constant
sf = silica fume content, % by mass of cementitious material
w/cm = water-to-cementitious materials ratio

The model contains five terms (plus the constant). The first term is linear in silica fume content, the second is linear in w/cm, the third term is a cross product, and the fourth and fifth terms are quadratic in silica fume content and w/cm, respectively. The model is more complex than that for the 28-day modulus of elasticity of the full-depth concretes. A plateau effect similar to that seen for the 28-day full-depth concrete strength model is apparent here. It is of interest that the models of modulus of elasticity are exactly reverse to the models of strength for

the same mixtures. That is, while the model of full-depth concrete strength is quadratic, the model of full-depth concrete modulus of elasticity is linear, and while the model of overlay concrete strength is linear, the model of overlay concrete modulus of elasticity is quadratic. Since many research studies have established rather definite relationships between compressive strength and modulus, there appears to be no physical explanation of why they would follow different models. Again, it is believed this is simply due to the extra terms in some models enabling reduction of the residuals in the model. Similar outcomes were seen for the models of 90-day modulus of elasticity for the full-depth and overlay concretes (not shown). The model of full depth concretes was linear in w/cm only (no effect of silica fume content), and the model of overlay concrete was linear in both w/cm and silica fume content. These contrasted with the model of the 90-day strength data, which was linear in silica fume content and w/cm and quadratic in silica fume content for both the full-depth and overlay concretes.

Comparison analyses were also carried out on modulus of elasticity for the Type K and Type I/II cement concretes and the slurry and densified forms of silica fume. No significant differences in modulus of elasticity were found between the two types of cement or two forms of silica fume.

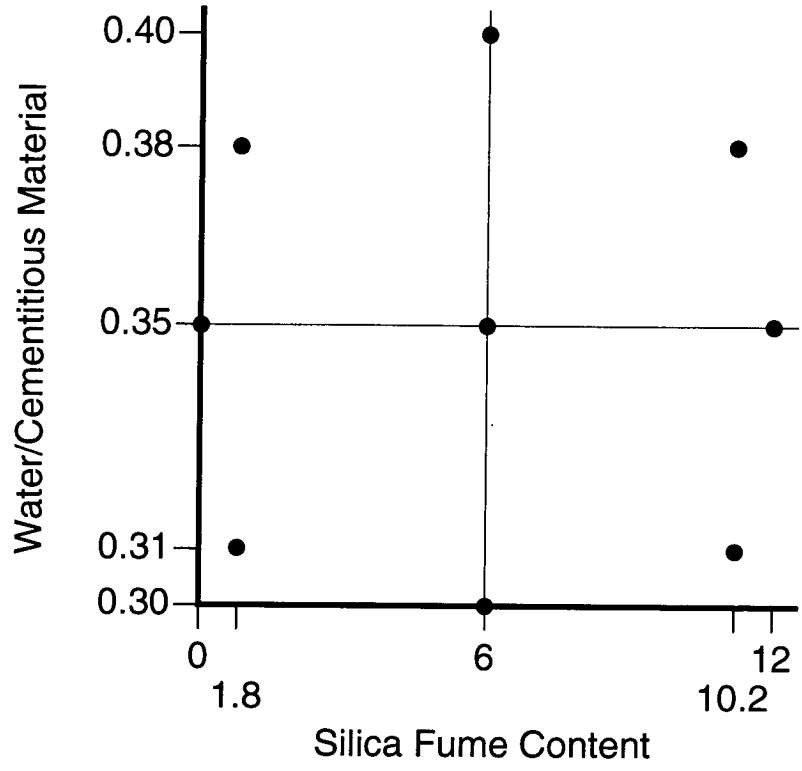

Figure C-1a. Central-composite design for full-depth mixtures.

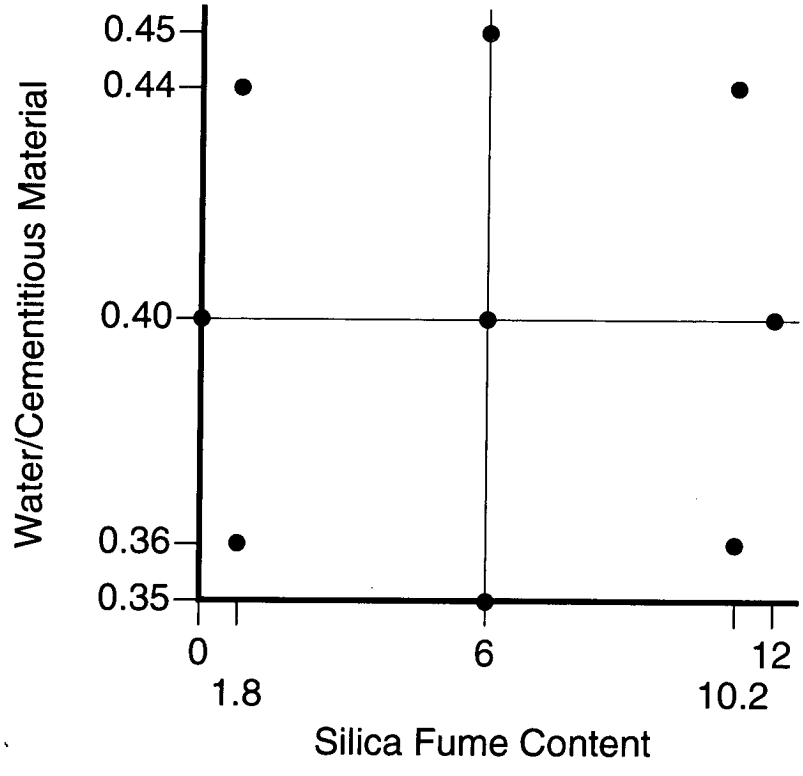

Figure C-1b. Central-composite design for overlay mixtures.

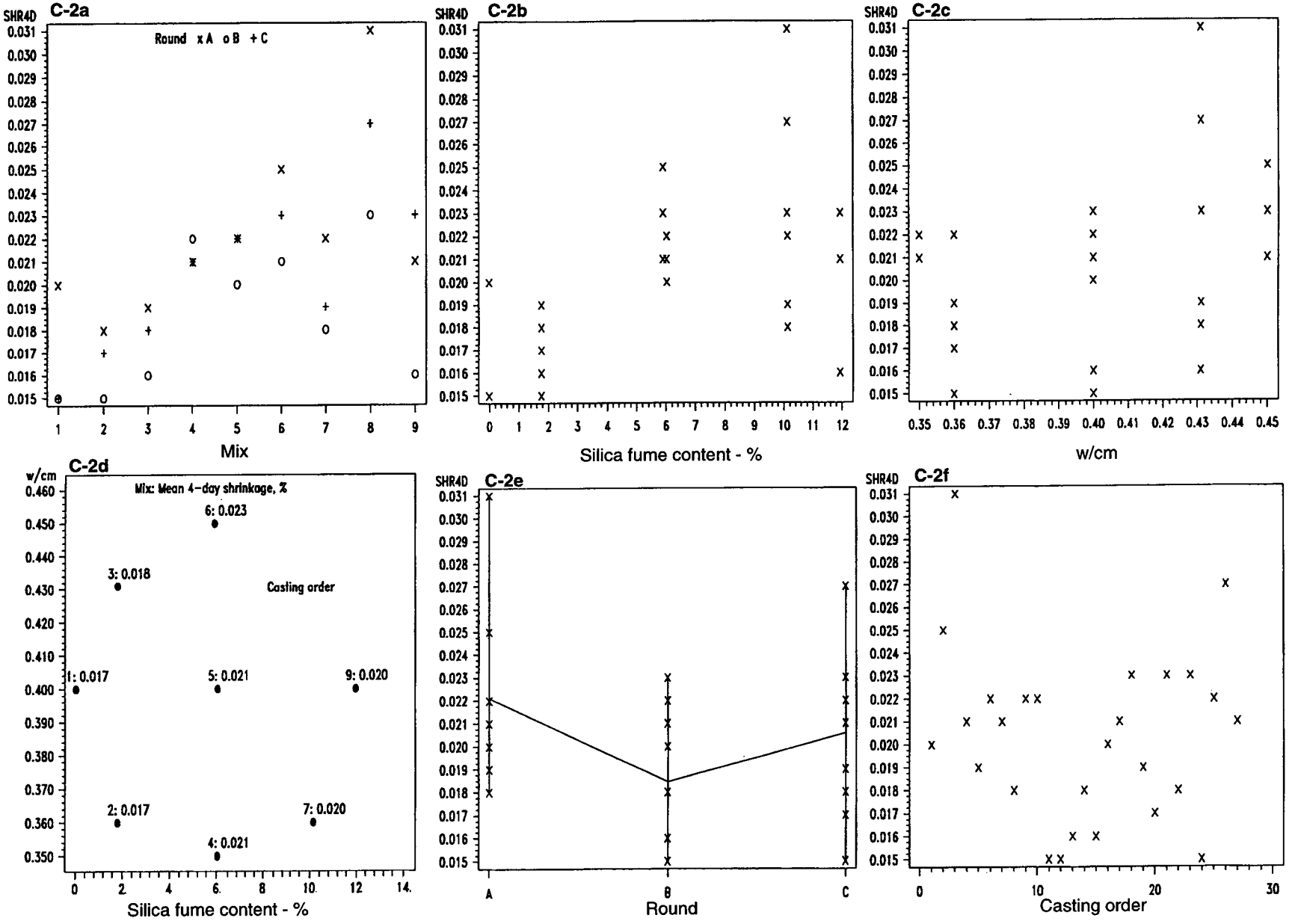

Figures C-2a through f. Exploratory data analyses for 4-day shrinkage of full-depth concrete mixtures.

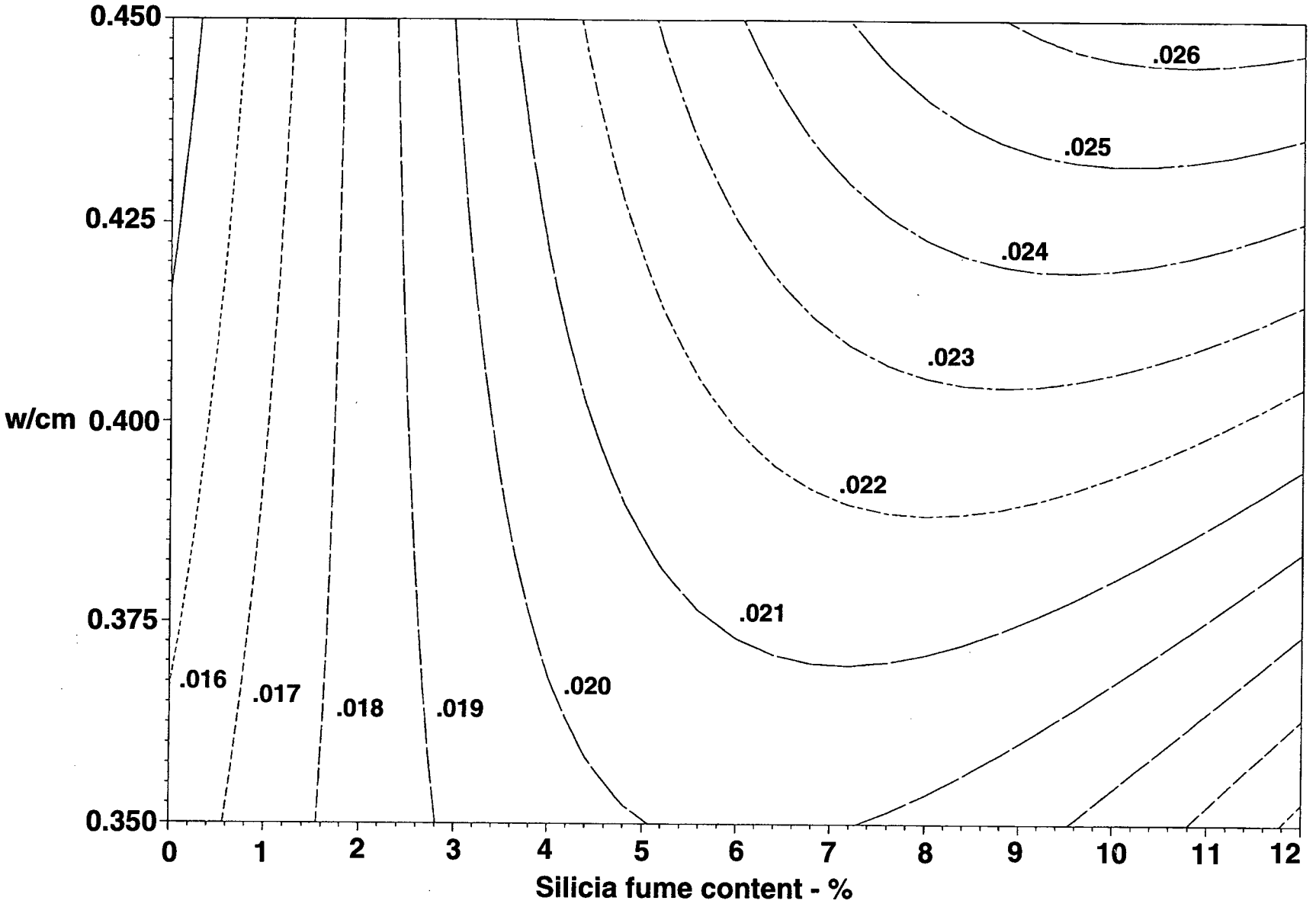

Figure C-3. Contour plots for 4-day shrinkage of full-depth concrete mixtures.

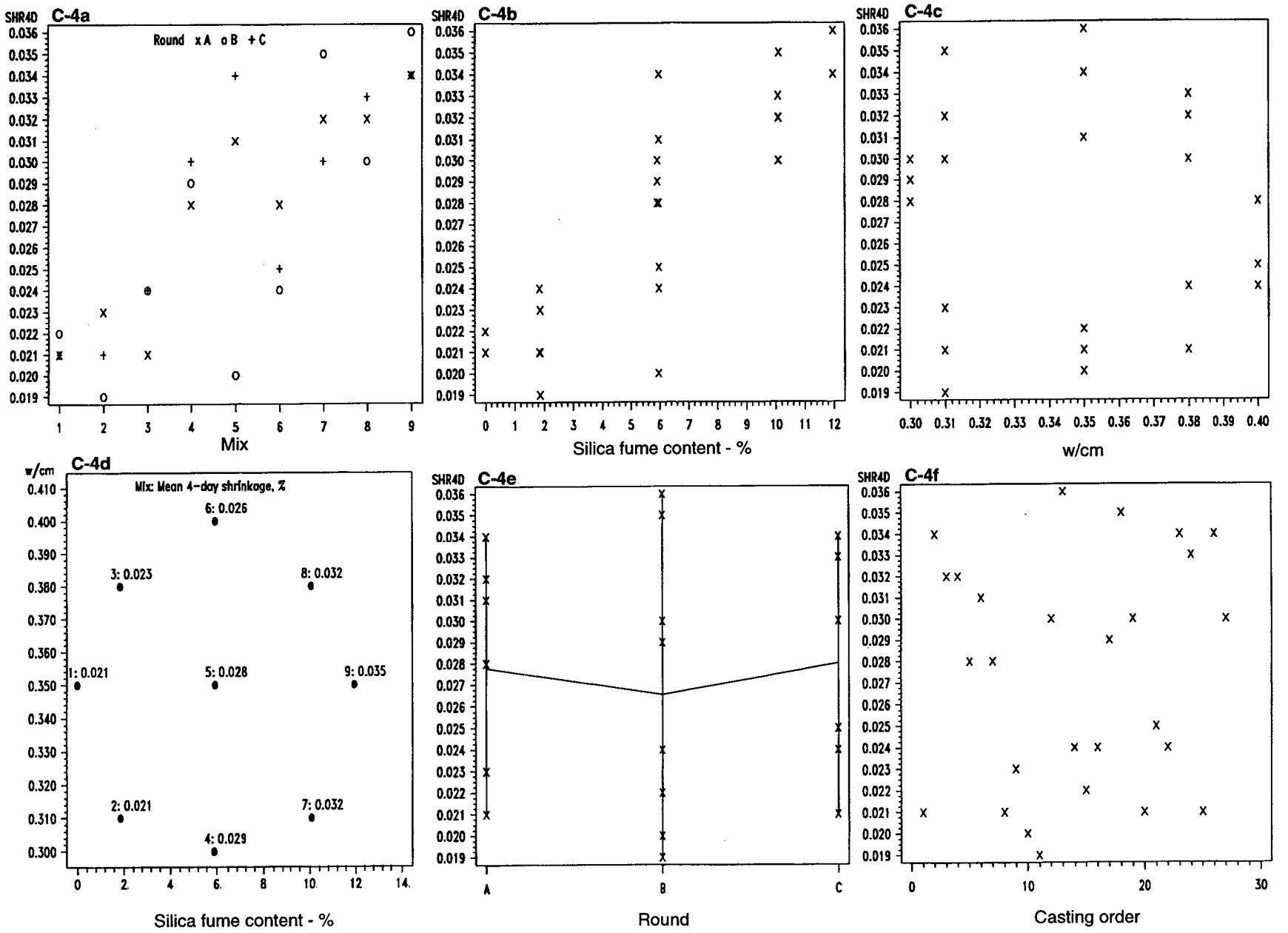

Figures C-4a through f. Exploratory data analyses for 4-day shrinkage of overlay concrete mixtures.

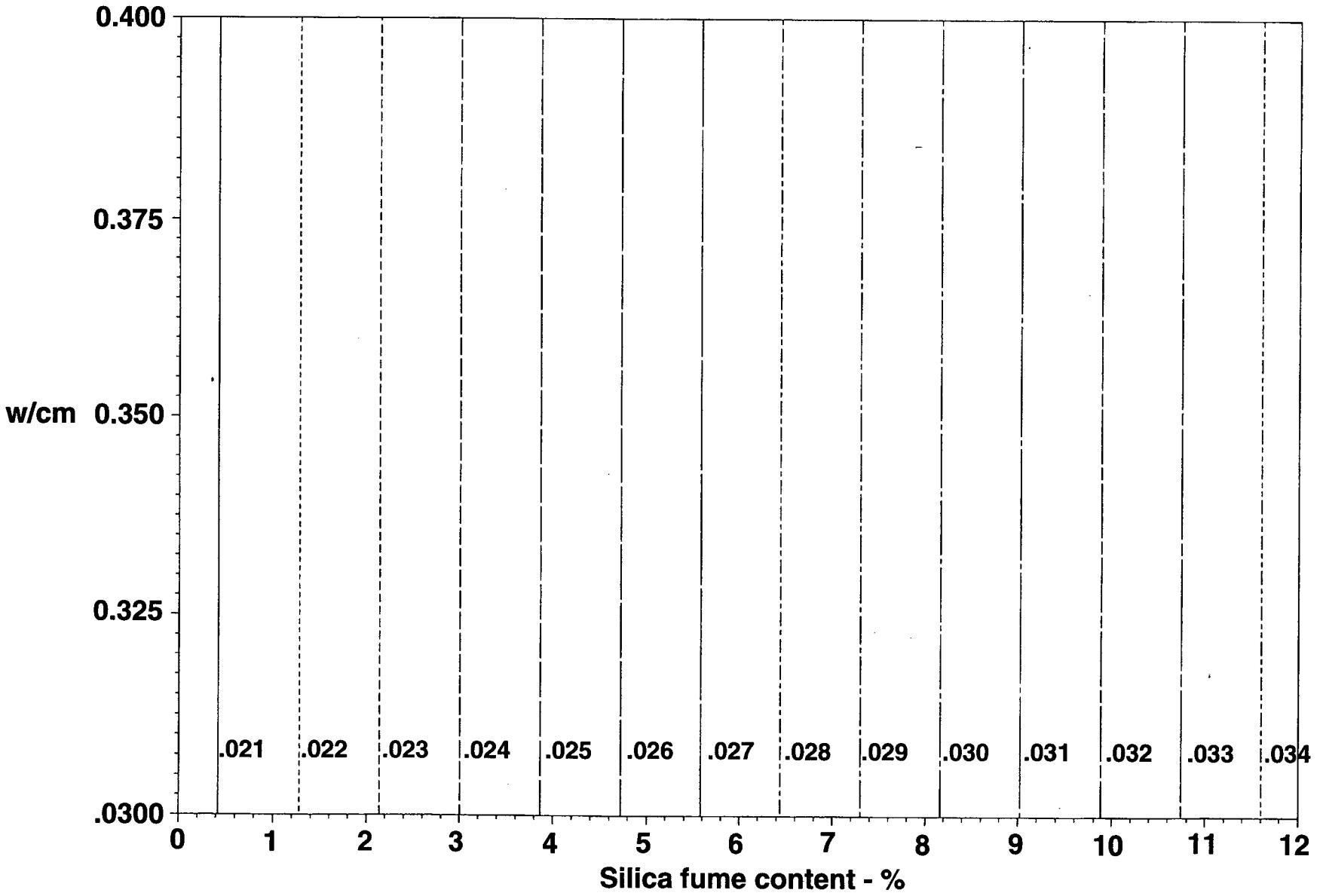

Figure C-5. Contour plots for 4-day shrinkage of overlay concrete mixtures.

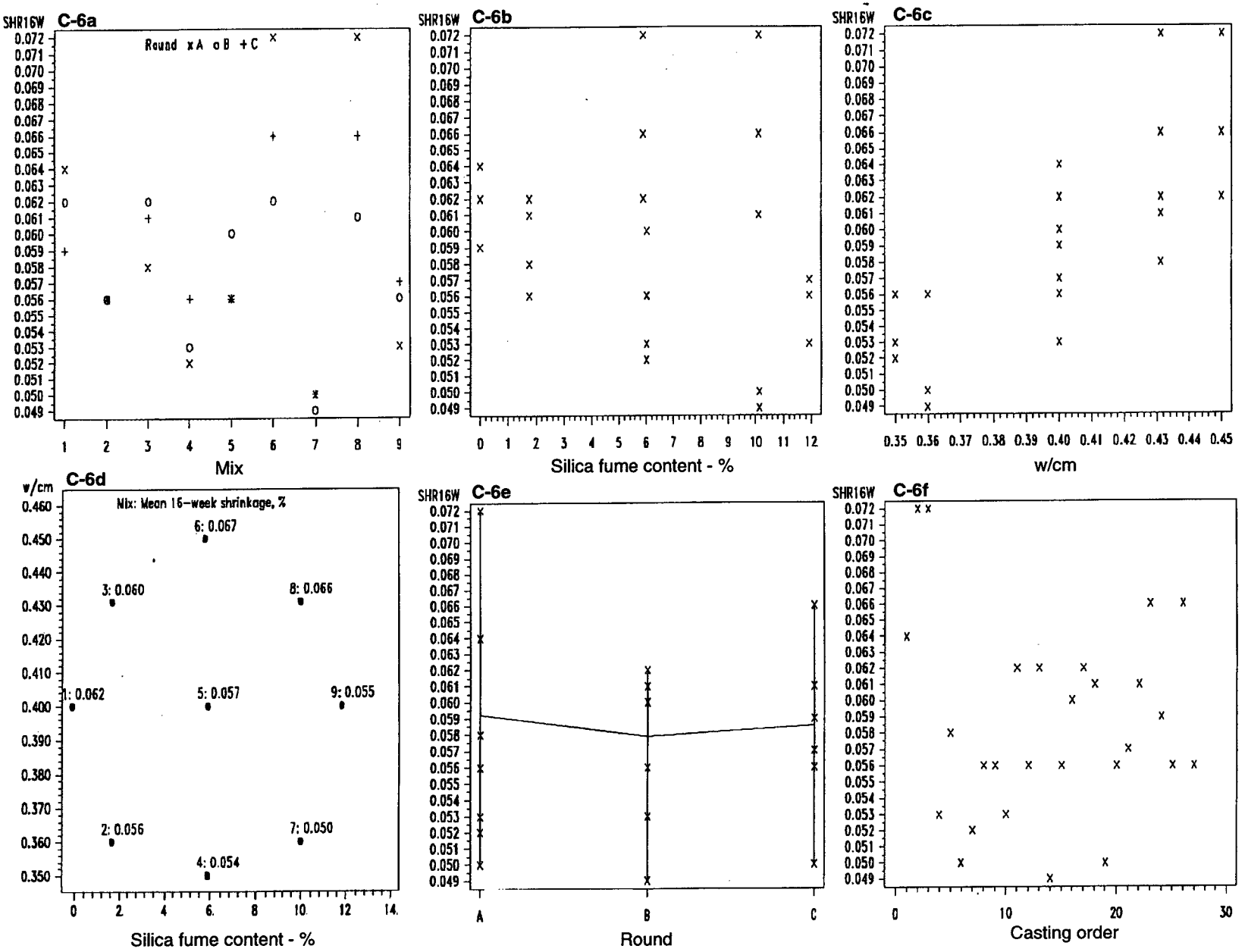

Figures C-6a through f. Exploratory data analyses for 16-week shrinkage of full-depth concrete mixtures.

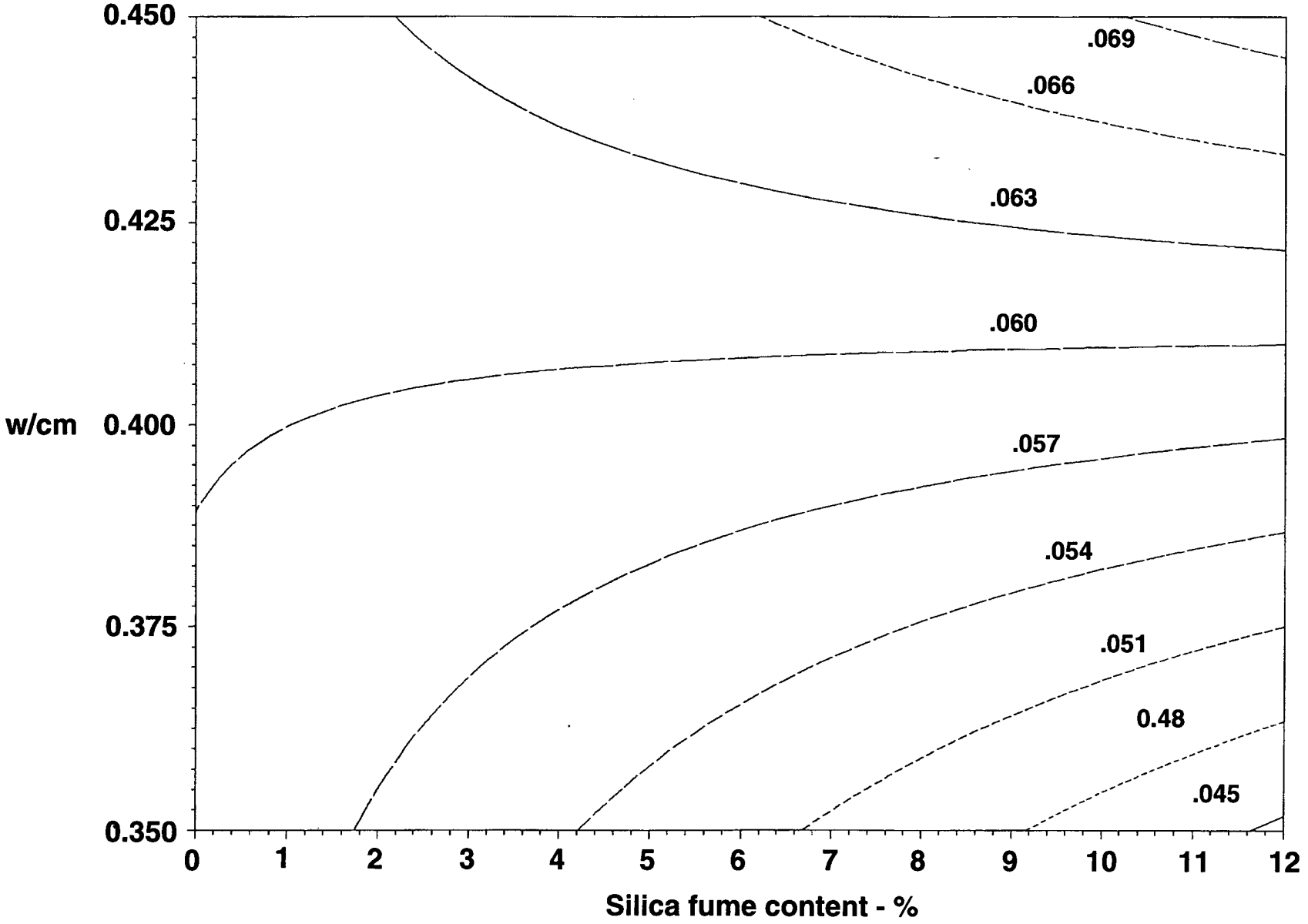

Figure C-7. Contour plots for 16-week shrinkage of full-depth concrete mixtures.

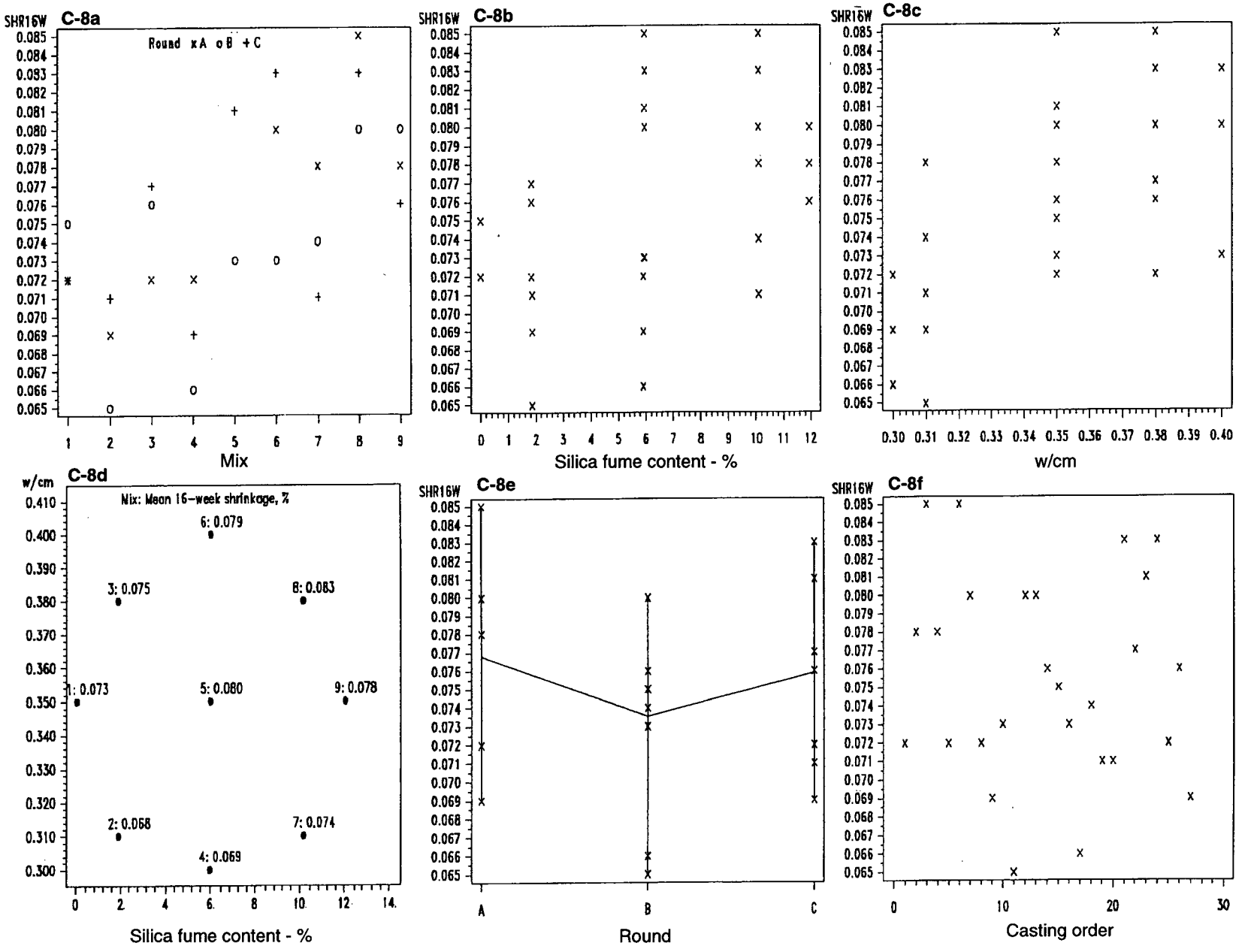

Figures C-8a through f. Exploratory data analyses for 16-week shrinkage of overlay concrete mixtures.

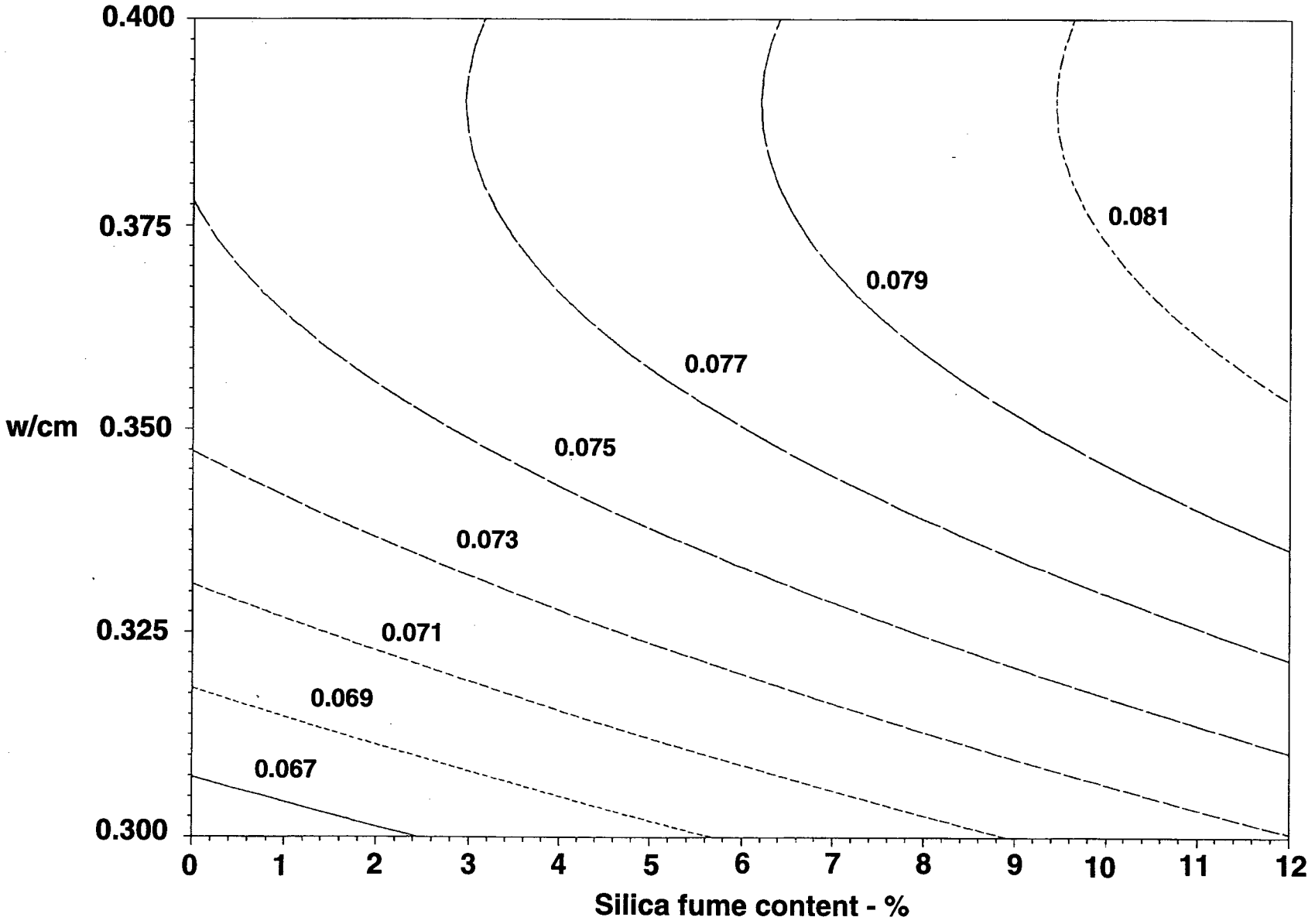

Figure C-9. Contour plots for 16-week shrinkage of overlay concrete mixtures.

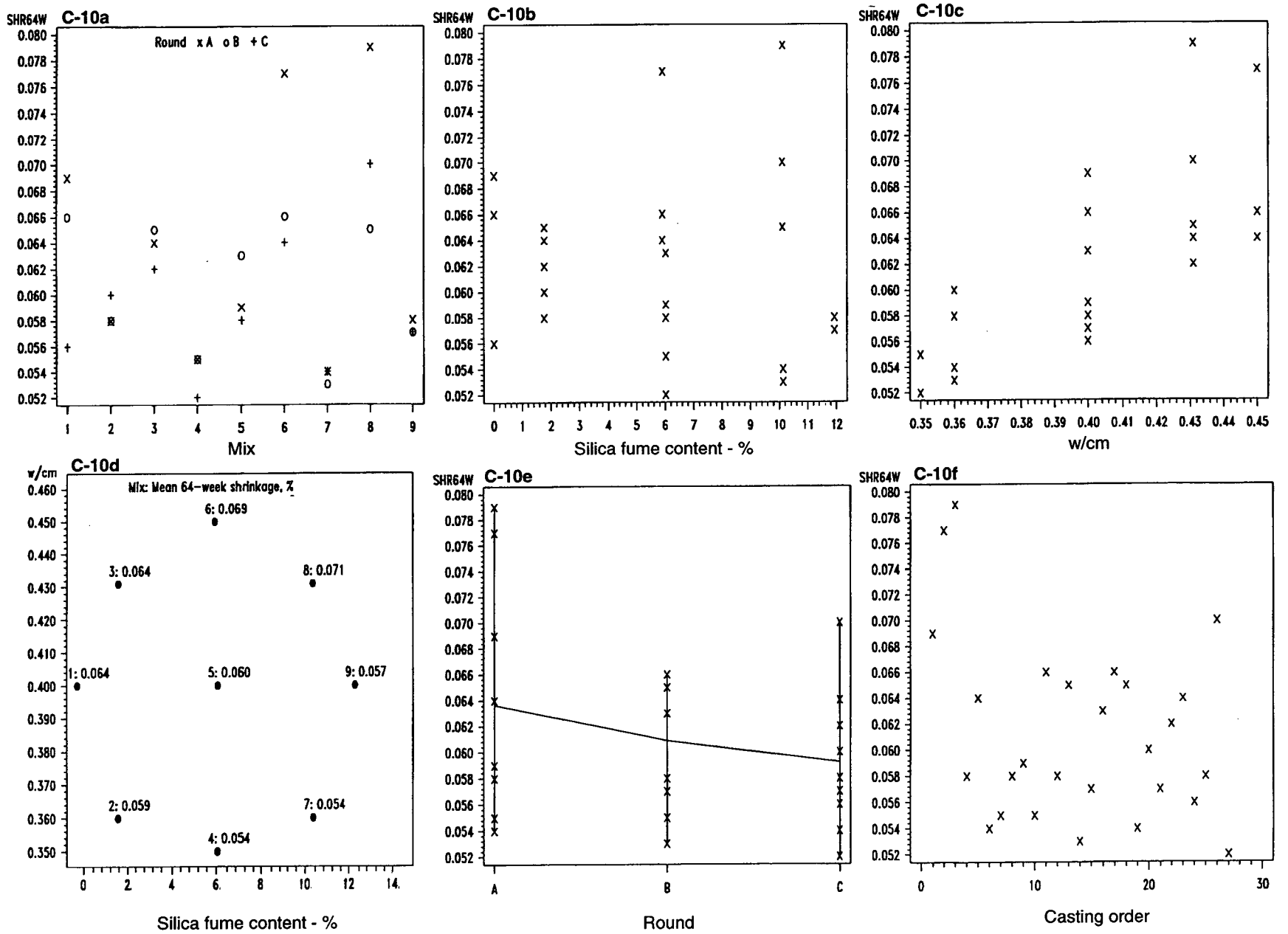

Figures C-10a through f. Exploratory data analyses for 64-week shrinkage of full-depth concrete mixtures.

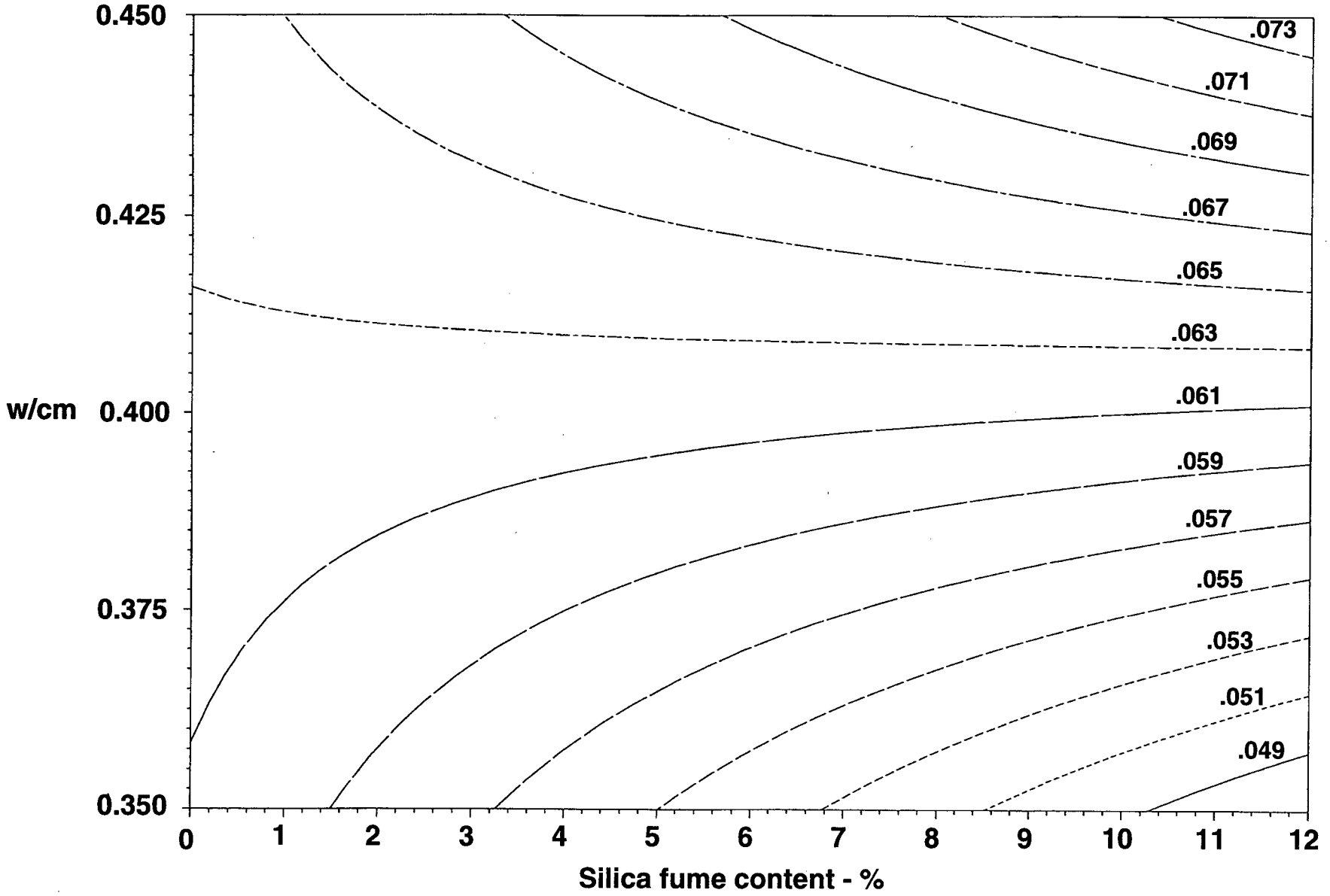

Figure C-11. Contour plots for 64-week shrinkage of full-depth concrete mixtures.

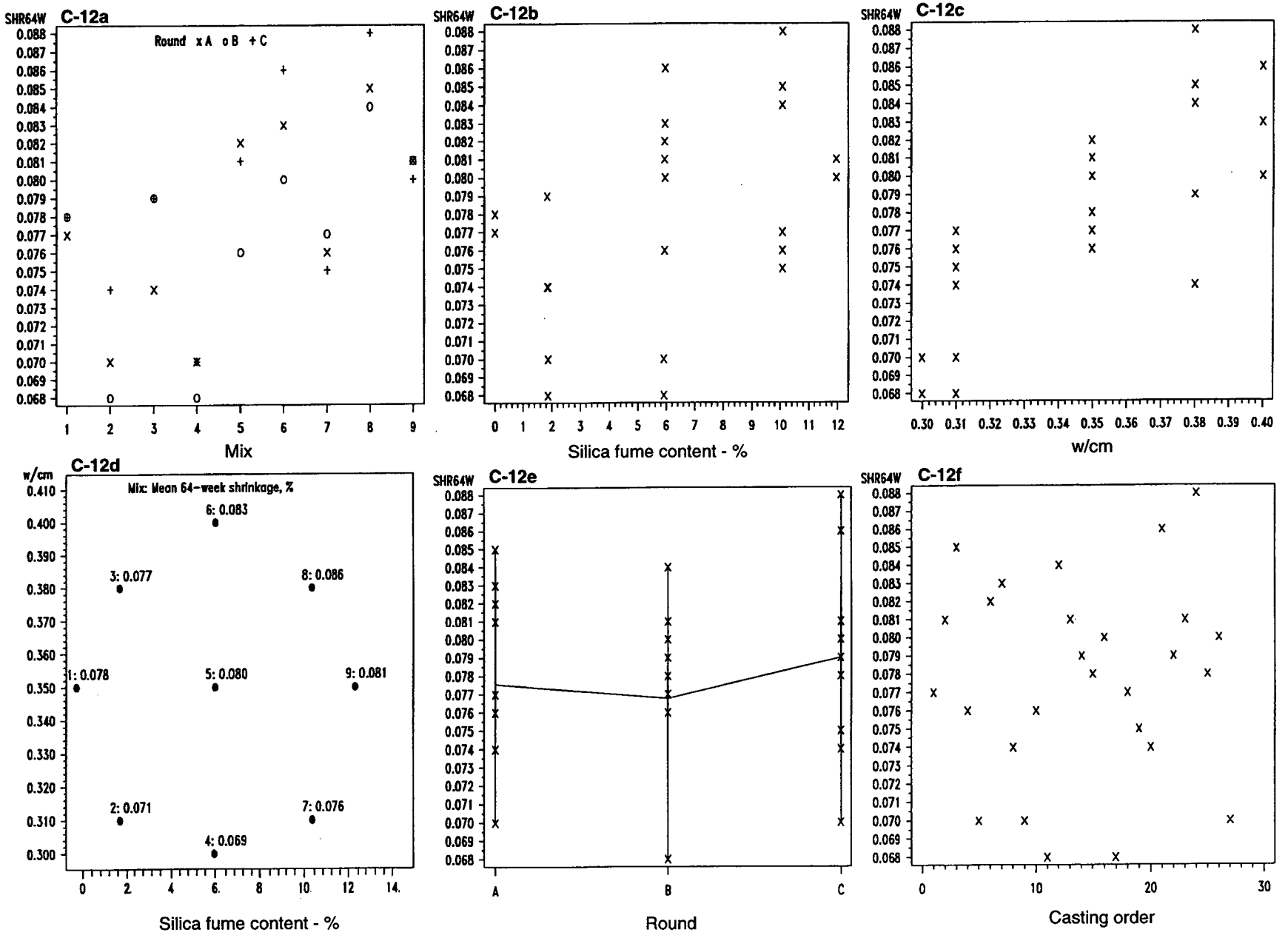

Figures C-12a through f. Exploratory data analyses for 64-week shrinkage of overlay concrete mixtures.

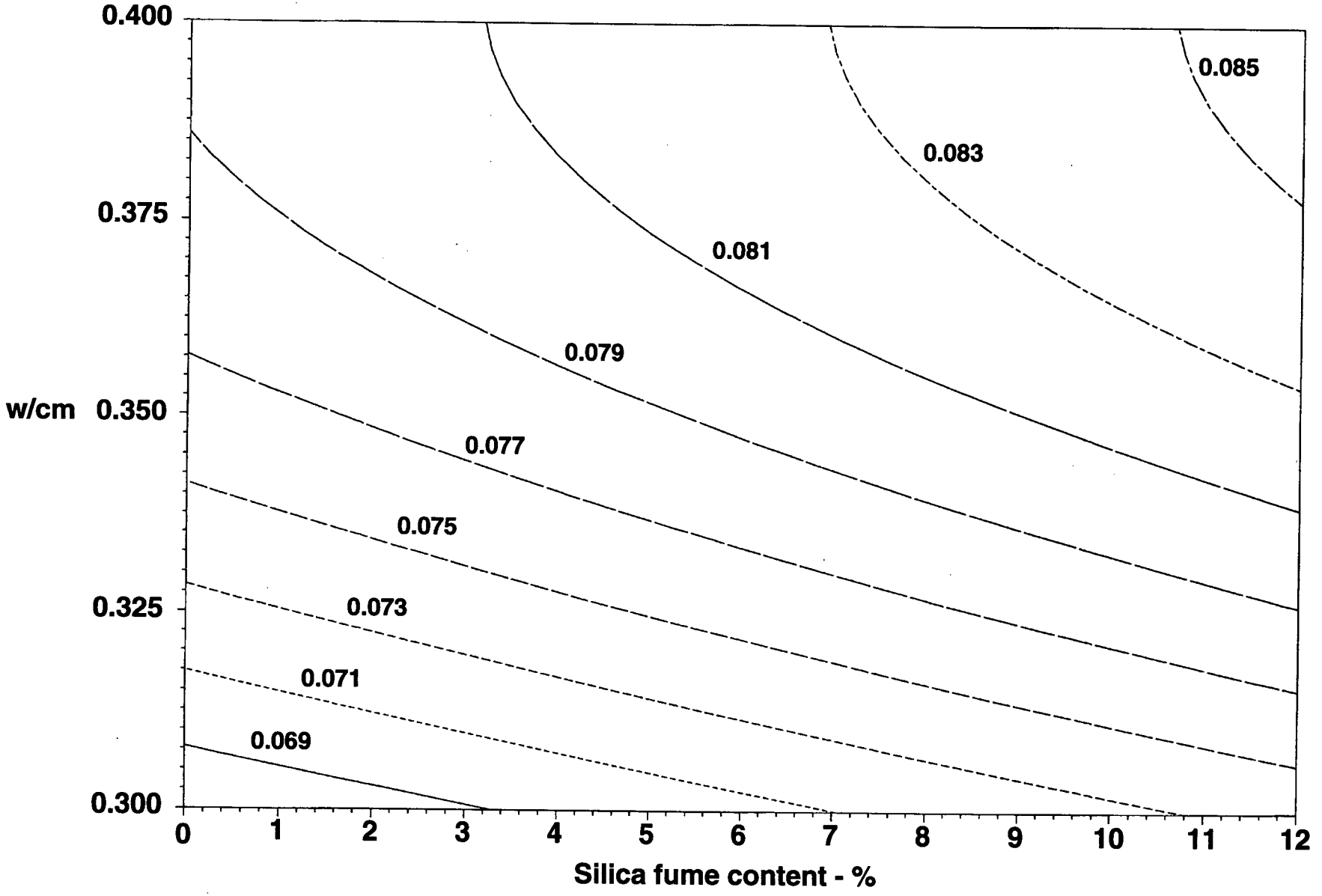

Figure C-13. Contour plots for 64-week shrinkage of overlay concrete mixtures.

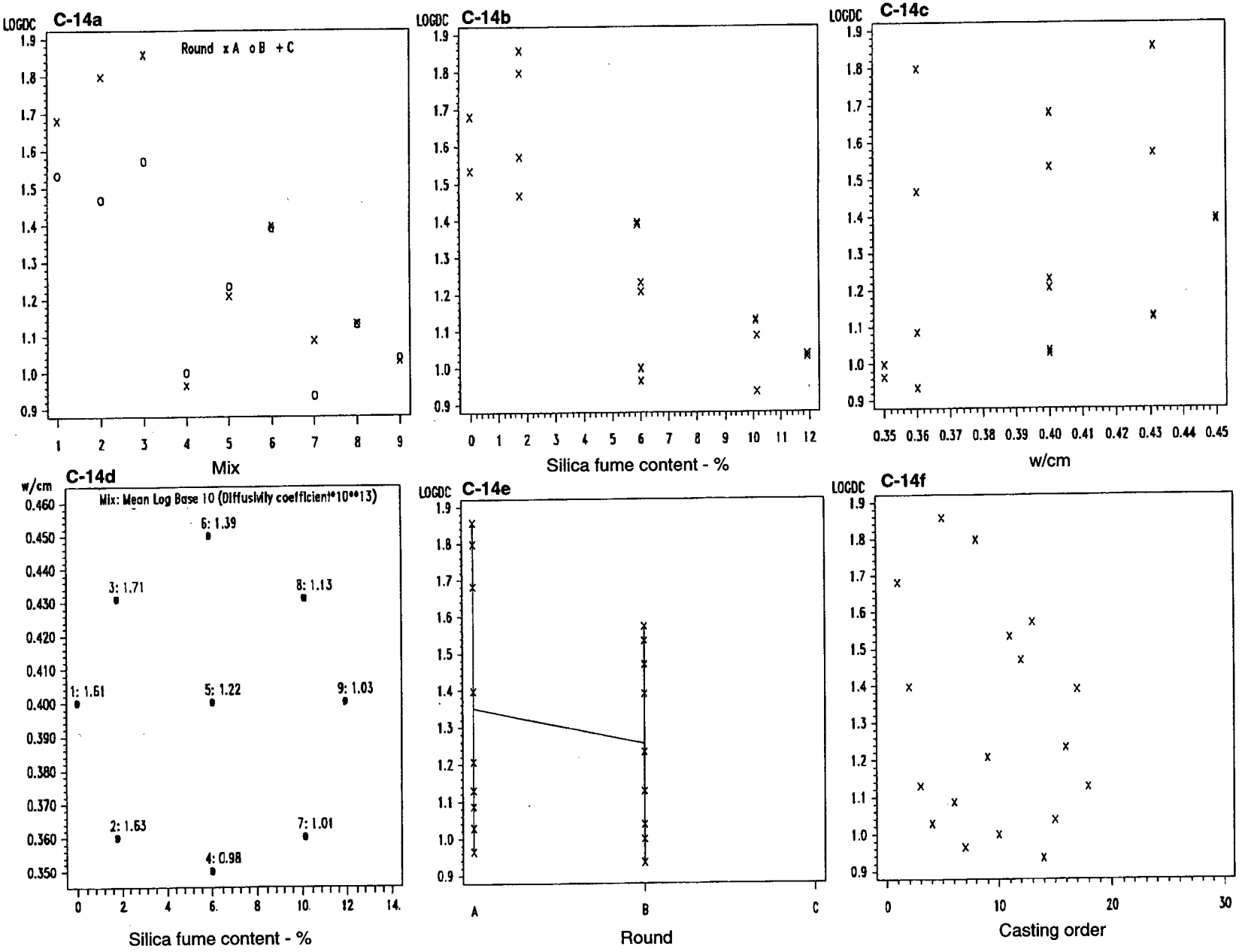

Figures C-14a through f. Exploratory data analyses for diffusivity coefficients (log transform) of full-depth concrete mixtures.

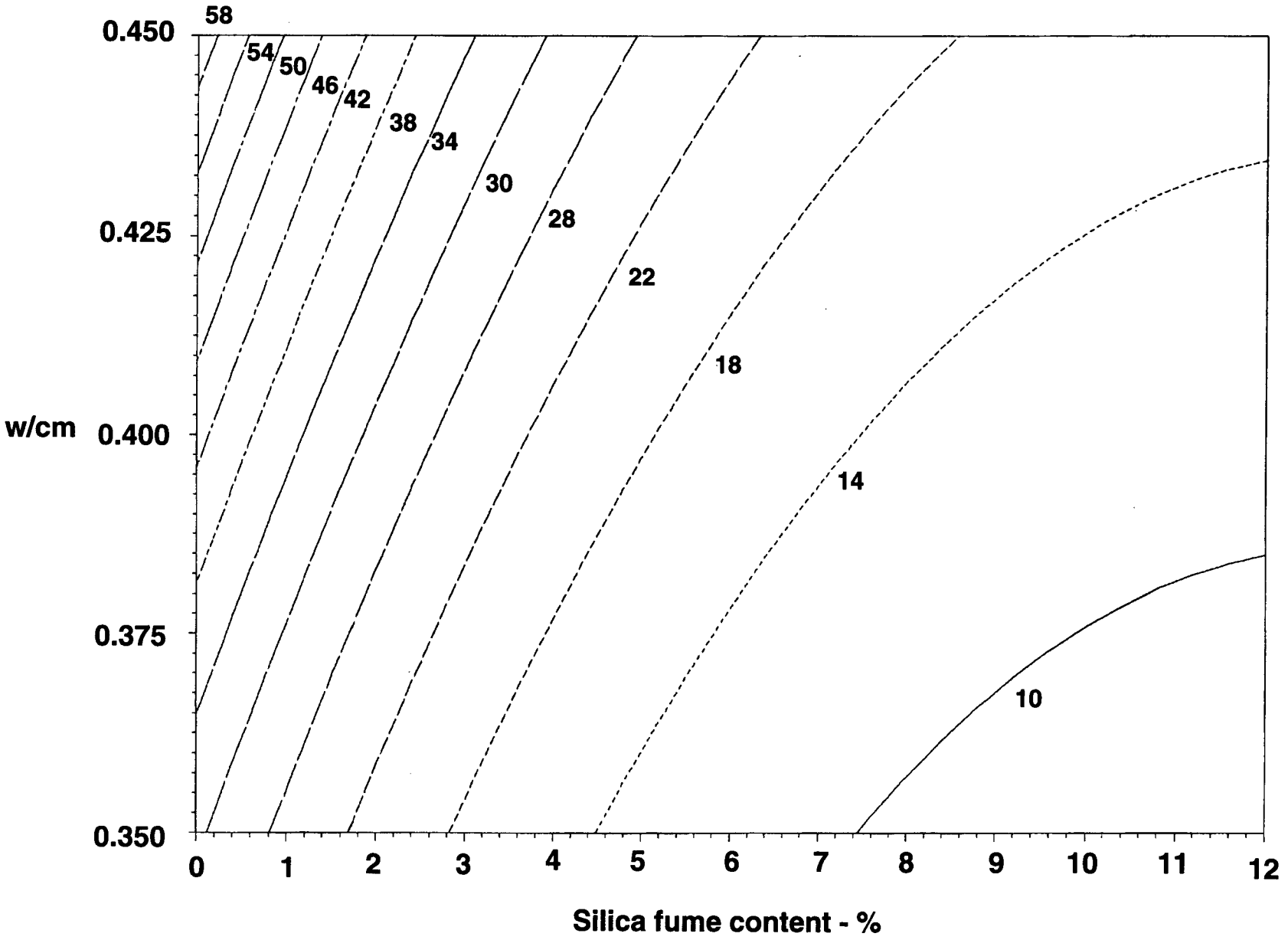

Figure C-15. Contour plots for diffusivity coefficients of full-depth concrete mixtures.

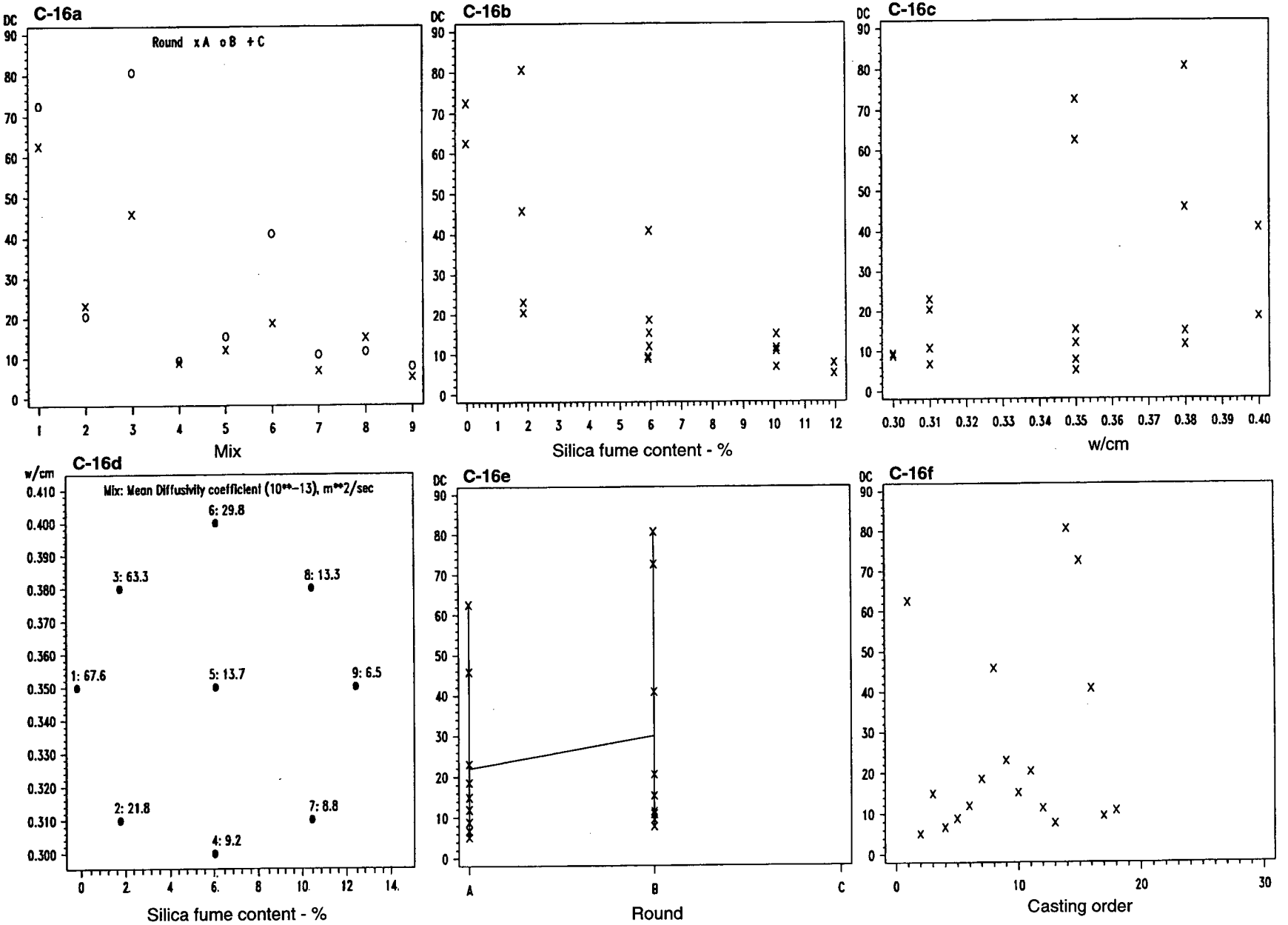

Figures C-16a through f. Exploratory data analyses for diffusivity coefficients (log transform) of overlay concrete mixtures.

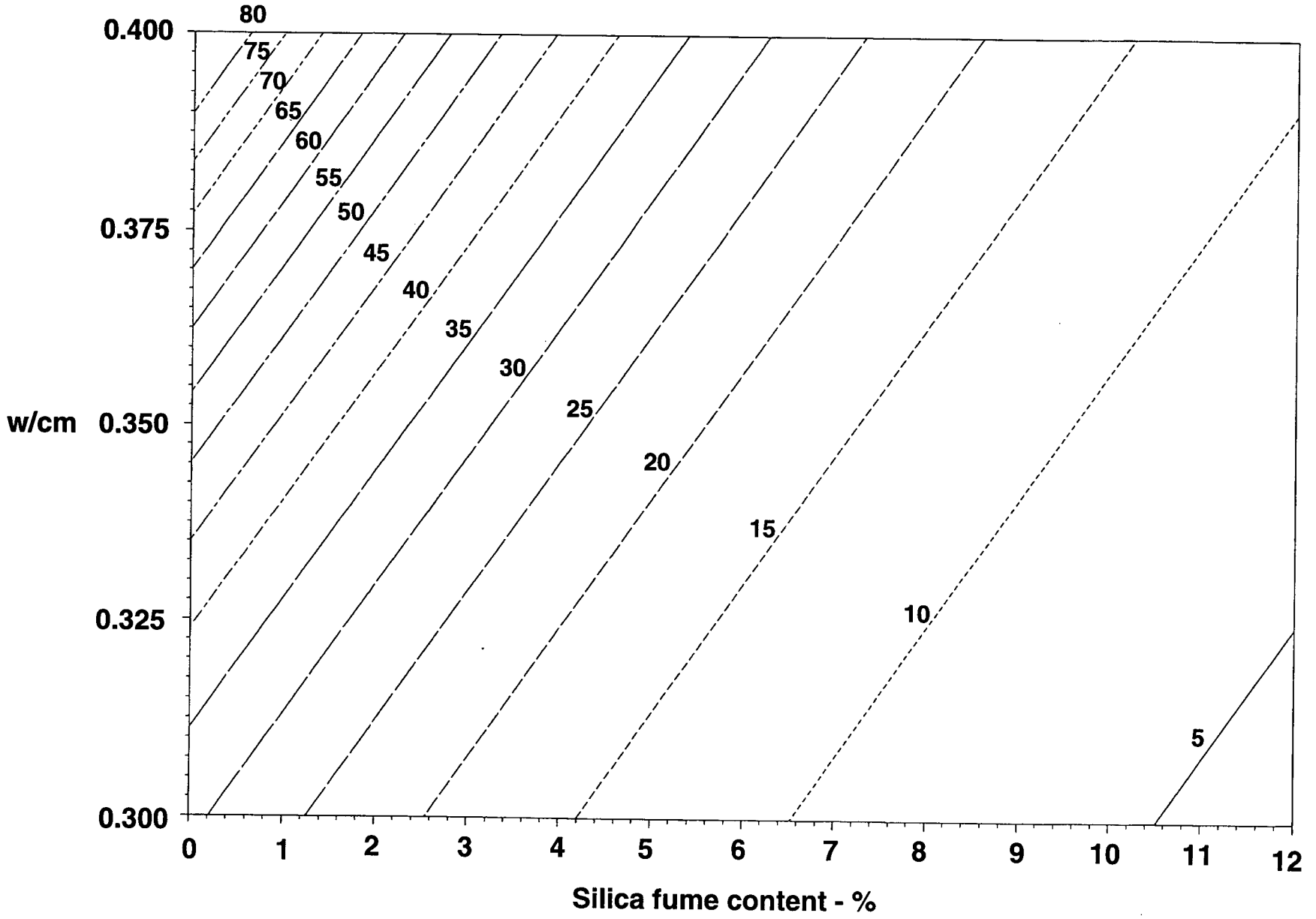

Figure C-17. Contour plots for diffusivity coefficients of overlay concrete mixtures.

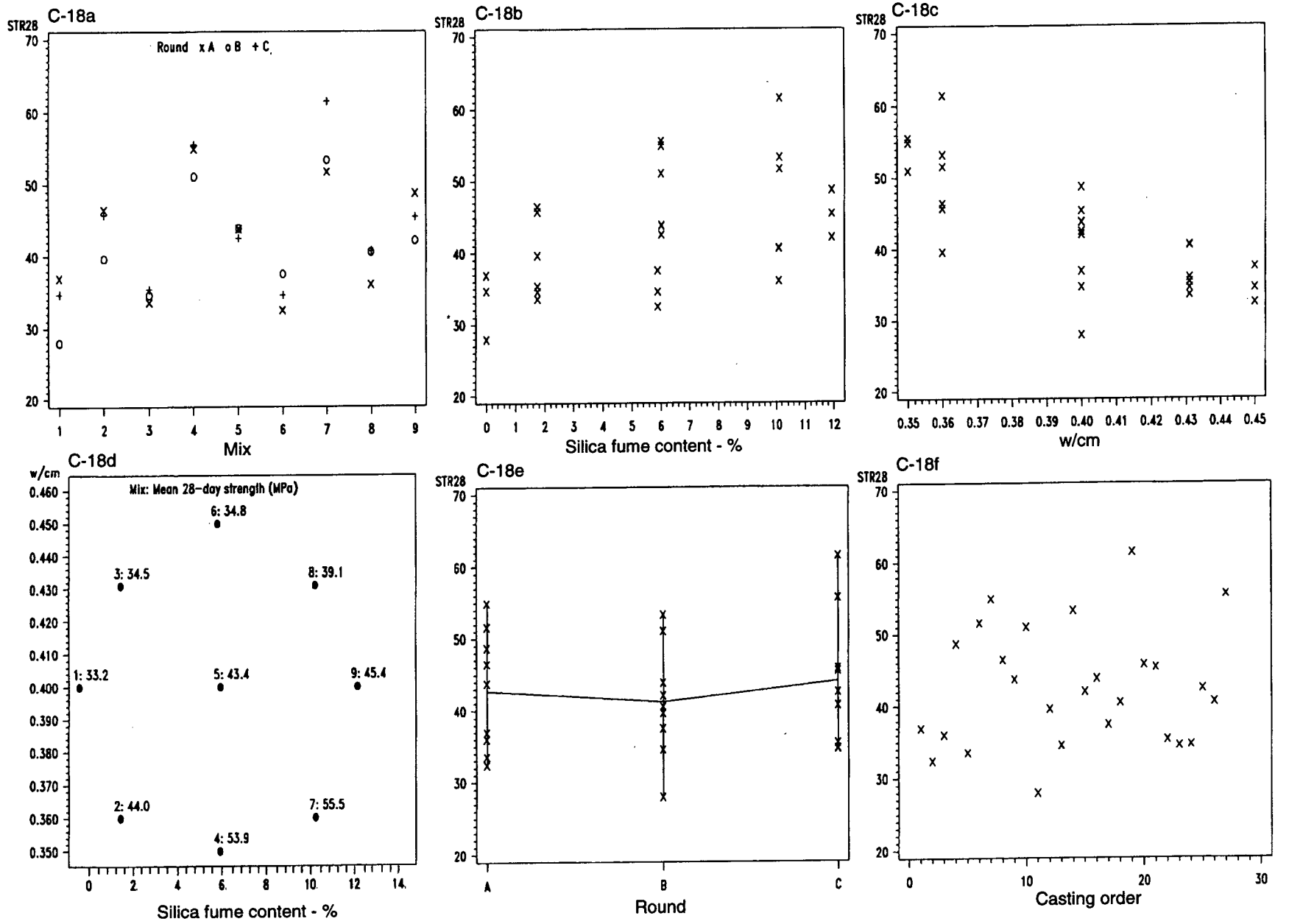

Figures C-18a through f. Exploratory data analyses for 28-day compressive strength of full-depth concrete mixtures.

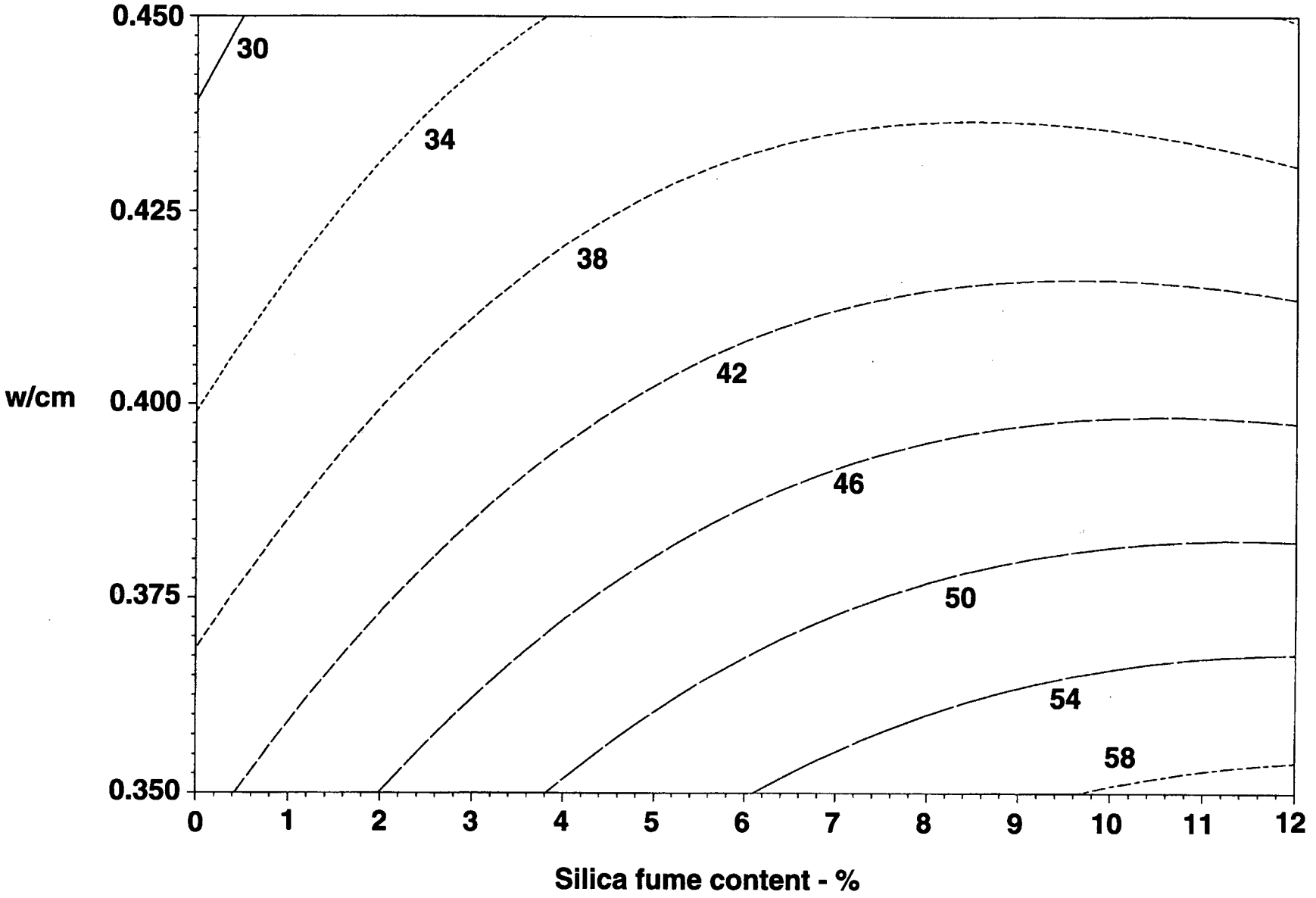

Figure C-19. Contour plots for 28-day compressive strength of full-depth concrete mixtures.

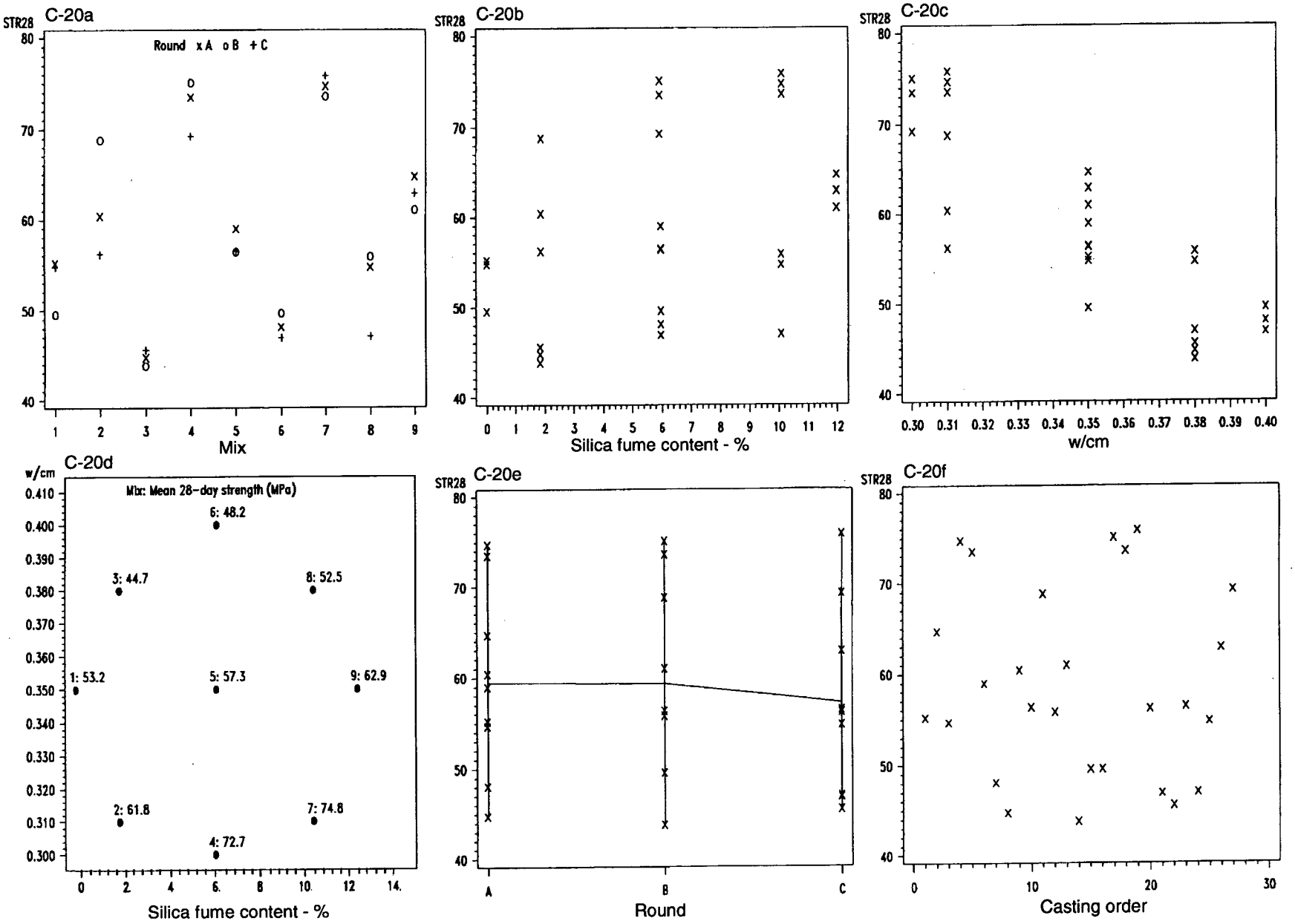

Figure C-20a through f. Exploratory data analyses for 28-day compressive strength of overlay concrete mixtures.

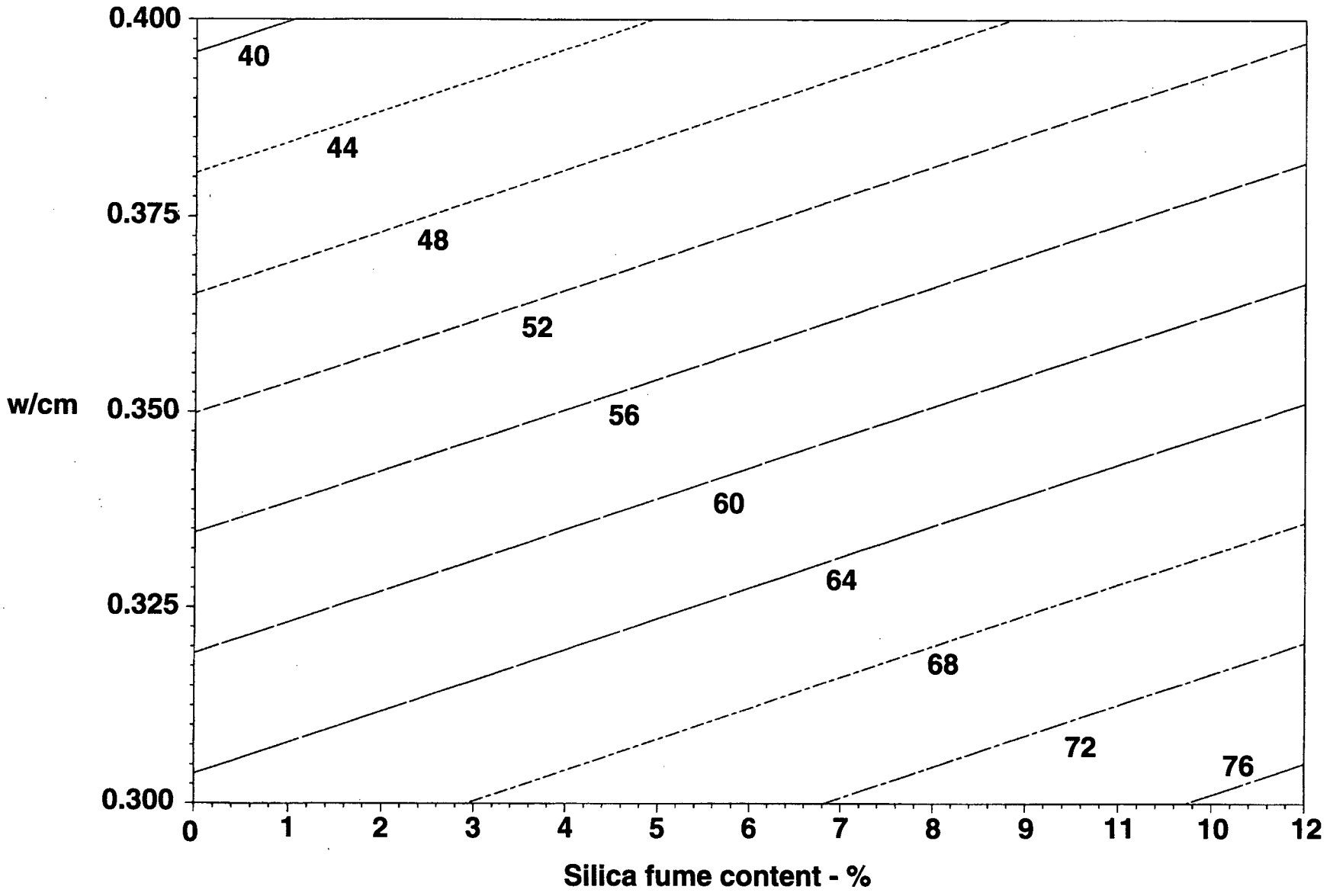

Figure C-21. Contour plots for 28-day compressive strength of overlay concrete mixtures.

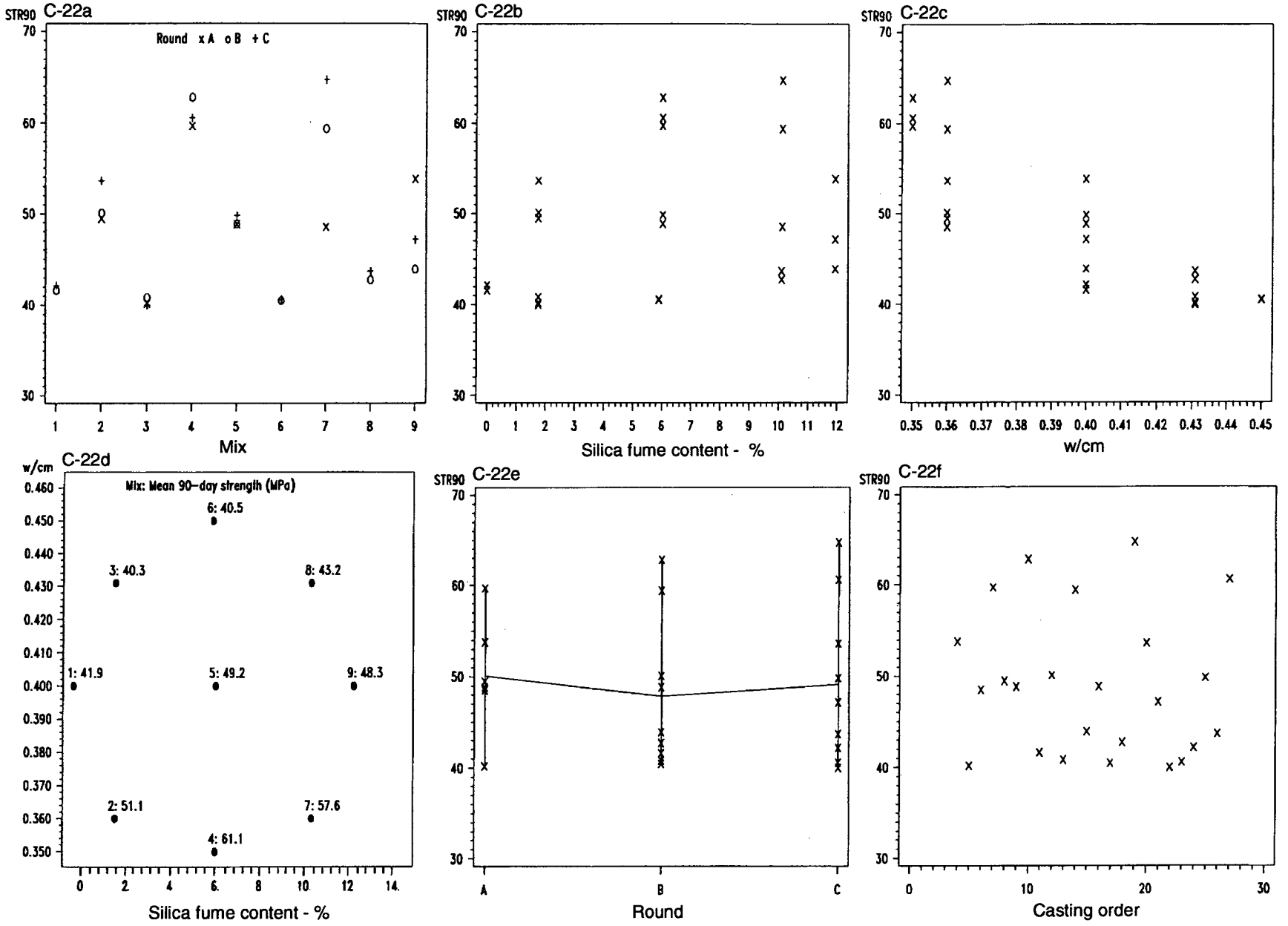

Figures C-22a through f. Exploratory data analyses for 90-day compressive strength of full-depth concrete mixtures.

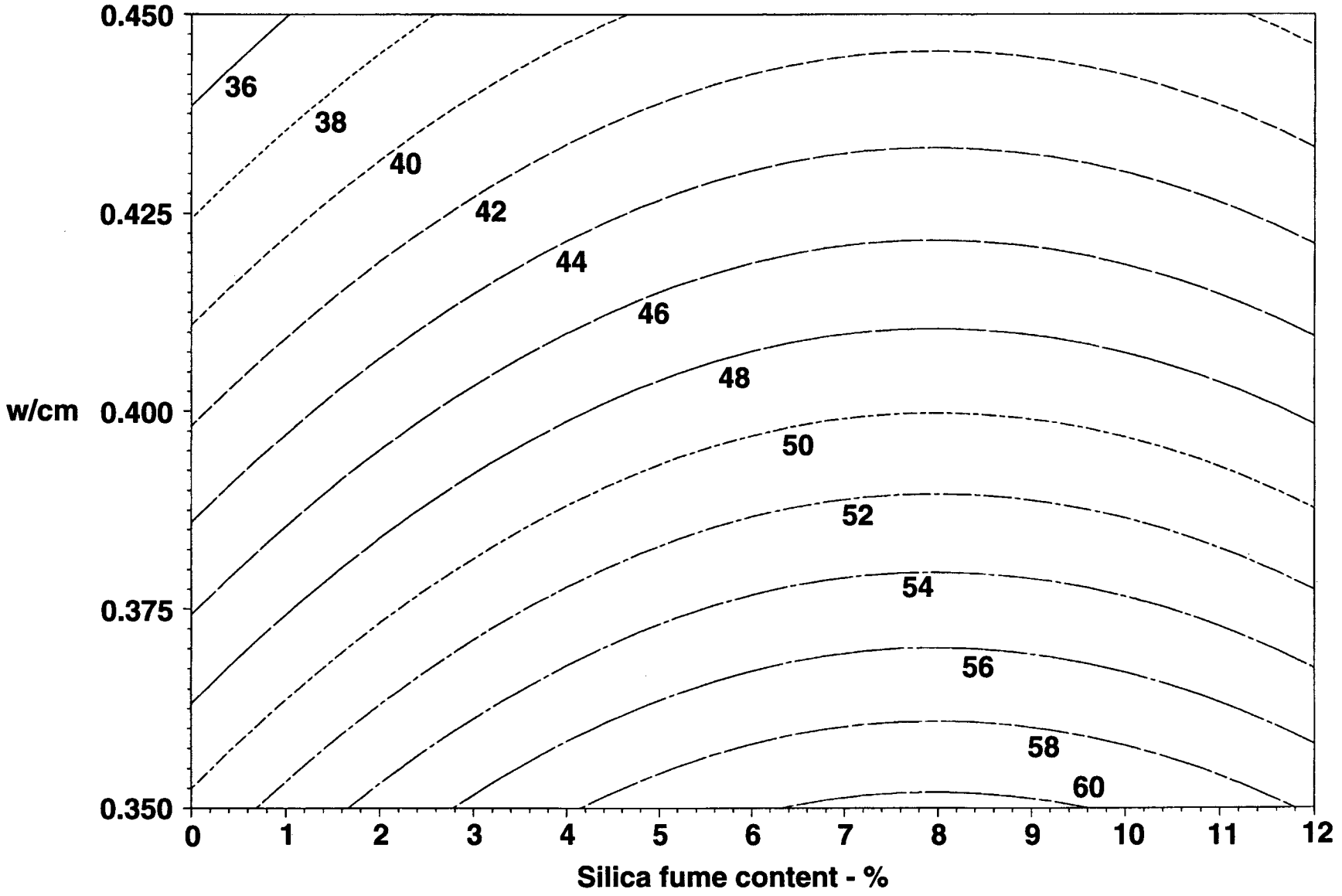

Figure C-23. Contour plots for 90-day compressive strength of full-depth concrete mixtures.

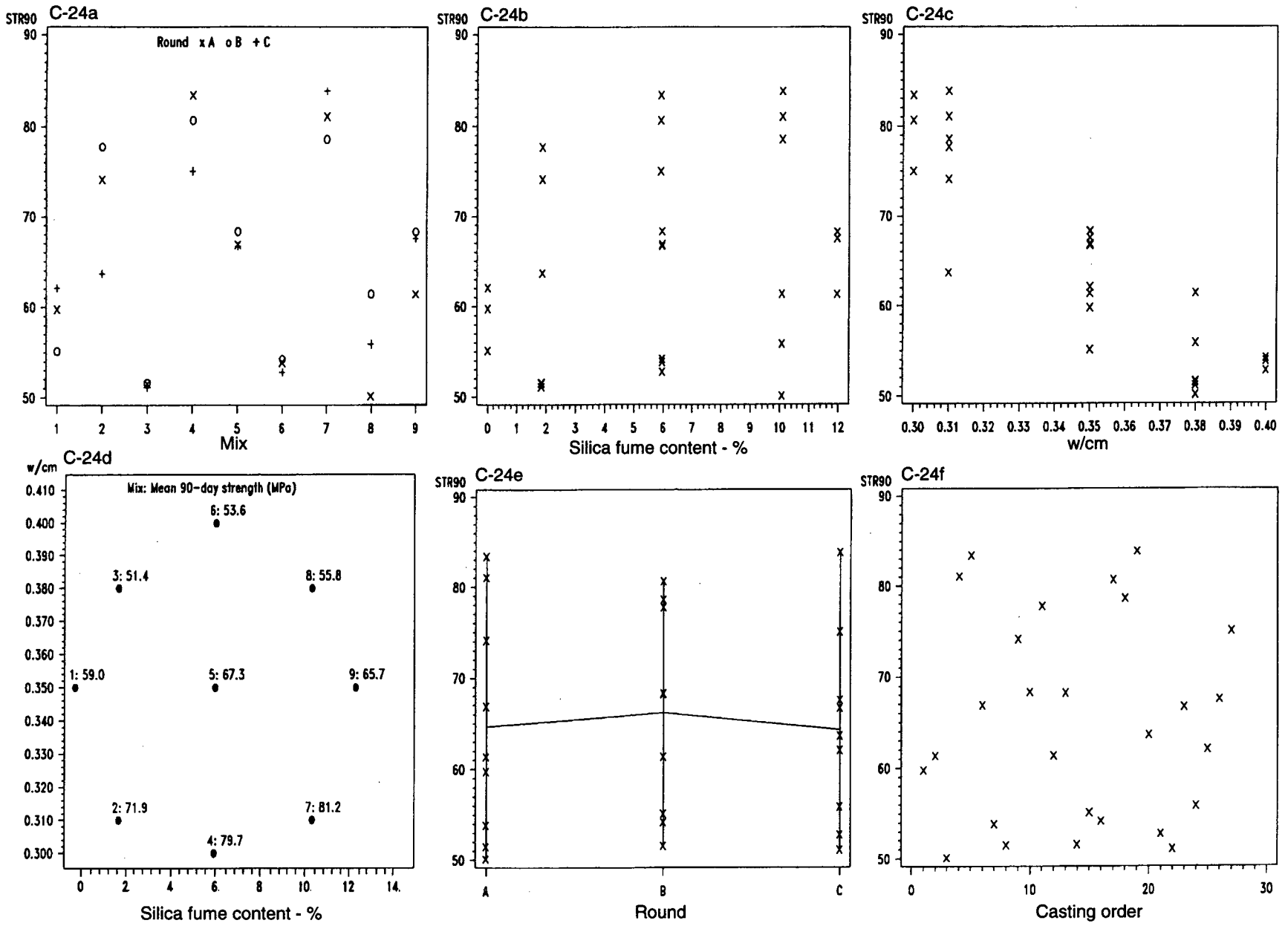

Figures C-24a through f. Exploratory data analyses for 90-day compressive strength of overlay concrete mixtures.

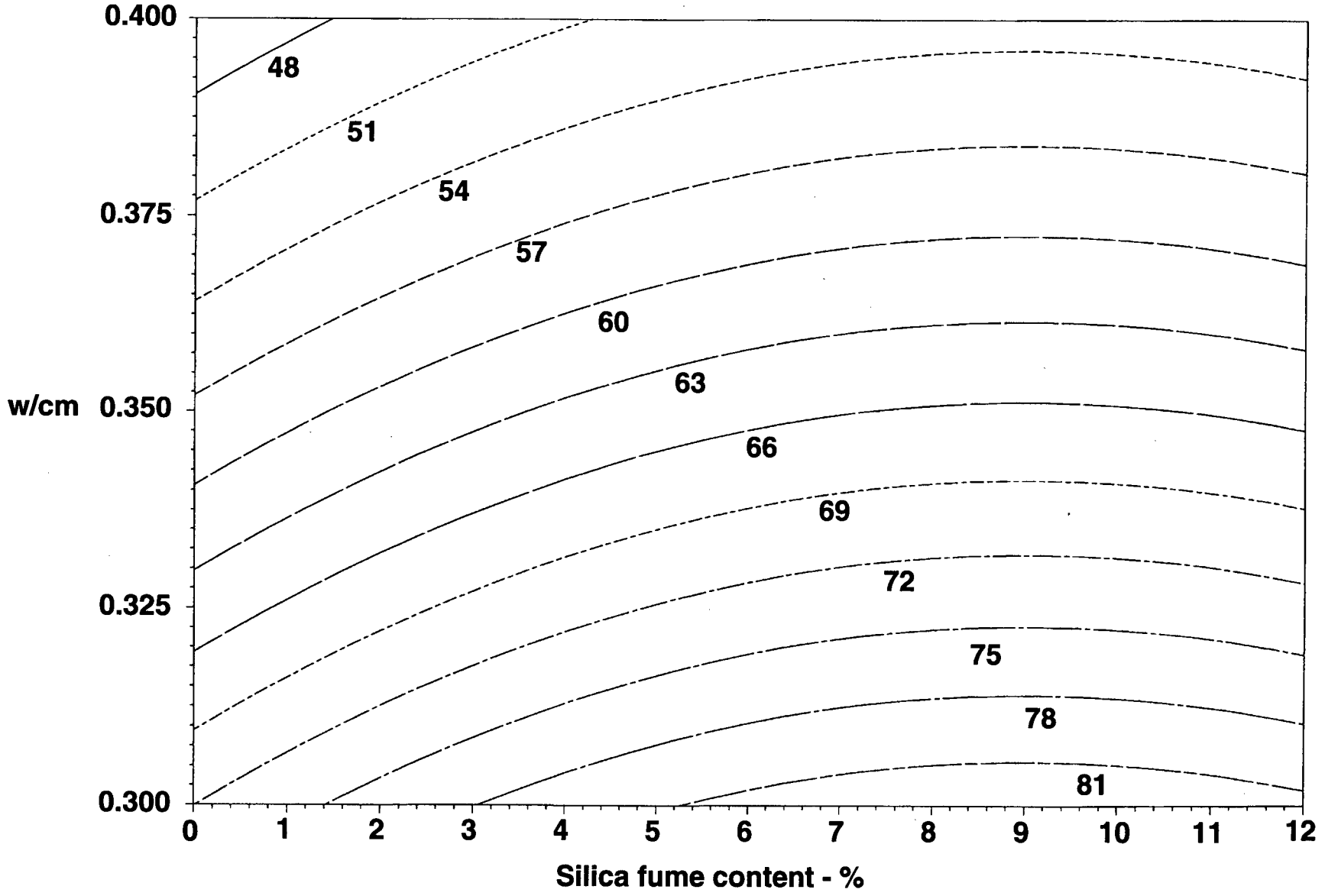

Figure C-25. Contour plot for 90-day compressive strength of overlay concrete mixtures.

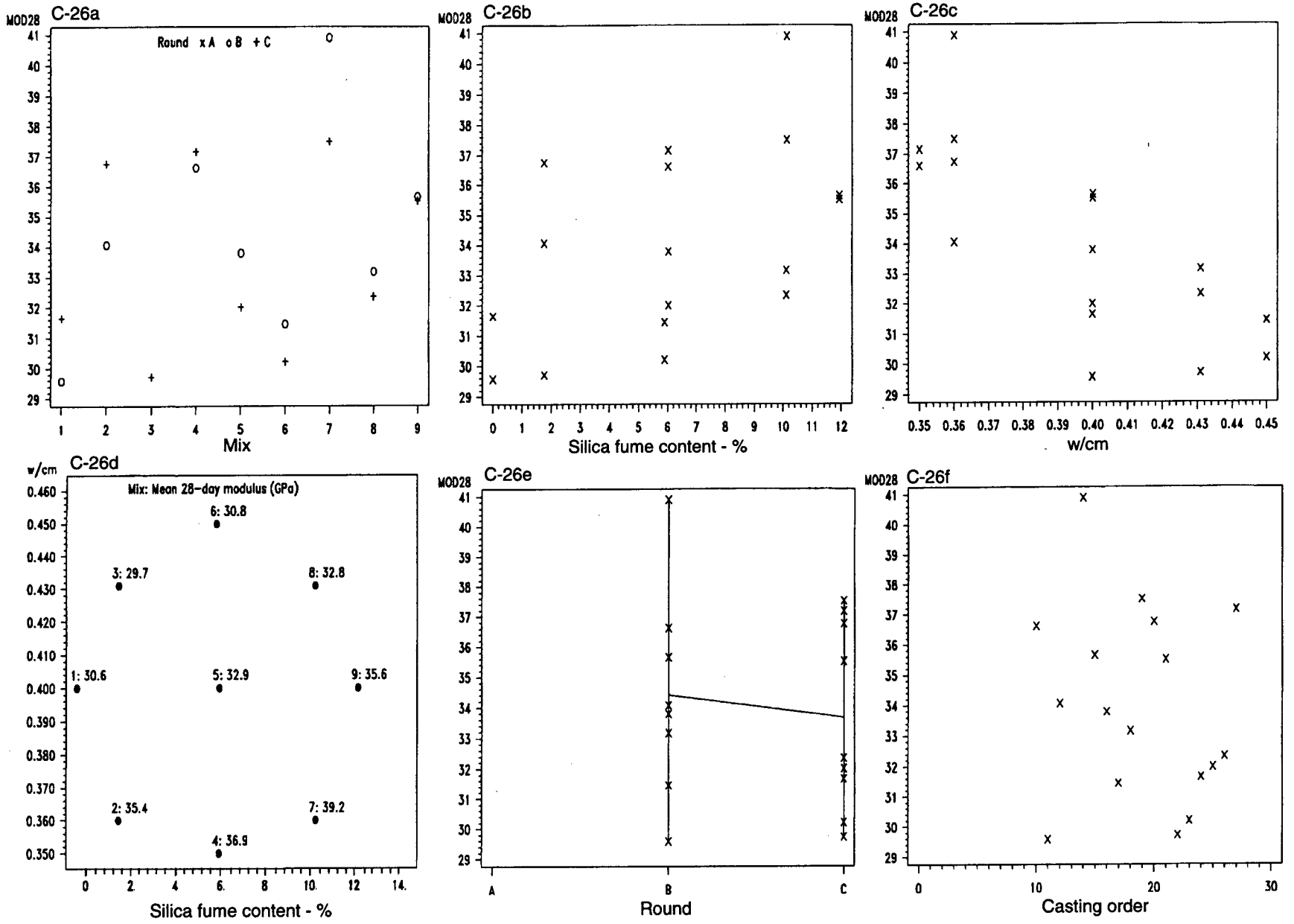

Figures C-26a through f. Exploratory data analyses for 28-day elastic modulus of full-depth concrete mixtures.

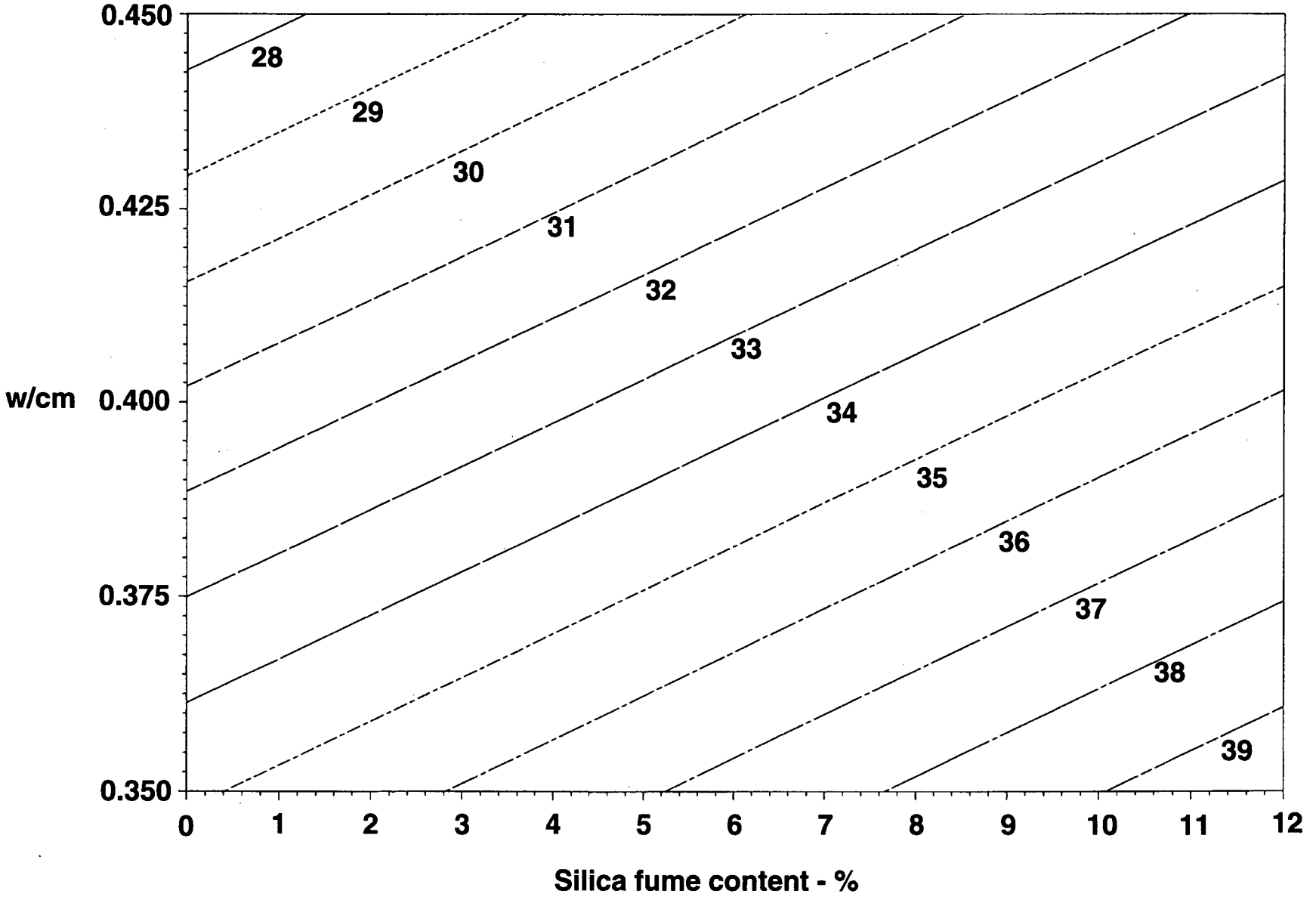

Figure C-27. Contour plots for 28-day elastic modulus for full-depth concrete mixtures.

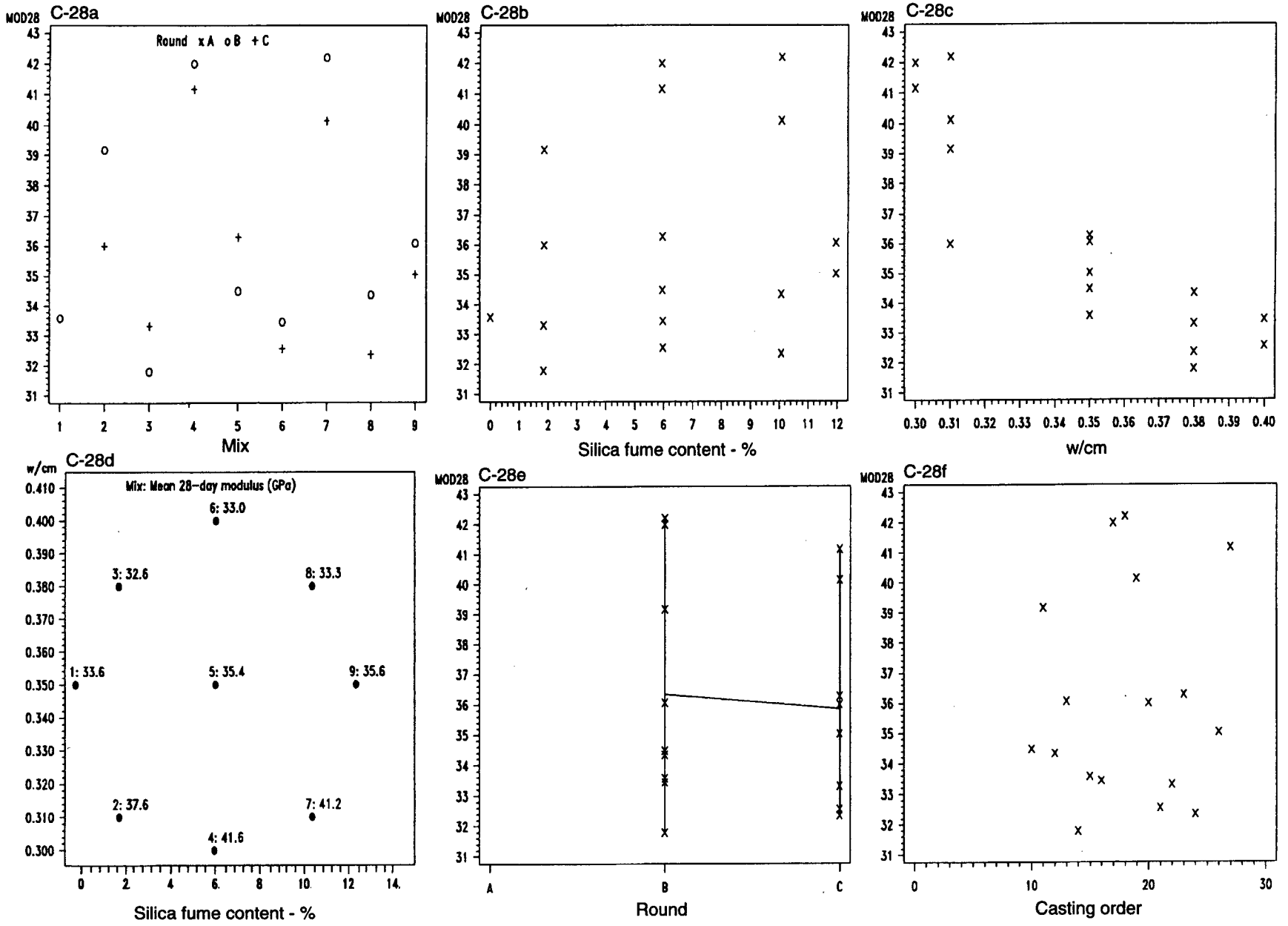

Figures C-28a through f. Exploratory data analyses for 28-day elastic modulus of overlay concrete mixtures.

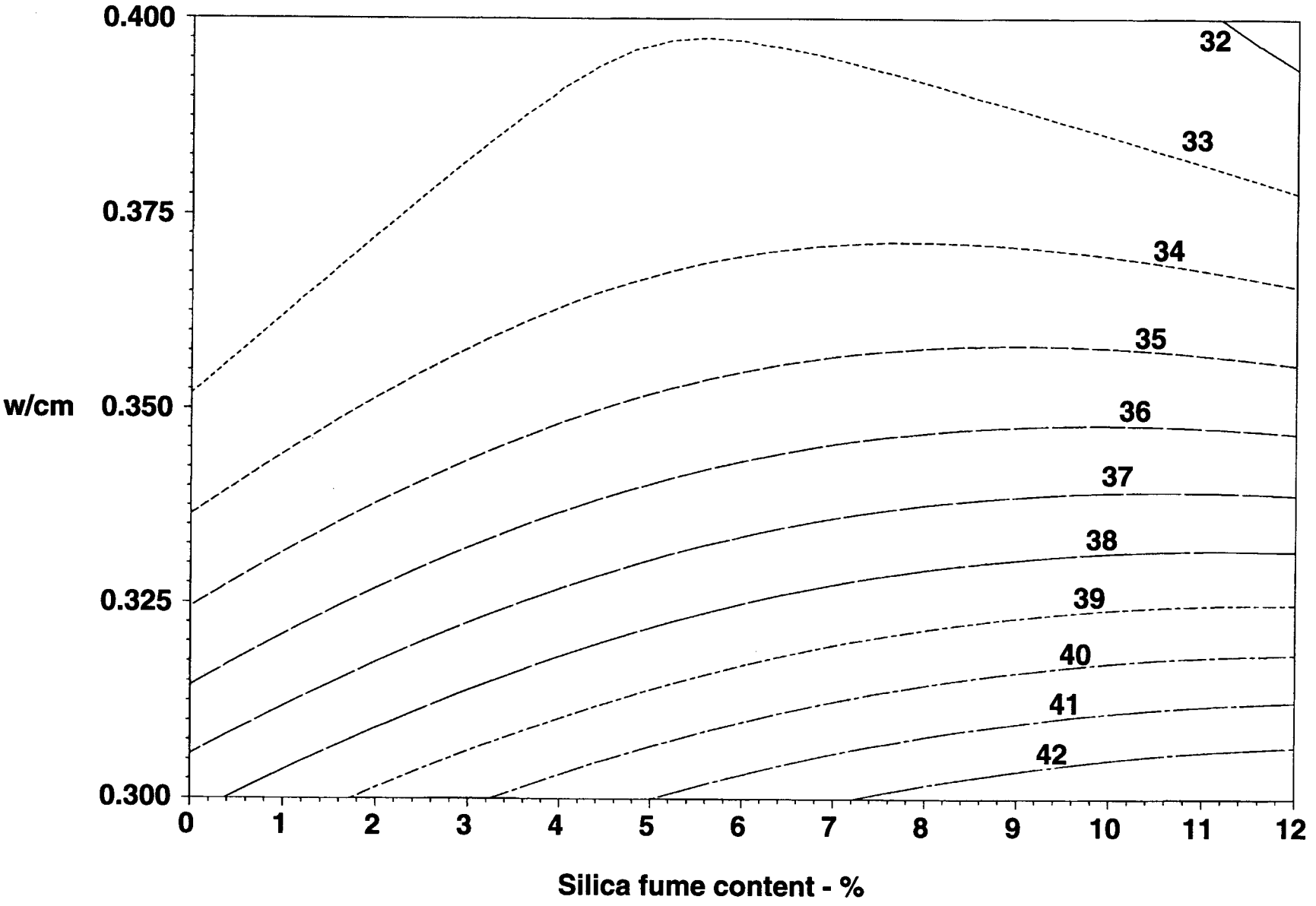

Figure C-29. Contour plots for 28-day elastic modulus of overlay concrete mixtures.

Table C-1. Mean difference and 95% confidence interval for shrinkage of concretes made with Type K and Type I/II cements.

	Shrinkage Difference (Type K-I/II) - %	
Test Age	Mean Difference	95% Confidence Interval
4-day	0.00400	± 0.00286
1-week	0.00467	± 0.00297
2-week	0.00667	±0.00274
4-week	0.00833	±0.00291
8-week	0.00542	±0.00265
16-week	0.00567	±0.00274
44-week	0.0070	±0.00290
64-week	0.0091	±0.00365

Table C-2. Mean difference and 95% confidence interval for shrinkage of concretes made with silica fume slurry and dry densified silica fume.

	Shrinkage Difference (Slurry-Densified) - %	
Test Age	Mean Difference	95% Confidence Interval
4-day	-0.00046	± 0.00125
1-week	0.00050	± 0.00296
2-week	0.00342	±0.00284
4-week	0.00275	±0.00317
8-week	0.00158	±0.00249
16-week	-0.00025	±0.00267
44-week	0.00058	±0.00193
64-week	-0.00167	±0.00219

Table C-3. Analysis of variance of Phase II data on tendency to crack.

Source	DF	Sum of Squares	Mean Square	F Value	P_r
Model	21	11.326602	0.539362	4.80	0.0001
Error	68	7.637173	0.112311		
Corrected Total	89	18.963775			
Silica fume	2	2.1059087	1.0079544	8.97	0.0003
w/cm	2	0.5934018	0.2967009	2.64	0.0785
w/cm x silica fume	4	0.3511801	0.0877950	0.78	0.5410
Cure	1	5.6150047	5.6150047	49.99	0.0001
Cure x w/cm	2	0.2434548	0.1217274	1.08	0.3441
Cure x silica fume	2	1.4023956	0.7011978	6.24	0.0032
Cure x silica fume x w/cm	4	0.4523557	0.1130889	1.01	0.4101
Round	4	0.6529005	0.1632251	1.45	0.2261

Table C-4. Analysis of variance of Phase II cracking data for concretes cured one day.

Source	DF	Sum of Squares	Mean Square	F Value	P_r
Model	12	3.1323291	0.2610366	3.04	0.0060
Error	32	2.7499639	0.0859364		
Corrected Total	44	5.8824030			
Silica fume	2	2.7089175	1.3544587	15.76	0.0001
w/cm	2	0.0923055	0.0461527	0.54	0.5896
w/cm x silica fume	4	0.1152722	0.0288181	0.34	0.8521
Round	4	0.2159439	0.0539860	0.63	0.6459

Table C-5. Mean difference and 95% confidence interval for difference between the means of the log of days to cracking for concretes cured one day.

Silica fume contnens	Mean Difference	95% Confidence Interval
0 and 9 percent	0.4660	± 0.263
0 and 6 percent	0.5617	± 0.263
6 and 9 percent	0.0956	± 0.263

Table C-6. Analysis of variance of Phase II cracking data for concretes cured seven days.

Source	DF	Sum of Squares	Mean Square	F Value	P_r
Model	12	2.9535907	0.2461326	1.75	0.1029
Error	32	4.5127769	0.1410243		
Corrected Total	44	7.4663676			
Silica fume	2	0.7093869	0.3546934	2.52	0.0967
w/cm	2	0.7445511	0.3722756	2.64	0.0869
w/cm x silica fume	4	0.6882636	0.1720659	1.22	0.3217
Round	4	0.8113891	0.2028473	1.44	0.2440

Table C-7. Mean difference and 95% confidence interval for compressive strengths of concretes made with Type K and Type I/II cements.

	Strength Difference (Type K-I/II) - MPa	
Test Age	Mean Difference	95% Confidence Interval
7-day	4.77	± 1.57
28-day	6.14	± 2.71
56-day	5.91	± 2.07
90-day	4.76	± 3.06

1MPa = 145 lbf/in^2

Table C-8. Mean difference and 95% confidence interval for compressive strengths of concretes made with silica fume slurry and dry densified silica fume.

	Strength Difference (Type K-I/II) - MPa	
Test Age	Mean Difference	95% Confidence Interval
7-day	-0.36	± 3.40
28-day	-1.11	± 3.85
56-day	5.83	± 4.37
90-day	0.77	± 3.52

1MPa = 145 lbf/in^2

APPENDIX D

PLAN FOR FIELD INSTALLATION

The silica fume contents, mix designs, and curing procedures for concretes to be used in the full-depth and overlay placement of highway bridge decks have been optimized in this laboratory study. The optimum silica fume contents which give acceptable strengths and shrinkage levels, low chloride diffusivity, and less tendency to crack were defined. However, in order to verify the long-term performance of these concretes under typical field conditions, a controlled field study is necessary. The effects of severe environments, and installation and construction procedures on long-term performance of such concretes need to be evaluated. The placement of a full-depth reinforced concrete highway bridge deck is recommended for this evaluation.

SITE SELECTION

The first step of this plan will be to locate an acceptable field site, such as a newly constructed bridge or bridge deck replacement. A letter explaining the purpose and the importance of the study will be prepared and sent to state highway agencies. A list of candidates' sites in the states which are willing to participate in the study will then be prepared. Because the cooperation of state highway agencies is critical for this study, the prior commitment of the agencies to participate must be secured. Since chloride diffusivity will be evaluated, it is recommended that the selected site be in a state where deicing salts are regularly applied. The size of the bridge, traffic counts, and geographical location are other factors to be considered in the selection process.

EXPERIMENTAL DESIGN

Selection of Test Materials

The materials needed for this study are commercially available. Most of the materials can be procured from local sources, with the exception of some admixtures which can be easily obtained from distributors. The properties of all materials should be determined before starting the program. The required materials are:

- Silica fume. Slurry or densified silica fume can be used. It is recommended that the silica fume used in the construction should be obtained from a single source, and should meet AASHTO M 307.

- Aggregates. Coarse and fine aggregates meeting AASHTO M 6 and M 80 can be obtained from local sources. It is advisable that the aggregates not contain chlorides, as these will interfere with the collection and analysis of chloride profile data.

- Cement. Type I/II portland cement meeting AASHTO M 85 and Type K cement meeting ASTM C 845 will be included. Type I/II cement can be obtained from local sources. Type K is available from only one supplier in the United States.

- Alternative cementitious materials. In addition to silica fume, fly ash is also needed; either class F or C meeting AASHTO M 295 may be used. The particular ash used can be selected based on availability and state highway agency specifications.

- Admixtures. Air-entraining and high-range water reducing admixtures are needed for all proposed mixes. Commercially available admixtures meeting AASHTO 154 and AASHTO 194 can be utilized in the study.

- Shrinkage-reducing admixture. This is a newly developed admixture which is commercially available and can be easily procured. There are as yet no AASHTO or ASTM specifications covering its use.

Design of test mixes

Four different mixture designs will be considered in this study. Mixture designations and mixture proportions are shown in Table D-1. Mixture I contains 6% silica fume by weight of cementitious material at w/cm of 0.40. This mix was designated as 5F in Appendix A of this report. Mixture II contains 6% silica fume and 20% fly ash by weight of cementitious materials with a maximum w/cm ratio of 0.40. AASHTO Type I/II cement is to be used in these two mixes. Mixture III contains Type K cement and 6% silica fume, and Mixture IV is the same as Mixture I except that a shrinkage reducing admixture is used.

Trial Mixtures

For each proposed mixture, trial batches should be prepared in the laboratory. It is strongly recommended that the same materials that will be used in the field should be used in the laboratory trials. Mixture proportions should be adjusted in order to obtain the fresh concrete properties (slump, air content, and unit weight) specified for the particular placement. Once these specified

properties are achieved, specimens will be prepared for compressive strength to verify that the specified strength has been achieved. The final mixture proportions will be selected after the completion of this task.

Layout of Test Sections

A two-lane bridge is recommended for this study. Each lane of the selected bridge will be divided into four sections. Two sections will be constructed using each mixture, but will be cured differently. A layout of a typical bridge is shown in Figure D-1.

Design of Experimental Variables

The laboratory study showed that mixture design and curing procedures are the most important factors controlling the performance of silica fume concrete. Therefore, mixture design and curing procedures are the variables that will be chosen for the recommended field study. As mentioned above, four different mixtures will be used. Two adjacent sections will be constructed using each mixture and then moist-cured for seven days, the minimum curing time for silica fume concrete which is recommended based on the results of this study. At the end of the seven-day moist curing, one of each of the duplicate sections will be sprayed with curing compound and the other will be air-cured. The contribution of the increased curing time afforded by the use of the curing compound can thereby be evaluated.

FIELD SITE INSTALLATION

Once the site is selected, the installation plans can be prepared. Field site installation involves coordination with the contractor and the state highway agency, scheduling of the concrete placement, instrumentation of the test sections, batching, and placement and curing procedures.

Contractor/Highway Agency Coordination

Coordination with the contractor and the state highway agency is essential for successful completion of the field evaluation. Information needed from the contractor includes sources and properties of the materials, concrete production processes, location of the batch plant, and type of placement equipment (e.g., pumping vs. other techniques). Quality control procedures should be coordinated with the state highway agency. It is important to ensure that all fresh concrete testing for slump, air content, and unit weight be done at least once for each section. In addition, the

microwave oven method (AASHTO TP23) can be used in the field to measure the water content of as-delivered concrete as an additional quality control measure. Since four different types of concrete will be used in the construction of the bridge deck, coordination with the ready-mix concrete supplier is also essential for properly carrying out the work.

Placement Scheduling

Placement scheduling should be arranged between the contractor and the state highway agency. Weather has to be taken into consideration. Arrangements should be made to accomodate rain or delays due to weather. Timing of the placement should be planned based on the size of bridge and the volume of concrete to be produced each day and the time it takes to cast each section.

Instrumentation of Test Sections

Before casting, a thermocouple tree consisting of five thermocouples will be placed in the center of every section. Thermocouple wires will be extended to the side of the bridge and connected to a data logger for monitoring. In addition, after the concrete is placed, shrinkage pins (gage studs) for measurement of length changes will be placed in the deck at each section before the concrete hardens. Pins will be placed in such a way as to be flush with the surface, so they will not be damaged when the bridge is opened to traffic.

Batching and Placement

As mentioned above, it is important to work with the contractor and the concrete supplier during batching of the concrete in order to ensure that the concrete is delivered as specified. If possible, field trial batches should be prepared before the casting of the actual bridge sections, and the properties of the fresh concrete should be measured. Aggregate moisture should be checked periodically. The types and dosages of admixtures should be checked, especially if the admixture (e.g., superplasticizer) is to be batched on site.

Before placement, the properties of the fresh concrete are to be measured at least once for every section. Measurements of the water content using the microwave oven method are also recommended for every section. Placement and consolidation procedures should follow the state specifications for bridge deck construction.

Curing Procedures

As mentioned earlier, since curing is critical for silica fume concrete, extra attention should be paid to maintain the required curing. All sections should be moist-cured under wet burlap for seven days. Burlap sheets should not be allowed to dry during the curing period. Water hoses should be used to keep the burlap wet during the entire curing period. The burlap should be covered with plastic sheets to prevent evaporation. At the end of the seven days of moist curing, one section constructed with each mixture will be sprayed with curing compound. The curing materials and application rate should meet AASHTO M 148 and state specifications.

FIELD INSTALLATION TESTING

Test specimens will be prepared from each concrete during placement. In situ testing will start as soon as the placement is completed.

In Situ Testing

Temperature measurement in each section will start immediately after the section is completed. Measurements will be taken every half hour in the first 24 hours, then every hour for the rest of the curing period. Initial measurements of length change will be taken after the gage studs are fixed on the deck. Impact-echo testing equipment will be used to measure the initial primary wave speed of the concrete 24 hours after placement of concrete at selected locations on each section. This initial reading will aid in monitoring changes in concrete quality with time, as the wave speed is a measure of the integrity of the concrete member. A significant decrease in wave speed is an indication of the formation of microcracks in the concrete.

Type and Preparation of Test Specimens

Nine 100 x 200 mm (4 x 8 in) cylinders, three 75 x 75 x 285 mm (3 x 3 x 11-1/4 in) shrinkage test beams, and one 305 x 305 x 75 mm (12 x 12 x 3 in) slab will be prepared from the concrete used in each section. In addition, restrained shrinkage rings identical to those used in the testing for cracking tendency (see Appendix B) will also be cast. The cylinders and beams will be moist cured in their molds in the field until set, then water-cured for 24 hours before transfer to the laboratory. The slabs will be cured in the field similarly to the curing of the actual bridge deck sections. Restrained shrinkage rings will be cured along with the slabs, then subjected to the bridge environment.

Schedule of Testing

The compressive strength will be tested at 3, 7, and 28 days. Three cylinders will be tested at each age. The length change of the beams will be measured at 4, 7, 14, and 28 days, and 8, 16, 44, and 64 weeks. At the end of the 14-day curing, the slabs will be transferred to the laboratory and used for the 6-month chloride ponding test as discussed in Appendix B of this report. Restrained shrinkage rings will be monitored until the occurence of the first crack. At the discretion of the test agency, AASHTO T 277 tests may also be performed on companion test cylinders if it is desired to obtain further correlation data with the results of the ponding tests.

LONG-TERM MONITORING

The most important aspect of this recommended study is the long-term monitoring of the performance of silica fume concrete mixtures under actual field conditions when subjected to traffic loading, weather, and other field variables.

Monitoring Frequency and Schedule

The bridge sections will be inspected at the ages of 1 and 6 months in the first year and then at the ages of 1, 2, and 4 years.

Visual Assessment and Characterization of Distress

Visual assessment consists of inspection of the bridge deck surface. It includes mapping of all visible cracks, measurement of crack widths, and documenting any sign of distress such as scaling or deterioration near joints. Distressed areas on the bridge deck will be documented photographically. These procedures will be performed on every section.

Nondestructive Testing

The SHRP surface air permeameter (AASHTO TP26) will be used to measure the surface air permeability. Initial readings and reading at later ages will be taken and compared. The increase in air permeability can serve as an indication of surface distress. The bridge deck will be sounded using a chain drag to locate any signs of delamination. The impact-echo technique will be used to measure crack depths and monitor their propagation with time. The impact-echo device will also be used to monitor changes in wave speeds with time, as previously discussed.

Coring and Laboratory Testing of Cores

Cores will be taken only if distress occurs. Cores will be obtained in distressed areas and petrographically analyzed to establish probable cause of distress. Companion cores in areas not showing distress will be taken for comparison purposes.

Periodic and Final Reports

Progress reports will be prepared after installation and after each field survey. All distresses will be documented. At the end of the project, a final report will be prepared summarizing the performance of all sections. Based on the outcome of the study, conclusions and recommendations will be given regarding the use and performance of silica fume concrete in field bridge decks.

COOPERATIVE FEATURES

Cooperation of the state highway agency in the conduct of this field research program is essential. The state highway agency must agree to provide convenient and safe access to the site, traffic control during periodic surveys, and permission to extract core samples from distressed sections. In addition, the cooperation of the Federal Highway Administration (FHWA) will be requested for loan of special SHRP equipment items which are needed for periodic nondestructive evaluation of the test sections.

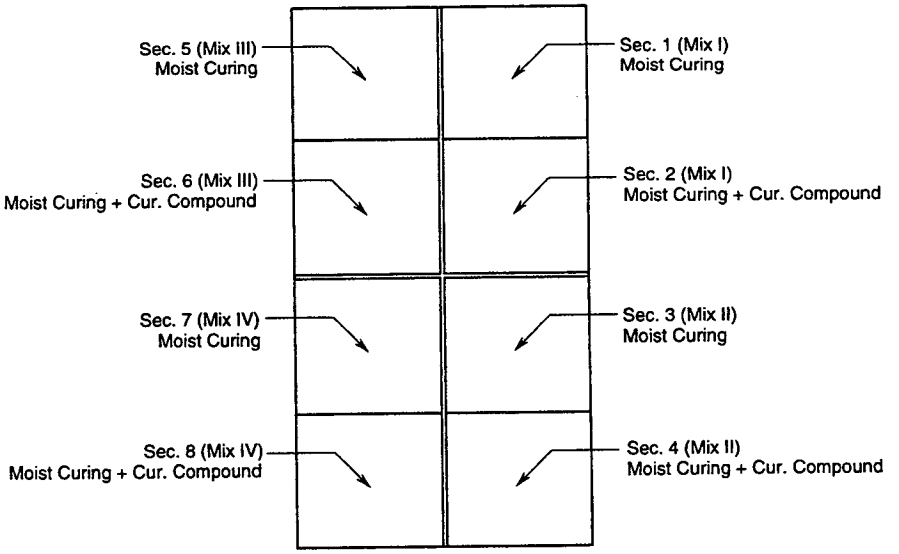

Figure D-1. Plan layout of typical two-lane bridge.

Table D-1. Mixture proportions of the proposed mixtures.

Material		Quantities (kg/m^3)			
		Mixture Designation			
		Mix I	Mix II	Mix III	Mix IV
(SSD) Base	% Silica Fume	6.0	6.0	6.0	6.0
	w/cm	0.4	0.4	0.4	0.4
Cement Type I		340	300		340
Cement Type K		—	—	340	—
Silica Fume		22	25	22	22
Fly Ash		—	80	—	—
Fine Aggregate		720	680	705	720
Coarse Aggregate		1050	1040	1030	1050
Water		146	120	146	146
AEA-mL/Kg		As required	As required	As required	As required
HRWR - mL/kg		"	—	"	"
Shrinkage-Reducing Admixture mL/kg		—	—	—	As specified
Set-Retarding Water Reducer mL/kg		—	As specified	—	"

The **Transportation Research Board** is a unit of the National Research Council, which serves the National Academy of Sciences and the National Academy of Engineering. The Board's mission is to promote innovation and progress in transportation by stimulating and conducting research, facilitating the dissemination of information, and encouraging the implementation of research results. The Board's varied activities annually draw on approximately 4,000 engineers, scientists, and other transportation researchers and practitioners from the public and private sectors and academia, all of whom contribute their expertise in the public interest. The program is supported by state transportation departments, federal agencies including the component administrations of the U.S. Department of Transportation, and other organizations and individuals interested in the development of transportation.

The National Academy of Sciences is a private, nonprofit, self-perpetuating society of distinguished scholars engaged in scientific and engineering research, dedicated to the furtherance of science and technology and to their use for the general welfare. Upon the authority of the charter granted to it by the Congress in 1863, the Academy has a mandate that requires it to advise the federal government on scientific and technical matters. Dr. Bruce M. Alberts is president of the National Academy of Sciences.

The National Academy of Engineering was established in 1964, under the charter of the National Academy of Sciences, as a parallel organization of outstanding engineers. It is autonomous in its administration and in the selection of its members, sharing with the National Academy of Sciences the responsibility for advising the federal government. The National Academy of Engineering also sponsors engineering programs aimed at meeting national needs, encourages education and research, and recognizes the superior achievements of engineers. Dr. William A. Wulf is president of the National Academy of Engineering.

The Institute of Medicine was established in 1970 by the National Academy of Sciences to secure the services of eminent members of appropriate professions in the examination of policy matters pertaining to the health of the public. The Institute acts under the responsibility given to the National Academy of Sciences by its congressional charter to be an adviser to the federal government and, upon its own initiative, to identify issues of medical care, research, and education. Dr. Kenneth I. Shine is president of the Institute of Medicine.

The National Research Council was organized by the National Academy of Sciences in 1916 to associate the broad community of science and technology with the Academy's purpose of furthering knowledge and advising the federal government. Functioning in accordance with general policies determined by the Academy, the Council has become the principal operating agency of both the National Academy of Sciences and the National Academy of Engineering in providing services to the government, the public, and the scientific and engineering communities. The Council is administered jointly by both the Academies and the Institute of Medicine. Dr. Bruce M. Alberts and Dr. William A. Wulf are chairman and vice chairman, respectively, of the National Research Council.

Abbreviations used without definitions in TRB publications:

AASHO	American Association of State Highway Officials
AASHTO	American Association of State Highway and Transportation Officials
ASCE	American Society of Civil Engineers
ASME	American Society of Mechanical Engineers
ASTM	American Society for Testing and Materials
FAA	Federal Aviation Administration
FHWA	Federal Highway Administration
FRA	Federal Railroad Administration
FTA	Federal Transit Administration
IEEE	Institute of Electrical and Electronics Engineers
ITE	Institute of Transportation Engineers
NCHRP	National Cooperative Highway Research Program
NCTRP	National Cooperative Transit Research and Development Program
NHTSA	National Highway Traffic Safety Administration
SAE	Society of Automotive Engineers
TCRP	Transit Cooperative Research Program
TRB	Transportation Research Board

Transportation Research Board
National Research Council
2101 Constitution Avenue, N.W.
Washington, D.C. 20418

ADDRESS CORRECTION REQUESTED